

**Assessing The Impact Of Showerhead Design Choices On Consumer Exposure  
To Drinking Water-Associated Pathogens That Can Cause Infections In The  
Immunocompromised**

by

**Sarah Pitell**

Bachelor of Arts, Biochemistry and Molecular Biology, College of Wooster, 2019

Master of Science, Civil Engineering, University of Pittsburgh, 2022

Submitted to the Graduate Faculty of the  
Swanson School of Engineering in partial fulfillment  
of the requirements for the degree of  
Doctor of Philosophy

University of Pittsburgh

2024

UNIVERSITY OF PITTSBURGH  
SWANSON SCHOOL OF ENGINEERING

This dissertation was presented

by

**Sarah Pitell**

It was defended on

March 1, 2023

and approved by

Dr. Vikas Khanna, Professor, Civil and Environmental Engineering

Dr. Meng Wang, Assistant Professor, Civil and Environmental Engineering

Dr. Janet Stout, Associate Professor, Civil and Environmental Engineering, Executive Vice  
President and Founder of Special Pathogens Laboratory

Dr. William DePas, Assistant Professor, Department of Pediatrics, Division of Infectious  
Diseases

Dr. Leanne Gilbertson, Associate Professor, Civil and Environmental Engineering, Duke  
University

**Dissertation Director: Dr. Sarah Haig, Assistant Professor, Civil and Environmental  
Engineering**

Copyright © by Sarah Pitell

2024

# **Assessing The Impact Of Showerhead Design Choices On Consumer Exposure To Drinking Water-Associated Pathogens That Can Cause Infections In The Immunocompromised**

Sarah Pitell, PhD in Civil Engineering

University of Pittsburgh, 2024

Respiratory infections from drinking water-associated pathogens that can cause infections in the immunocompromised (DWPIs) are responsible for >145,000 human infections annually and cost the US economy billions. Cases are rapidly increasing in the United States as susceptible populations increase (e.g., those at either age extreme or currently living with a weakened immune system), and currently outpace illness caused by regulated fecal-borne pathogens. DWPIs thrive in building plumbing biofilms, with several recent studies showing a clear link between the strains of DWPIs found in household water and the strains infecting people. Although DWPI exposure can occur through a variety of pathways, inhalation of shower water associated aerosols are most likely a source of infection. Because DWPI proliferation occurs mainly in building plumbing, studying how consumer choices at the point of use (e.g., showerhead type and water use patterns) affect users' potential DWPI exposure is critical to helping vulnerable groups make informed decisions about their plumbing to reduce health risks.

This work focused specifically on quantitatively assessing the impacts that different showerhead setups had on the microbiome and DWPI exposure risk posed by shower water and shower-water associated aerosols. Through full-scale shower and biofilm reactor experimentation, the findings from this work have shown that antimicrobial additives such as silver do not reduce DWPIs in the shower system, and that showerhead material choice, flow rate, and changes in water

use habits impact the microbiome. An especially important finding from this work is that showerhead age (days of use) is a major factor in explaining microbial dynamics in shower water and associated aerosols and consequently should be considered when developing new DWPI microbial risk assessments. Overall, this body of work provides consumers and building managers with unbiased and empirical data to empower and inform them to make choices that are best for their specific situations, as well as provide valuable insights for DWPI mitigation.

## Table Of Contents

<b>Committee Membership Page.....</b>	<b>ii</b>
<b>Abstract .....</b>	<b>iv</b>
<b>Table Of Contents.....</b>	<b>vi</b>
<b>List Of Tables.....</b>	<b>xii</b>
<b>List Of Figures .....</b>	<b>xiv</b>
<b>Acknowledgements.....</b>	<b>xxiv</b>
<b>List Of Abbreviations.....</b>	<b>xxvi</b>
<b>1.0 Introduction.....</b>	<b>1</b>
<b>1.1 DWPIs As An Emerging Public Health Concern.....</b>	<b>1</b>
<b>1.2 Shower Systems As A Potential Point Of Exposure To DWPIs .....</b>	<b>3</b>
<b>1.3 Responding To Novel Water Utilization Strategies And Its Effects On DWPIs .....</b>	<b>5</b>
<b>1.4 Thesis Objectives And Hypotheses .....</b>	<b>7</b>
<b>2.0 Specific Aim 1.0: The Impact Of Antimicrobial Showerheads On The Prevalence And Abundance Of DWPIs In Shower Water And Shower Water-Associated Aerosols .....</b>	<b>10</b>

<b>2.1 Introduction.....</b>	<b>11</b>
<b>2.2 Research Approach .....</b>	<b>14</b>
<b>2.2.1 INHALE Shower Laboratory Set Up And Tested Showerheads.....</b>	<b>14</b>
<b>2.2.2 Shower Water And Shower Water Associated Bioaerosol Collection.....</b>	<b>16</b>
<b>2.2.3 Water Quality Measurements.....</b>	<b>17</b>
<b>2.2.4 DWPI Quantification .....</b>	<b>18</b>
<b>2.2.5 16S rRNA Gene Amplicon Sequencing .....</b>	<b>19</b>
<b>2.2.6 Statistical Analysis.....</b>	<b>19</b>
<b>2.3 Results And Discussion .....</b>	<b>21</b>
<b>2.3.1 Showerhead Type Did Not Impact Shower Water Chemistry .....</b>	<b>21</b>
<b>2.3.2 DWPI Presence And Abundance Was Unaffected By Showerhead Type....</b>	<b>21</b>
<b>2.3.3 Aerosolization Behavior Of DWPIs Is Species-Specific .....</b>	<b>25</b>
<b>2.3.4 Microbial Community Dynamics Were Phase (Water And Aerosol) And Showerhead Age Dependent.....</b>	<b>30</b>
<b>2.4 Conclusions.....</b>	<b>34</b>
<b>3.0 Specific Aim 2.0: Evaluate The Efficacy Of Silver In The Showering System.....</b>	<b>36</b>
<b>3.1 Introduction.....</b>	<b>38</b>

<b>3.2 Research Approach .....</b>	<b>40</b>
<b>3.2.1 INHALE Shower Laboratory Experimental Design And Sampling Regime .....</b>	<b>40</b>
<b>3.2.2 Showerhead Materials Testing .....</b>	<b>41</b>
<b>3.2.3 Water And Biofilm Sample Collection From Showerheads .....</b>	<b>42</b>
<b>3.2.4 Water Quality Measurements.....</b>	<b>44</b>
<b>3.2.5 DWPI Culturing.....</b>	<b>44</b>
<b>3.2.6 DWPI Absolute Abundance Quantification .....</b>	<b>45</b>
<b>3.2.7 Biofilm Imaging Using Optical Coherence Tomography.....</b>	<b>45</b>
<b>3.2.8 16S rRNA Sequencing.....</b>	<b>46</b>
<b>3.2.9 Silver Nitrate Exposure To <i>M. abscessus</i> Biofilms In A CDC Biofilm Reactor .....</b>	<b>46</b>
<b>3.2.10 Statistical Analysis.....</b>	<b>50</b>
<b>3.3 Results And Discussion .....</b>	<b>50</b>
<b>3.3.1 Silver-Containing Showerheads Minimally Impacted Metal Composition In Shower Water .....</b>	<b>50</b>
<b>3.3.2 Silver-Containing Showerheads Did Not Impact Viable DWPI Concentrations In Shower Water.....</b>	<b>54</b>

3.3.3 Microbial Community Membership Varied Between Showerhead Type In Shower Water .....	58
3.3.4 Showerhead Age Influenced The Microbiota In Water Samples .....	63
3.3.5 Shower-Associated Biofilms Contained Complex Microbial Communities.	66
3.3.6 Shower Hose Biofilm Topography Was Influenced By Material Type .....	72
3.3.7 Response To Silver Nitrate By <i>M. abscessus</i> Biofilms Was Dose-Dependent .....	75
3.4 6 Conclusions.....	80
<b>4.0 Specific Aim 3.0: Examining The Impacts Of Shower Use Patterns On DWPIs And The Microbiome.....</b>	<b>85</b>
4.1 Introduction.....	87
4.2 Research Approach .....	90
4.2.1 Methodology Used After The COVID-19 Shutdown .....	90
4.2.2 Methodology Used To Assess Water-Conserving Showerheads.....	91
4.2.3 Methodology Used In Both Studies.....	93
4.2.4 16S rRNA Sequencing.....	93
4.2.5 Statistical Analysis.....	93

<b>4.3 Results And Discussion .....</b>	<b>94</b>
<b>4.3.1 Microbial Water Quality Was Severely Impacted By Prolonged Stagnation .....</b>	<b>94</b>
<b>4.3.2 Water-Conserving Showerheads Decreased Microbial Concentrations In Shower Water, But Increased The Concentrations Of Aerosols Containing Gram-Negative Bacteria .....</b>	<b>97</b>
<b>4.3.3 Microbial Community Membership Varied With Flow Rate.....</b>	<b>101</b>
<b>4.3.4 Showerhead Age Is The Key Factor That Influenced Microbial Dynamics .....</b>	<b>104</b>
<b>4.4 Conclusions.....</b>	<b>106</b>
<b>5.0 Concluding Remarks And Recommendations To Stakeholders.....</b>	<b>108</b>
<b>5.1 Overall Summary .....</b>	<b>108</b>
<b>5.2 Considerations For Future Research .....</b>	<b>109</b>
<b>5.3 Considerations For Consumers And Building Managers.....</b>	<b>111</b>
<b>5.3.1 Material Choice Does Not Impact DWPI Densities In Shower Water Or Aerosols .....</b>	<b>111</b>
<b>5.3.2 Water-Conserving Showerheads Increase Aerosol Generation And Containment Of Potentially Pathogenic Microorganisms.....</b>	<b>112</b>

<b>5.3.3 Shower Water Usage And Management Practices.....</b>	<b>113</b>
<b>Appendix A Chapter 2 Supplementary Information .....</b>	<b>115</b>
<b>Appendix B : Chapter 3 Supplementary Information .....</b>	<b>126</b>
<b>Appendix C : Chapter 4 Supplementary Information.....</b>	<b>142</b>
<b>Bibliography .....</b>	<b>148</b>

## List Of Tables

<b>Table 1: Summary of generated linear models. In the model components column, ± indicates positive or negative association and the percent of the variance explained by each variable is superscripted.....</b>	<b>29</b>
<b>Table 2: Summary of showerheads used in Chapter 3. ....</b>	<b>41</b>
<b>Table 3: Total and dissolved metals recovered in shower water from different showerhead types in mg/L. Significance in analyte concentrations between head types were determined via one-way analysis of variants (ANOVA). .Error! Bookmark not defined.</b>	
<b>Table 4: Summary of generated linear models in the first draw and flush samples. In the model components column, the percent of the variance explained by each variable is superscripted. All response variables were transformed to achieve normality as described in parentheses in the model column. ....</b>	<b>96</b>
<b>Table 5: Average aerosolization partitioning percentages for DWPIs and total bacteria..</b>	<b>100</b>
<b>Appendix A Table 1: Different physical and chemical water quality parameters measured in this study and corresponding analytical method used. ....</b>	<b>119</b>
<b>Appendix A Table 2: Molecular primers, thresholds, and assay sensitivity for ddPCR analysis. ....</b>	<b>120</b>
<b>Appendix A Table 3: Average values of water quality parameters.....</b>	<b>121</b>

**Appendix A Table 4: Average aerosol partitioning values of DWPIs and total bacteria by head type.....124**

**Appendix B Table 1: Different physical and chemical water quality parameters measured in this study and corresponding analytical method used .....134**

**Appendix B Table 2: Molecular primers, thresholds, and assay sensitivity for ddPCR analysis.....135**

**Appendix B Table 3: Average values of water quality parameters.....136**

**Appendix B Table 4: Summary of generated linear models in water samples. In the model components column,  $\pm$  indicates positive or negative association and the percent of the variance explained by each variable is superscripted. ....137**

**Appendix B Table 5: Average diversity values of water samples  $\pm$  standard deviation. Sample size is denoted in parentheses under value. ....138**

**Appendix B Table 6: Average diversity values of biofilm samples  $\pm$  standard deviation for A. hose samples and B. swab samples.....139**

## List Of Figures

- Figure 1: Diagram illustrating the particle size which can be deposited at different locations in the respiratory system .....2**
- Figure 2: Schematic of full-scale shower laboratory set-up. The blue X indicates the aerosol sampling port in the Plexiglass door, the black X indicates where the copper pipe from the hot water heater connects to the shower stall, and the red X's correspond to each showerhead position. ....15**
- Figure 3: Absolute gene copy concentration of total bacteria (orange), *Legionella pneumophila* (green), *Pseudomonas aeruginosa* (blue), and nontuberculous mycobacteria (yellow) observed across 84 days of shower operation in ABS Plastic, silter-based, and silver-embedded showerheads in shower water. Each showerhead type shows all the data collected from three experimental showerhead replicates...22**
- Figure 4: Stacked barplots of the average absolute abundance of *Legionella pneumophila* (green), *Pseudomonas aeruginosa* (yellow), and nontuberculous mycobacteria (blue) within bio-respirable shower water-associated aerosols (<10 um) produced during an 8-minute shower using ABS Plastic showerhead, Silver-embedded showerhead, and Filter-based showerhead. Averages are based on triplicates of each showerhead type. ....26**
- Figure 5: Partitioning percentages of A *Legionella pneumophila*, B *Pseudomonas aeruginosa*, C nontuberculous mycobacteria, and D total bacteria based on biofilm growth stage;**

initial (0 -13 days), early (14-42 days) and mature (43-84 days) using all data collected from all showerhead types.....28

Figure 6: Stacked barplots showing the top ten most abundance phyla A. and genera B. in shower water and shower water-associated aerosols. Data illustrate the average abundance observed across all showerhead types and all timepoints. ....31

Figure 7: Heatmap showing the abundances of the fifteen least abundant genera produced in A. aerosol samples and B. water samples by each shower head type .....33

Figure 8: Top ten most abundant genera by biofilm establishment period for A. water and B. aerosol samples. Each bar represents an average across all showerhead types....34

Figure 9: Quantification of DWPIs by showerhead type. A. Enumeration of *Mycobacterium gordonae* (light yellow) and *Mycobacterium phocacium/mucogenicum* (light brown) in culture. The red line labeled “LOD” refers to the upper limit of detection of the culturing method. B. Microbial densities of *Legionella pneumophila* (dark orange), *Pseudomonas aeruginosa* (dark blue), nontuberculous mycobacteria (gold), and total bacteria (green).....55

Figure 10: The overlap and proportion of core genera (84% relative abundance on average) in each showerhead type. A. Venn diagram illustrating the shared and unique genera between different showerhead types, and B. Pie charts showing the relative abundance of core genera in each showerhead type. All other shared genera constituting <30% relative abundance each were combined in the “shared other

genera” category, and all genera not present in all showerhead types were combined in the “unique” category. ....59

**Figure 11: Average relative abundance and standard deviation of statistically significant functional traits in water samples by showerhead type obtained from PICRUSt analysis. ....61**

**Figure 12: Viable concentrations of A. *Mycobacterium gordonae* and B. *Mycobacterium mucogenicum / phocaicum* for ABS plastic (red), metal (yellow), silver-coated copper mesh (green), silver-embedded (blue), and silver mesh (purple) showerheads by biofilm formation stage. Significant differences at p-values <0.05, <0.01 and <0.001 are denoted by \*, \*\*, and \*\*\* respectively.....64**

**Figure 13: Absolute quantification of DWPI biofilm densities in A. swab samples before (n=18) and after (n=18) the 12 week long sampling campaign and B. hose samples of different showerhead types (n=3) after 12 weeks of daily use.....68**

**Figure 14: Ten most abundant genera from A. swab samples taken from the plumbing outlet before the shower hose before (n=18) and after (n=18) the 12 week long sampling campaign and B. hose samples of different showerhead types (n=3) taken from the hose to the showerhead after 12 weeks of daily use.....71**

**Figure 15: Representative 3D renderings generated from OCT images taken from A. ABS plastic shower hoses, B. hoses containing pure silver mesh, and C. shower hoses with the addition of silver-coated copper mesh in the hose. ....73**

**Figure 16: Recovered *M. abscessus* biofilms after reactor operation for clinical (red) and environmental (blue) isolates quantified using A. plate counts (n=8), and B. ddPCR results (n=1). Significance in A. is denoted by brackets, but there were not enough samples to determine significance for B.....76**

**Figure 17: Fluorescent microscopy results of representative sections of *M. abscessus* biofilms recovered after 7 days of reactor operation by isolate (row) and exposure condition (column). Green indicates the presence of biomass, and total biovolume (abbreviated b.v.) was included on each image that was quantified from zstack data. ....78**

**Figure 18: Planktonic vs. aggregate *M. abscessus* ratios (ranges in parentheses) for A. clinical (0–163) and B. environmental (0–100) isolates for the initial inoculates and after silver exposure (each tile is one technical replicate (n = 9 per isolate × condition × time). Blue cells represent a smaller ratio, signifying a larger proportion of aggregated *M. abscessus* cells, while white/red cells represent a higher ratio (larger proportion of planktonic *M. abscessus* cells). The white cells represent the 50th percentile. The ratios were obtained by dividing the planktonic OD600 measurements by the aggregate OD600 measurements. C. The values from A. and B. were normalized to the results of the isolates taken from the reactor with no added silver. ....83**

**Figure 19: Microbial abundances in shower water (n=9) over time before (red) and after (blue) 5 minutes of flushing after 95 days of stagnation (day 0). *Legionella pneumophila* quantified with Legiolert A., and ddPCR analysis B., Nontuberculous mycobacteria quantified with ddPCR C., and total bacteria quantified with ddPCR**

**D. Significant differences as determined with paired Wilcoxon tests are denoted by brackets, with black brackets indicating differences between the paired first draw and flush samples, red brackets denoting differences between first draw samples, and blue brackets denoting differences between flushed samples. Significance was indicated by asterisks, with \* , \*\*, and \*\*\*denote p-values of  $\leq 0.05$ ,  $\leq 0.01$ , and  $\leq 0.001$ , respectively.....95**

**Figure 20: Box and whisker plots showing the absolute densities of *L. pneumophila* (LP, green), Nontuberculous mycobacteria (NTM, yellow), and total bacteria (TOT, orange) by showerhead flow rate in A. shower water and B. shower water associated aerosols (<10um). Data is aggregated across the whole 8-week experimental timeframe (n=18). Significant differences are denoted by brackets, with \* and \*\* denoting p-values of < 0.05 and < 0.01, respectively.....98**

**Figure 21: Box and whisker plots showing the absolute numbers of aerosolized particles by showerhead flow rate between the diameters of A. 0.3  $\mu\text{m}$  – 5  $\mu\text{m}$  and B. 2  $\mu\text{m}$  – 5  $\mu\text{m}$ . Data is aggregated across the whole 8 -week experimental timeframe (n=18).....99**

**Figure 22: Relative abundance of the 30 most abundant bacterial genera in all samples. In the figure, Burkholderia1 and Lachnospiraceae sp.2 refer to Burkholderia-Caballeronia-Paraburkholderia and Lachnospiraceae NK4A136 group, respectively. Every heatmap box is correlated to a sample, and is organized by day sampled as well as flow rate.....102**

**Appendix A Figure 1: Absolute gene copy concentrations in shower water over time by showerhead type. A. *L. pneumophila*, B. *P. aeruginosa*, C. NTM, and D. total bacteria**

observed across 14 weeks of operation in ABS plastic (green), filter-based antimicrobial (yellow), and silver-embedded (blue) showerheads in shower water associated aerosols. Each showerhead type shows all the data collected from three experimental showerhead replicates for that specific time point.....115

**Appendix A Figure 2: Absolute gene copy concentrations in shower water associated aerosols over time. A. *L. pneumophila*, B. *P. aeruginosa*, C. NTM, and D. total bacteria observed across 14 weeks of operation in ABS plastic (green), filter-based antimicrobial (yellow), and silver-embedded (blue) showerheads in shower water associated aerosols. Each showerhead type shows all the data collected from three experimental showerhead replicates for that specific time point.....116**

**Appendix A Figure 3: Absolute gene copy concentrations in shower water over time. A. *L. pneumophila*, B. *P. aeruginosa*, C. NTM, and D. total bacteria observed across 14 weeks of operation in ABS plastic (green), filter-based antimicrobial (yellow), and silver-embedded (blue) showerheads in shower water. Each showerhead type shows all the data collected from three experimental showerhead replicates for that specific time point. ....117**

**Appendix A Figure 4: Non-metric Multidimensional Scaling plot by A. sample type, B. biofilm age bin of water samples, and C. showerhead type of water samples.....118**

**Appendix A Procedure 1: Threshold determination for ddPCR quantification .....125**

**Appendix B Figure 1: Summary of SEM-EDS analysis conducted on silver-containing inserts of the silver-embedded head A. Annotated diagram of the sampling sites of the shower**

insert, with A1 being the ‘top’ of the insert, A2 being taken from the side wall, and A3 being the ‘bottom’ of the insert. B. Representative EDS scan from an insert with red corresponding to sampling site A1, blue corresponding to sampling site A2, and yellow corresponding to sampling site A3. C. Representative SEM image taken from the showerhead insert, with maps of i. oxygen and ii. titanium. ....126

Appendix B Figure 2: CDC Biofilm Reactor Schematic. A. Annotated diagram of a CDC Biofilm Reactor, and B. A representative experimental reactor set up. The red star indicates the location of the influent, the yellow star indicates the location of the reactor itself, and the blue star indicates the location of the pump. ....127

Appendix B Figure 3: Non-metric Multidimensional Scaling plot of water samples by showerhead type .....128

Appendix B Figure 4: Shannon diversity calculated from water samples by showerhead type .....129

Appendix B Figure 5: Viable concentrations of A. *L. pneumophila*, B. *P. aeruginosa*, C. *M. gordonae*, D. NTM, E. total bacteria, and F. *M. mucogenicum/phocaicum* for ABS plastic (red), metal (yellow), silver-coated copper mesh (green), silver-embedded (blue), and silver mesh (purple) showerheads by biofilm formation stage. Significant differences are marked with a colored bracket and star corresponding to the showerhead type and p-value (\* =  $p \leq 0.05$ , \*\* =  $p \leq 0.01$ , \*\*\* =  $p \leq 0.001$ ) .....130

Appendix B Figure 6: Visual discoloration cause by silver nitrate of the reactors with 480 mg Ag<sup>+</sup>/L\*min (A.) and 4800 mg Ag<sup>+</sup>/L\*min (B.) after 7 days of reactor operation. ..131

**Appendix B Figure 7: Average log reduction ± standard deviation of environmental (dark blue) and clinical (dark red) *M. abscessus* exposed to various silver nitrate concentrations for 10 minutes (light grey) or 100 minutes (dark grey). Each bar represents n=3 samples. The initial inoculate concentration for environmental and clinical isolates were 2.8 x 10<sup>6</sup> cfu/mL and 3.4 x 10<sup>6</sup> cfu/mL, respectively. ....132**

**Appendix B Figure 8: Planktonic vs. aggregate *M. abscessus* ratios (ranges in parentheses) for clinical (0–163) and B. environmental (0–41) isolates for the initial inoculates (each tile is one technical replicate, for a total of n = 9 per isolate × time). Green cells represent a smaller ratio, signifying a larger proportion of aggregated *M. abscessus* cells, while yellow cells represent a higher ratio, signifying a larger proportion of planktonic *M. abscessus* cells. The dark yellow cells represent the 50th percentile. The ratios were obtained by dividing the planktonic OD600 measurements by the aggregate OD600 measurements.....133**

**Appendix B Procedure 1: CDC Biofilm Reactor Method Development .....140**

**Appendix C Figure 1: Absolute gene copy concentrations in shower water and associated aerosols by showerhead flow rate. A. *L. pneumophila* in shower aerosols, B. NTM in shower aerosols, C. total bacteria in shower aerosols, D. *L. pneumophila* in shower water, E. NTM in shower water, and F. total bacteria in shower water observed for all three showerheads. Each showerhead type shows all the data collected from all replicates for that specific showerhead. ....142**

**Appendix C Figure 2: Diversity of water and aerosol samples. A. Non-metric multidimensional scaling (NMDS) plots of bacterial OTUs represented by the Bray–**

Curtis dissimilarity index. Comparison of B. richness and C. diversity of bacterial OTUs in air and water samples estimated by the Chao1 estimator and Shannon index, respectively Significant differences are marked with a colored bracket and star corresponding to the showerhead type and p-value (\* =  $p \leq 0.05$ , \*\* =  $p \leq 0.01$ , \*\*\* =  $p \leq 0.001$ ).....143

Appendix C Figure 3: Alpha diversity of aerosol samples. The effects of flow rate on A. Chao1 estimator of richness and B. Shannon index diversity. The effects of showerhead age on C. Chao1 estimator of richness and C. Shannon index diversity. Significance and the statistical analysis used are contained in the upper right hand corner of each plot. ....144

Appendix C Figure 4: Alpha diversity of water samples. The effects of flow rate on A. Chao1 estimator of richness and B. Shannon index diversity. The effects of showerhead age on C. Chao1 estimator of richness and C. Shannon index diversity. Significance and the statistical analysis used are contained in the upper right hand corner of each plot. ....145

Appendix C Figure 5: Significant functional traits in water samples by flow rate obtained from PICRUST analysis. ....146

Appendix C Figure 6: Absolute gene copy concentrations in shower water and associated aerosols over time. A. *L. pneumophila* in shower water, B. NTM in shower water, C. total bacteria in shower water, D. *L. pneumophila* in shower aerosols, E. NTM in shower aerosols, and F. total bacteria in shower aerosols observed for all three

**showerheads. Each showerhead type shows all the data collected from all replicates  
for that specific showerhead.....147**

## Acknowledgements

I would like to firstly acknowledge those that were influential in the outcomes of this body of work: I am grateful for the opportunities provided by my committee chair and primary investigator on my research projects during my Ph.D., Dr. Sarah-Jane Haig, as well as my committee members Dr. Leanne Gilbertson, Dr. Janet Stout, Dr. Vikas Khanna, Dr. Meng Wang, and Dr. Will DePas. In this case, more cooks in the kitchen greatly improved the final dish (that dish being my thesis); thank you all for your feedback, suggestions, and encouragement during this process. I would also like to acknowledge those just as instrumental for my success employed at the University of Pittsburgh, namely Dan and the rest of the operations and maintenance staff, Ms. Cheryl Morand, Ms. Alysia Grogan, and the rest of the front office staff, and Dr. Dave Malehorn and Charles “Scooter” Hager. I would not have been able to conduct the research contained in this dissertation without their ample support. I would also like to thank the University of Pittsburgh as well as the Swanson School of Engineering’s Civil and Environmental Engineering department for their facilities and teaching/research assistantship opportunities that made pursuing this degree possible. In the same vein, I would like to thank the University of Pittsburgh’s Central Research Development Fund and the National Science Foundation’s CBET- 1935378 for their financial support.

I would not have gotten to this point in this journey without my colleague, lab sibling, and dear friend Isaiah Spencer-Williams, who has seen the Good, the Bad, and the Ugly of the last five years of my life. Isaiah, thank you for being my other brain cell in and out of the lab: there is no one I would rather share this experience with. I also want to acknowledge the other members of

the lab group, Mima Ohwobete, Mariia Nikitina, and Cheolwoon Woo, who have provided unquantifiable amounts of technical and emotional support during their respective tenures in the group, as well as all who went through the ‘revolving door’ of the Haig lab with a specific emphasis on Evan Trump. Evan, I am so proud of all you accomplished while working with me and after: thank you for letting me grow as a mentor and as a friend.

I would also like to thank my previous scholarly mentors for investing their time, energy, and resources into me at the beginning of my academic journey. Specifically, I would like to highlight Dr. Paul Edmiston as the most influential mentor of my life. Dr. E.: thank you from the bottom of my heart for taking a chance on an over-eager 18 year-old that sat in the front of your 8 am introduction to chemistry class. Not only did you give me the skills I needed to be successful in the lab, you fostered my curiosity of the world around me and taught me how to answer the questions that meant something to me (both research and otherwise). It has been one of life’s greatest joys to keep in touch through my time at Pitt, and I will never be able to thank you enough for your support over the past 9 years.

This thesis is dedicated to my village. For those that were here when I chose to come home to Pittsburgh, those that needed to leave my life before this moment, and those that hopped on this crazy train partway through. Although this has been the greatest period of challenge in my life, I have also never experienced a time where there has been this much love and joy. Specifically, I would like to acknowledge my biological family (my mother Lisa and late father Michael Pitell and my brother Matthew Pitell) and my chosen family, who are legion. Finally, I express my deepest gratitude to those during this journey that chose to show me kindness and compassion when I needed it most.

## List Of Abbreviations

ABS – Acrylonitrile Butadiene Styrene

ANOVA – Analysis of Variance

ANSI – American National Standards Institute

ASTM – American Society for Testing and Materials

CCA – Canonical Correspondence Analysis

CDC – Center for Disease Control

CSI– Copper Silver Ionization

CSTR – Continuously Stirred Tank Reactor

ddPCR – Droplet Digital Polymerase Chain Reaction

DNA –Deoxyribonucleic Acid

DOC – Dissolved Organic Carbon

DW- Drinking Water

DWPI – Drinking Water-Associated Pathogens that Infect the Immunocompromised

EDS – Energy Dispersive X-Ray Spectroscopy

EPA – Environmental Protection Agency

ICP-MS – Inductively Coupled Plasma Mass Spectrometry

ISO – International Organization for Standardization

KEGG – Kyoto Encyclopedia of Genes and Genomes

NMDS – Non-metric Multidimensional Scaling

NSF – National Sanitation Foundation

NTM – Nontuberculous Mycobacteria

OCT – Optical Coherence Tomography

OTUs – Operational Taxonomic Units

RDA – Redundancy Analysis

RNA – Ribonucleic Acid

RT-ddPCR – Reverse Transcriptase-Droplet Digital Polymerase Chain Reaction

SEM – Scanning Electron Microscopy

TOC – Total Organic Carbon

UV – Ultraviolet radiation

VBNC-Viable but not Culturable

## 1.0 Introduction

### 1.1 DWPIs As An Emerging Public Health Concern

Respiratory infections from drinking water-associated pathogens that can cause infections in the immunocompromised (DWPIs)<sup>1</sup> cost the US economy \$2.39 billion annually<sup>2</sup>. Today, the incidence of waterborne disease outbreaks in the United States attributed to DWPIs; which are not regulated by the US EPA, (e.g., *Legionella pneumophila*, nontuberculous mycobacteria (NTM), *Pseudomonas aeruginosa* amongst others) appear to be increasing<sup>3-6</sup>. For example, the incidences of legionellosis and non-tuberculous mycobacterial pulmonary disease increased 225%<sup>7</sup> and 300%<sup>8</sup> from 2000- 2017, respectively, and was responsible for a majority of waterborne outbreaks between 2015-2020<sup>9</sup>. This far exceeds disease incidence caused by regulated fecal-borne pathogens<sup>2,4</sup>. These respiratory infections clinically present as an atypical pneumonia that is often chronic and difficult to treat<sup>5,10-13</sup>, and tend to infect the very young, the very old, and those with immunosuppressing conditions (e.g., those with cancer or certain genetic diseases) or underlying lung issues<sup>1,14,15</sup>. Furthermore, recent evidence has suggested that even otherwise healthy people can become infected with NTM after repeated exposure, so developing mitigation strategies for DWPI exposure are essential to protecting public health<sup>16</sup>. While present naturally in the environment (surface water, soil)<sup>17</sup>, DWPIs are typically not quantified in finished drinking water (DW) leaving the treatment plant, but can multiply within the distribution network and in building water systems, often within biofilms<sup>18</sup>. Environmental conditions in building plumbing favor the formation of biofilms, allowing DWPIs to persist and grow<sup>6,19-21</sup> likely explaining their higher

abundance in building plumbing<sup>22</sup> and recent connection to several clinical infections<sup>16,23</sup>. DWPIs are also often difficult to accurately quantify using culturing (a common enumeration method in drinking water) due to these microorganisms' ability to enter a viable, but not culturable (VBNC) state<sup>24-26</sup> where they are still infectious, causing false negative samples during culturing alone. Although human exposure to DWPIs occurs through a variety of pathways, inhalation of DW aerosols produced during showering or by hot tubs and therapy pools have been linked to pulmonary infections<sup>1,19,24,27</sup>. Current data in DWPI disease pathology suggests that upon inhalation, the microorganisms travel to the alveoli and evade macrophage inactivation, allowing these microorganisms to cause a disease state<sup>28-30</sup>. In order for this to happen, DWPIs must be contained in a bioaerosol that is between 2  $\mu\text{m}$  and 5  $\mu\text{m}$  in diameter: if the particle is bigger, then it will settle before traveling into the lower respiratory tract<sup>31</sup> and particles smaller than 2  $\mu\text{m}$  cannot contain a single microorganism<sup>32</sup> (Figure 1).

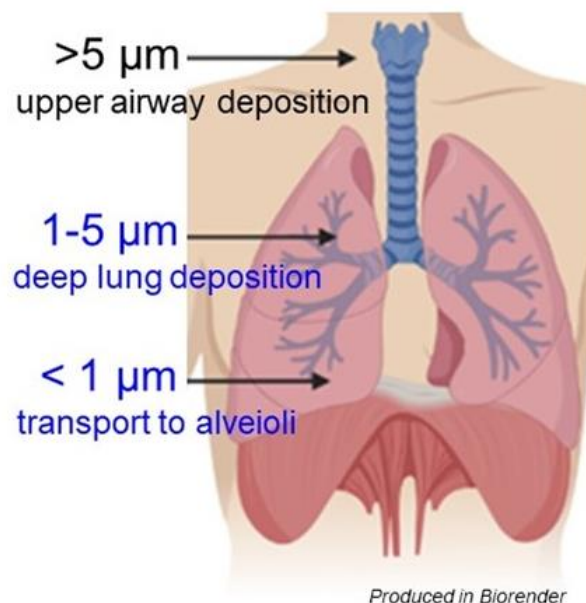


**Figure 1: Diagram illustrating the particle size which can be deposited at different locations in the respiratory system**

Despite these observations, majority of the DWPI research in the DW transect focuses on biogeographical surveys to identify locations where these organisms can be found and linkages with physiochemical parameters, but critical steps in the DWPI transmission pathway— aerosolization and persistence in indoor air remains poorly understood; specifically, little is known about how consumer choices (e.g., showerhead type and water use behaviors) influences indoor air quality.

## **1.2 Shower Systems As A Potential Point Of Exposure To DWPIs**

Although any interaction with unsterilized DW could result in a potential DWPI infection, showering has been identified to be a meaningful place of exposure for non-point source disease incidence<sup>1,16,33,34</sup>. The average American household uses on average 1100 L of DW every day, and 20% of this amount can be attributed to showering alone<sup>35</sup>. The volume of water used during showering coupled with how this water accounts for over half of the water usage that involves direct consumer- DW contact<sup>35</sup> can translate to a larger potential risk of DWPI exposure. Additionally, showering is a frequent behavior for most people with an average duration of 8 minutes per day for the American adult<sup>36</sup>, so the consistency and duration of DW contact increases risk profile. DWPI aerosolization is the hypothetical route of exposure due to the microorganisms needing to enter the lower respiratory tract, and showers are an ideal environment for aerosol generation and dispersal. The shower environment during operation and for a while after retains a high relative humidity level without proper ventilation, and introducing hot water into the shower system is more likely to generate aerosols than cold<sup>27</sup>, with showers emitting up to 65 million aerosols during the course of an average use<sup>37,38</sup>. A large amount of these aerosols are created

when the bulk water exits the showerhead, which is often placed within the average adult's respirable zone (close to the nose and mouth). Perhaps the strongest evidence to suggest that showers are a meaningful place of exposure for DWPIs is that multiple studies have identified DWPIs in shower water<sup>34,39,40</sup>, shower water-associated aerosols<sup>27,33,41</sup>, and within the biofilms of the shower hoses<sup>6,42-44</sup>, with several studies isolating environmental DWPIs that match clinical pulmonary isolates<sup>16,34,40</sup>.

Biofilms have been postulated to influence DWPIs in the water due to the dynamic attachment and detachment of microorganisms<sup>45</sup> and the observed DWPI membership in shower biofilms<sup>6,42,43,46</sup>. Despite limited understanding of DW biofilm formation kinetics, evidence suggests a time-dependent colonization process in operational settings. Previous research has identified distinct phases of community composition that potentially impact the presence and abundance of DWPIs, as evidenced in studies conducted on pristine plumbing rigs before and after 30 days of continuous operation<sup>47</sup>. However, to the best of the author's knowledge, no studies have yet reported long-term biofilm succession in DW plumbing.

The current evidence clearly shows showers to be a source of DWPI exposure, however managing DWPIs within the shower system is challenging because DWPI proliferation typically occurs in building plumbing<sup>48</sup> as these microorganisms cannot be mitigated in the distribution system or at the DW treatment plant. Therefore to effectively manage DWPIs building-wide mitigation strategies (e.g., copper-silver ionization (CSI), reverse osmosis or other filtration systems at the building water inlet, thermal or chemical shocking, etc.) can be used. However these solutions are expensive, not feasible to employ at a residential scale due to the additional monitoring and skilled operation needed to run these systems, and ultimately offer questionable

efficacy in reducing DWPI loads in the long term<sup>49–52</sup>. Instead, addressing DWPI loads at the point of use (POU) where the water exits the pipe for use is becoming increasingly popular for consumers and companies alike<sup>53–55</sup>. POU devices such as showerheads are cheaper than more systemic interventions, and they allow the individual user to decide what specific aspects of their water they want to impact (e.g., additional disinfection, removal of unregulated contaminants, water conservation). Although this seems like an attractive option for consumers, there are few legal guidelines that ensure the marketing claims of these showerheads are accurate in real-world use conditions. For example, antimicrobial showerheads can be marketed as such without any kind of third-party testing, and the testing that is done for some products follow ISO 22196:2011<sup>56</sup> to test the antimicrobial material alone, which does not simulate water use and focuses on quantifying microbial reduction of non-DWPI organisms (e.g., *Escherichia coli*) using culture-based methods alone. Antimicrobial showerheads in particular are a growing commerce sector globally<sup>55</sup>, and have a variety of different marketed technologies that claim to reduce microorganisms in their resulting shower water such as filter blocks or various silver-containing materials, but even if these technologies were effective during showering, no work has been conducted studying the effects these fixtures have on aerosols, the likely route of exposure. Because of the lack of reliable and true-to-use testing of these showerheads, there is little unbiased evidence available for consumers to aid them in choosing a showerhead that reduces their potential DWPI exposure.

### **1.3 Responding To Novel Water Utilization Strategies And Its Effects On DWPIs**

While respiratory infections caused by DWPIs are expected to increase in the upcoming years, DW quality and use patterns are also likely to change in response to external stressors.

Potable water scarcity will continue to become one of the greatest global engineering challenges as the population continues to increase<sup>57</sup> and climate change alters historic meteorological and hydrogeological trends<sup>58</sup>. Many regions are already experiencing the need to conserve DW at the consumer level to reduce the total water demand of a municipality, and showers are an intervention point to reduce total water usage<sup>59,60</sup>. The maximum flow rate for showerheads in the US is 9.5 L/min, however the US EPA's voluntary conservation WaterSense program certifies showerheads with flow rates less than 7.6 L/min<sup>59,60</sup>, with certain places such as Hawaii and California mandating even lower flow rates to reduce water use<sup>60</sup>. In order to get the same experience with less water, the pressure and flow path within the showerhead is altered<sup>59,60</sup>, leading to different transport dynamics within the shower system and thus may impact factors of the produced shower water (water quality) and shower water-associated aerosols (size and abundance of particles) which in turn may impact the shower microbiome. In particular the impacts of adopting these low-flow fixtures from a DWPI exposure standpoint have not been explored, so understanding how showerhead flow rate impacts bioaerosolization can help inform overall cost-benefit analysis of using these types of fixtures.

In addition to saving water at the POU in the shower stall, studying the effects of other changes in DW use patterns (period of no use / stagnation) from a microbial perspective is essential to improving choices made in times of crisis. Global shutdowns caused by the Covid-19 pandemic caused extreme changes in water use patterns: because of the stay-at-home orders, large buildings such as offices, schools, hotels, and dormitories were left vacant for extended periods of time with very limited water management plans in place. While it is known that extended water age increases microorganisms in DW<sup>48</sup>, the effects of prolonged stagnation in places of consistent water use had not been explored. Without this knowledge, building managers responsible for maintaining water

quality in these buildings followed arbitrary flushing guidelines in hopes of reducing the amount of DWPIs and other hallmarks of poor water quality to acceptable levels. Improving resiliency in water management responses will become increasingly more important as the landscape of DW management continues to rapidly change.

#### **1.4 Thesis Objectives And Hypotheses**

Immediate attention is required to gather unbiased information on how consumer choices in showers (including showerhead material, flow rate, and usage patterns) affect exposure to DWPIs. Furthermore, a more thorough understanding of how these choices impact the shower microbiome across water, aerosols, and biofilms is essential. Investigating parameters such as showerhead type (treatment strategy) and water age (how long the showerhead has been operational for) and their influence on relevant microorganisms is pivotal for informed global and individual decision-making regarding mitigation strategies. Moreover, this knowledge will contribute to the development of exposure and risk assessment models, streamlining decision-making processes in the future.

The following specific aims were pursued to characterize and assess how certain consumer level shower system specific decisions (e.g., showerhead type, flow rate and DW stagnation duration) impact DWPI presence and abundance and the greater microbiome in shower water, shower water-associated aerosols, and shower-related biofilms:

1. Assess the impact of different types of antimicrobial showerheads (chemically mediated and physiochemical) on the prevalence and abundance of DWPIs in shower water and shower

water-associated aerosols. It is hypothesized that antimicrobial showerheads will have the greatest reduction on microbial loads in both phases compared to non-antimicrobial showerheads.

2. Evaluate the efficacy of antimicrobial showerheads utilizing silver as their antimicrobial agent. It is hypothesized that showerheads containing silver regardless of form will produce shower water and biofilms with lower overall microbial and DWPI density than non-antimicrobial showerheads.
3. Examine the impacts of shower use patterns (e.g., extended stagnation and the adoption of low-flow showerheads) on DWPIs and the greater microbiome. Three hypotheses are proposed: 1) reducing the showerhead flow rate is expected to elevate the production of respirable aerosols and the proportion of DWPIs transitioning from shower water to shower water-associated aerosols, while also exerting a significant impact on the microbiome of both shower water 2) and associated aerosols. Thirdly, prolonged stagnation periods are anticipated to amplify DWPI densities in the shower water, whereas flushing regimes are predicted to diminish these densities.

Overall, this body of work characterizes the microbial landscape of the showering environment and aims to assess how POU intervention strategies (e.g., antimicrobial showerheads, water-conserving showerheads, and flushing regimes) impact DWPIs and the greater microbiome. By isolating these individual aspects in a full-scale laboratory built to accurately simulate a residential shower, the findings contained in this dissertation can be directly applied to real-world bathrooms. Understanding the effects of these specific interventions will allow building managers and DW users alike to make informed choices on how to reduce their total possible microbial exposures

from showering, and help guide them in responding to the rapidly evolving challenges of water safety in our ever-changing world.

## **2.0 Specific Aim 1.0: The Impact Of Antimicrobial Showerheads On The Prevalence And Abundance Of DWPIs In Shower Water And Shower Water-Associated Aerosols**

Specific Aim 1.0 was funded by The University of Pittsburgh's Central Research Development Fund and played no role in data collection or interpretation. This work was conducted with the support of Dr. Daniel Bain when running ICP-MS analysis, Dr. David Malehorn when running the TOC analyzer, and Isaiah Spencer-Williams for assistance with sequencing analysis. The results of Specific Aim 1.0 have been published in one journal publication and two conference proceedings:

### **Journal Article**

**Pitell, S.**, Haig, S.-J. Assessing the Impact of Anti-Microbial Showerheads on the Prevalence and Abundance of Opportunistic Pathogens in Shower Water and Shower Water-Associated Aerosols. *Frontiers in Microbiomes* **2023**, 2. <https://doi.org/10.3389/frmbi.2023.1292571>

### **Conference Proceedings**

1. **Pitell, S.**, Haig, S.-J. Exploring point-of-use risk management strategies for bioaerosols: effectiveness on antimicrobial showerheads on reducing opportunistic pathogen exposure. *Poster*. Gordon Research Conference Microbiology of the Built Environment (Waterville Valley, NH) 6/21/22
2. **Pitell, S.**, Haig, S.-J. A breath of fresh air: assessing anti-microbial showerheads' ability to reduce the aerosolization of opportunistic pathogens. *Presentation*. Association of

## 2.1 Introduction

As discussed in [Chapter 1](#), respiratory infections from drinking water-associated pathogens that can cause infections in the immunocompromised (DWPIs)<sup>1</sup> such as *Legionella pneumophila*, nontuberculous mycobacteria (NTM), and *Pseudomonas aeruginosa* are a major public health and economic issue in the United States<sup>2</sup>, with the shower identified as a possible intervention point for DWPI exposure. Previous work on DWPIs in showers have mainly focused on detection in the shower water<sup>34,39,40</sup>, linking abundances to physiochemical parameters<sup>22,24,48</sup>, or connecting environmental isolates to clinical strains<sup>16,40</sup>. While informative, there are crucial gaps in the current body of knowledge including in-depth characterization of the route of exposure (i.e., inhalation of produced aerosols) as well as what can be done to decrease DWPI infection risk. Additionally, experimental design shortcomings of these studies, such as the collection of grab samples that: (a) do not account for differences in the microbial load over the entire course of a shower, and (b) either assess one shower system or draw parallels across numerous systems without contextualization of different use patterns, materials, or other factors, lead to inaccurate DWPI risk assessment. Likewise, how plumbing material and shower usage / age (time since showerhead has been installed) impacts microbial load and community composition is unknown. As virgin plumbing is used, biofilms stemming from the DW microbiota are formed<sup>6,42,43,46,47</sup>; these biofilms are thought to influence the resulting microbial composition of both the shower water and aerosols, however these microbial adhesion and detachment events are poorly

characterized<sup>45</sup>. Some previous work conducted to evaluate initial colonization in virgin plumbing materials has found that the microbial composition of DW biofilms change over time, with marked differences occurring between the day of installation (day 0), before 30 days of use (early biofilm phase), and after 30 days of use (mature biofilm phase)<sup>47</sup>, which further highlights the need for longitudinal testing of the same outlet.

Given that the average adult showers for 8 minutes every day<sup>36</sup> and that building plumbing has consistently detectable DWPIs<sup>22,24</sup>, the most promising DWPI mitigation location would be at the final point of use (e.g., showerheads). Currently, to help reduce the risk posed by DWPIs in household and healthcare shower water, individuals and facility managers use a variety of approaches spanning from large-scale engineered solutions (periodic thermal<sup>52,61</sup> or chlorine shocking of building plumbing<sup>62</sup>) to more economic and tunable approaches such as the use of antimicrobial showerheads. The designs of antimicrobial showerheads fall into one of two categories: chemically mediated antimicrobial activity (e.g., use of silver and or copper) or physiochemical antimicrobial activity (e.g., filtration through a media bed or block<sup>63</sup>). Regardless of the type of antimicrobial showerhead, all claim to reduce or eliminate microorganisms from shower water. Such claims are substantiated by culture-dependent assessment approaches used by regulators to detect pathogens, even though it is widely known that these approaches can provide false-negative results if DWPIs exist in the VBNC<sup>64</sup> state, or if they are present below the method detection limit. Furthermore, manufacturers follow ISO 22196:2011<sup>56</sup> to test their antimicrobial material, which does not simulate the shower environment and focusses on quantifying microbial reduction of non DWPI organisms (e.g., *Escherichia coli*) using culture-based methods, and completely overlooks the exposure route – aerosols<sup>65–67</sup>.

Previous studies have assessed DWPI concentration in aerosols produced from showers, however, these studies although pioneering have many drawbacks; namely the microbial assessment in all aerosol size fractions <sup>40,68</sup> (including fractions which cannot be respired) <sup>33</sup>, unrealistic shower operation and sampling approach (i.e. collection for >1h) <sup>33</sup>, the use of hard impaction for collection <sup>40,68</sup>, which reduces recovery and can distort aerosol size, the lack of replication and temporal assessment. Given these shortcomings there is an immediate need to quantitatively assess the efficacy of antimicrobial showerheads on both their produced water and respirable shower water-associated aerosols (2  $\mu\text{m}$  – 5  $\mu\text{m}$ ) under realistic use conditions.

This study compared water quality, DWPI abundance and microbial community composition in shower water and respirable shower water-associated aerosols between antimicrobial and conventionally used acrylonitrile butadiene styrene (ABS) plastic showerheads using a custom full-scale shower laboratory to simulate real world showering conditions. Two antimicrobial showerheads were used in this study: one marketed to contain silver impregnated into the plastic, and the other contained a proprietary multi-stage filter. Shower water and their associated aerosols were collected from triplicates of each showerhead biweekly over the course of 14 weeks (84 days). All samples were analyzed for DWPI abundance using droplet digital PCR, microbial community dynamics using 16S rRNA amplicon sequencing, and a variety of physiochemical parameters.

## 2.2 Research Approach

### 2.2.1 INHALE Shower Laboratory Set Up And Tested Showerheads

The INHALE shower laboratory at the University of Pittsburgh, PA, consists of three full-scale shower stalls (Sterling Ensemble 34 in. x 42 in. x 77 in) connected to their own separate 50-gallon electric water heater (Bradford White Corporation, Model Number: RE350S6 – 1NCWW), using municipal water supplied by the City of Pittsburgh after transit through building plumbing. The water pressure feeding into the laboratory is 60 psi, with a 56 psi pressure measured at the outlet. In each stall, there are three showerheads that are controlled with independent valves, allowing for triplicate studies to be run (nine showerheads overall) (Figure 2). The INHALE laboratory was constructed with virgin copper piping for the plumbing, and contains a 1¾ thermomixing valve on the outlet of each water heater that is set so that the water coming out of the showerheads is 40 °C, the average shower temperature of Americans<sup>36</sup>. Each showerhead tested had an output flow of 2.5 gpm. A ¾” hole was drilled in each Plexiglas shower stall door 154 cm from the shower floor in order to collect bioaerosols present in the average American adult’s respirable zone<sup>69</sup>. Each showerhead was flushed daily for 8 minutes to simulate an average American’s shower<sup>36</sup> and to replicate real-world shower impacts on the biofilms within the pipes.

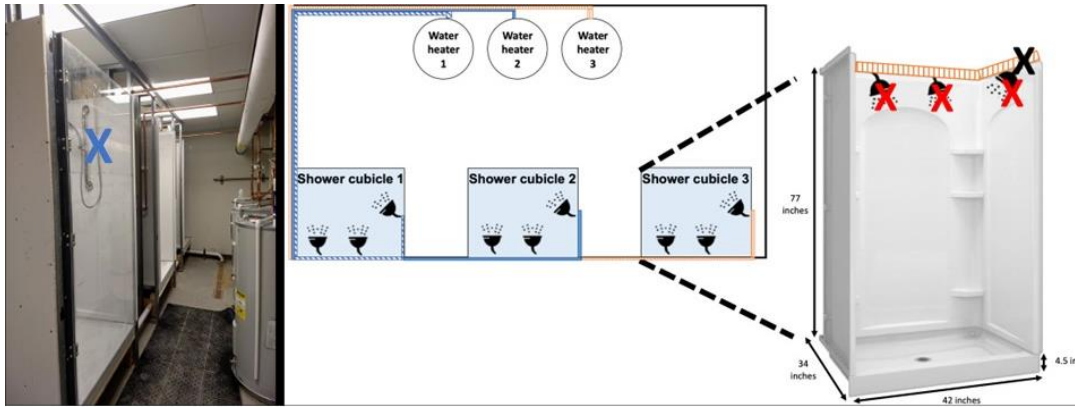


**Figure 2: Schematic of full-scale shower laboratory set-up. The blue X indicates the aerosol sampling port in the Plexiglass door, the black X indicates where the copper pipe from the hot water heater connects to the shower stall, and the red X's correspond to each showerhead position.**

Three different types of showerheads were installed in triplicate in the INHALE shower laboratory: a commonly used and widely available showerhead made from acrylonitrile butadiene styrene plastic (ABS) and two marketed antimicrobial showerheads (one containing silver nanoparticle technology embedded in the plastic polymer; referred to from here forward as silver embedded, and the other showerhead was an ABS plastic showerhead that contained an in-line proprietary filter containing zinc, calcium, and copper; referred to from here forward as filter-based). The silver-embedded showerhead was marketed to be bacteriostatic and to prevent the formation of biofilm inside the showerhead and hose. The filter-based showerhead is marketed to remove bacteria from the resulting shower water in addition to removing iron and chlorine. All tested showerheads were obtained directly from their respective manufacturers. Prior to the installation of the showerheads to be assessed, ABS heads were installed on each of the three outlets in each stall and flushed daily for 8-minutes for 1 month to eliminate water quality artifacts due to stagnation.

### **2.2.2 Shower Water And Shower Water Associated Bioaerosol Collection**

Water and respirable aerosols (<10 µm in diameter) samples were collected in tandem biweekly over the course of 3 months (yielding 7 sampling events in total) from each showerhead. This time frame was chosen following the manufacturer's guidelines to replace the silver-embedded showerhead after 60 days of use: the sampling period of 84 days allowed for studying its performance during its marketed effective treatment period, and past its recommended timeframe. The aerosol sampler was turned on at the same time as the shower, and an 8-minute composite water samples were taken at the same time as aerosol collection. The shower and aerosol sampler continued to run for a total of 20 minutes after the water was collected, when the shower and aerosol sampler was turned off. To prevent aerosol contamination from one showerhead to the others and to allow aerosol abundance to return to baseline, one showerhead at a time was sampled with a gap of at least 1 h between heads.

Briefly, water sampling entailed collecting a 1.5 L composite sample taken over 8 minutes after the shower water reached temperature for each head into a sterile Nalgene bottle. Allowing the water to reach showering temperature before sampling was to simulate what a person showering would come into contact with. 1 L was immediately filtered through a 0.2 µm polycarbonate filter (Millipore, Cork, Ireland) and the filter was stored at -20 °C prior to extraction, while the remaining water was used for water chemistry analysis. Deionized water was processed identically to the shower water samples as a negative control.

Bioaerosols were sampled using the 110A Spot Sampler by Aerosol Devices Inc. (Aerosol Devices, Fort Collins, CO), with the addition of a SCC1.829 cyclone (Mesa Labs, Lakewood, CO) that allowed for collection of respirable aerosols (<10  $\mu\text{m}$  in diameter). Following the approach of Nieto-Caballero *et al.*, 2019 bioaerosols were collected into 0.6 mL of RNAlater (ThermoFisher, Waltham, MA) using antistatic tubing for 20 minutes to ensure sufficient biomass was collected<sup>70</sup>. Samples were stored at -20 °C prior to extraction. Background samples were taken prior to each sampling event where aerosols were collected in the INHALE shower laboratory for 20 minutes with no showers running, and aerosol control samples were taken at sampling events 1, 4, and 7 by installing a HEPA filter in-line with the sample tubing.

### **2.2.3 Water Quality Measurements**

Twenty water quality parameters (Appendix A Table 1) were measured using previously described methods<sup>22</sup>. Ammonia<sup>71</sup>, orthophosphate<sup>72</sup>, free chlorine, and total chlorine<sup>73</sup> concentrations were determined at the time of collection using a portable DR900 spectrophotometer (Hach, Loveland, CO, USA). Temperature and pH were monitored onsite using a portable pH and temperature meter (HANNA Instruments, Woonsocket, RI). Total and dissolved organic carbon were measured using the Shimadzu TOC-L analyzer using the subtractive method (Shimadzu, Kyoto, Japan). Total and dissolved iron, lead, copper, silver, calcium and magnesium were determined using inductively coupled plasma mass spectrometry (PerkinElmer NexION 300 ICP-MS, PerkinElmer, Waltham, MA). Prior to analysis, all dissolved organic carbon and dissolved metal samples were prepared by passing water through a 0.45  $\mu\text{m}$  nylon syringe filter (ThermoFisher, Waltham, MA) primed with 5 mL of sample. Deionized water was processed in

the same way to samples as controls. All analyses, except pH, and temperature, were performed in triplicate and the coefficient of variation was at most 13%.

#### **2.2.4 DWPI Quantification**

DNA from collected water and aerosol samples were extracted using the Fast Spin DNA Extraction kit (MPBio, Irvine, CA), where the extracted DNA was eluted into 100  $\mu\text{L}$  of DES<sup>48</sup> and stored at  $-20\text{ }^{\circ}\text{C}$  until further analysis. Extraction controls were performed for each extraction kit where nothing was added to the extraction kit reagents, and filter controls were processed by extracting filters that had no material passed through it for each filter manufacturing batch. Absolute densities of total bacteria, *L. pneumophila*, *P. aeruginosa*, and NTM were determined using droplet digital polymerase chain reaction (ddPCR) (QX200, Bio-Rad, Hercules, CA) targeting the 16S rRNA gene and taxon specific genes, respectively (Appendix A Table 2). All samples were analyzed in duplicate along with negative controls (field blanks, extraction blanks, and ddPCR blanks of molecular grade water as the template) and gblock positive controls of each amplicon (Integrated DNA Technologies, Inc., Coralville, IA). Each 22  $\mu\text{L}$  ddPCR reaction contained 11  $\mu\text{L}$  of EvaGREEN supermix (Bio-Rad, Hercules, CA), 0.625 mg/mL bovine serum albumin (Invitrogen Corporation, Waltham, MA, USA), 0.2  $\mu\text{M}$  primers (Integrated DNA Technologies, Inc., Coralville, IA) (Appendix A Table 2), 7.57  $\mu\text{L}$  of water, and 2  $\mu\text{L}$  of the extracted template DNA at an assay specific dilution. Droplets were generated to a 20- $\mu\text{L}$  reaction volume using the automated droplet generation oil for EvaGREEN (Bio-Rad, Hercules, CA), and the plate was heat sealed. PCR was performed using a C1000 Touch thermal cycler (Bio-Rad Laboratories) within 15 min of droplet generation using the reaction conditions presented in Table A2 Within 1 h of PCR completion plates were ran on the droplet reader for quantification.

Thresholds were set for each ddPCR assay (Appendix A Procedure 1) and the absolute density of the target taxa were determined using Quantasoft v1.0.596 following the method described by Lievens *et al.*<sup>74</sup>. Paired water and aerosol samples were compared after DWPI quantification to assess DWPI partitioning by calculating the ratio of DWPIs in the aerosol phase and water phase.

### **2.2.5 16S rRNA Gene Amplicon Sequencing**

16S rRNA gene amplicon library preparation and sequencing were performed on water and aerosol samples at Argonne National Laboratory following the Illumina Earth Microbiome Protocol<sup>75</sup>. Samples were sequenced on an Illumina HiSeq2500 with a total of 1,633,966 raw reads generated. Microbiome analysis was performed using QIIME2 (version 2020.2) with quality filtering performed using the method described in Bolyen *et al.*<sup>76</sup>. Reads were assigned to operational taxonomic units (OTUs) using a 97% cutoff using the closed reference OTU-picking protocol in QIIME2 (version 2020.2) using the Silva (version 132.5) reference database. All data were processed using the University of Pittsburgh's Center for Research Computing cluster servers.

### **2.2.6 Statistical Analysis**

All data was visualized and analyzed using R statistical software (Version 4.0.5). Significant differences ( $p$ -values  $<0.05$ ) of parameters by head type, sample type, and over time were determined using analysis of variance (ANOVA) tests, and paired Mann Whitney U-tests. While alternative analyses, such as the sign test, could have been employed to assess statistical significance, the decision was made to utilize standard non-parametric tests due to the limited

understanding of temporal changes and their potential influence on biofilm composition. Power calculations were conducted in order to ensure that these statistical tests were valid. Linear mixed-effect models were developed to determine which physiochemical parameters impacted absolute abundances of DWPIs utilizing a stepwise forward and reverse approach to find the model with the lowest Akaike Information Criterion value<sup>77</sup>. Prior to model generation, all DWPIs abundances were transformed to ensure normal distributions, all physiochemical data were scaled, and all collinear variables were assessed and removed using a variance inflation factor (VIF) values <10. Power calculations revealed no more than five explanatory variables should be included in the models. Taxonomic data generated from sequencing were Hellinger transformed prior to analysis to minimize the impact of low abundances of many taxa<sup>78</sup>. Pairwise dissimilarities between samples were calculated based on the Bray-Curtis dissimilarity index, and examined for temporal and spatial patterns in the bacterial community structure by Non-metric Multidimensional Scaling as implemented in the Vegan package in R<sup>79</sup>. Significant differences in the microbial community compositions (Shannon diversity index, Chao's richness, and Pielou's evenness) based on showerhead age and sample type were determined by ANOVA. Relationships between environmental parameters and patterns in microbial community composition were examined by redundancy analysis (RDA) with significance tested by ANOVA after reducing the overall suite of environmental variables with variation inflation factor analysis (VIF)<sup>22</sup>.

## **2.3 Results And Discussion**

### **2.3.1 Showerhead Type Did Not Impact Shower Water Chemistry**

Overall, there was no significant difference in effluent showerhead water chemistry between any of the head types (ABS, silver-embedded, and filter-based), despite different materials used and marketing claims (Appendix A Table 3). In particular, it was surprising to observe no significant differences in the concentration of chemicals expected to leach from the showerheads (i.e., organic carbon from the ABS showerhead, organic carbon and silver from the silver-embedded showerhead, or organic carbon, calcium, and copper from the filter-based showerhead) during any point of the 84-day long sampling period. In terms of additional treatment besides the antimicrobial properties of the showerheads, the filter-based showerhead claimed to remove 95% of total chlorine. However, there was no significant difference in chlorine concentration between all head types, although the filter-based heads had the lowest absolute concentration of free and total chlorine when the average values were compared (Appendix A Table 3). It is challenging to determine if the filter-based head is effective at removing chlorine because it was tested using hot water at the point of use, where most of the chlorine residual has dissipated or volatilized by the time of testing regardless of head type.

### **2.3.2 DWPI Presence And Abundance Was Unaffected By Showerhead Type**

From a consumer perception perspective, the most likely reason for the use of antimicrobial showerheads is their efficacy at removing microorganisms from water. Both the silver-embedded and filter-based antimicrobial showerheads claim that they contain materials that are bactericidal

and bacteriostatic, yet there was no statistically significant difference in the absolute abundance of total bacteria or any DWPI between the antimicrobial showerheads and the ABS showerheads in both water exiting the showerhead and associated bioaerosols (Figure 3). When looking at DWPI abundances over time, there were no significant trends in the aerosol data due to the low biomass recovered for the DWPI targets (Appendix A Figure 3). In the water samples, there were no significant differences over time between showerhead type, but there were marked differences in the behavior of each DWPI. *L. pneumophila* and *P. aeruginosa* were detected transiently in the water samples in low concentrations (88 gene copies/L and  $3.9 \times 10^4$  gene copies/L, respectively), whereas NTM was consistently abundant and increased in concentration after day 42 of continuous use (Appendix A Figure 2).

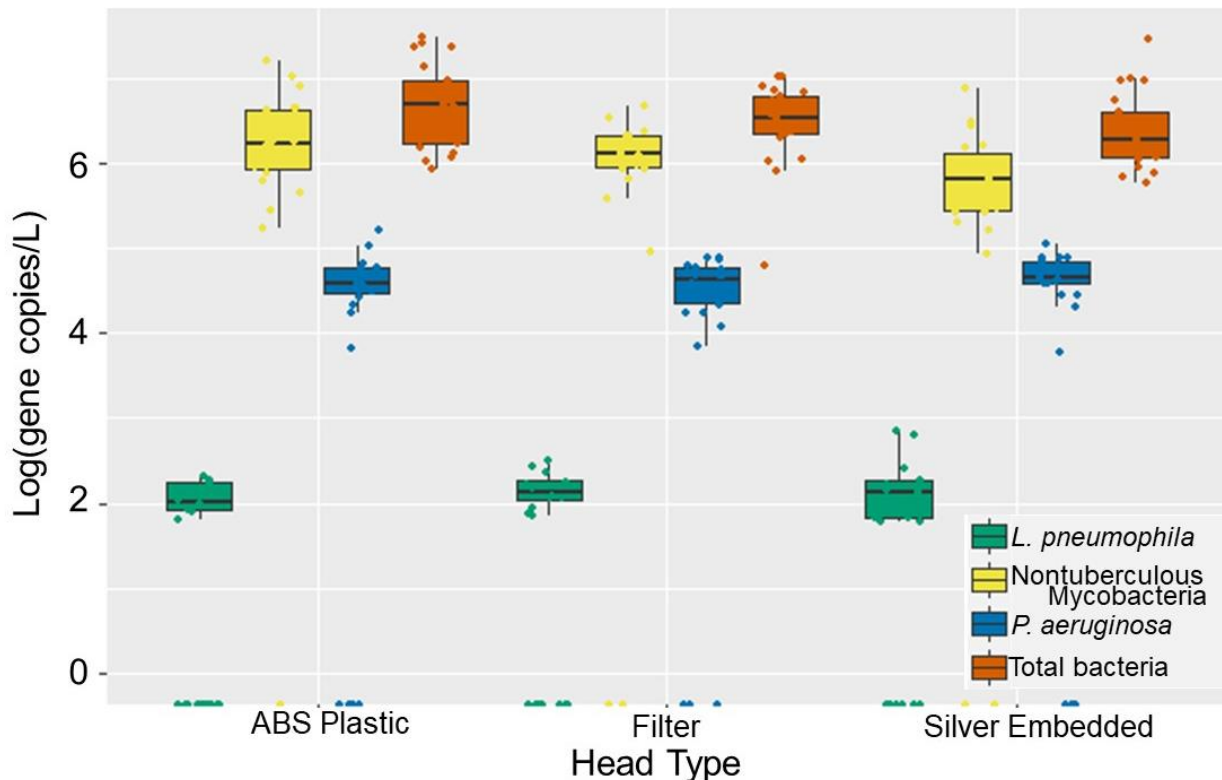


Figure 3: Absolute gene copy concentration of total bacteria (orange), *Legionella pneumophila* (green), *Pseudomonas aeruginosa* (blue), and nontuberculous mycobacteria (yellow) observed across 84 days of shower

**operation in ABS Plastic, silter-based, and silver-embedded showerheads in shower water. Each showerhead type shows all the data collected from three experimental showerhead replicates.**

The results of the amplicon sequencing corroborated the absolute quantification data: non metric multidimensional scaling (NMDS) analysis revealed no meaningful clustering in samples based on showerhead type (Appendix A Figure 4), and RDA analysis confirmed that showerhead type was not a significant parameter in explaining differences in the microbial community. The disparity between the marketing claims of these showerheads and their performance in a full-scale system could be due to a variety of factors, but likely are either due to material/ antimicrobial agent or application issues. From an antimicrobial agent perspective, it is possible that the tested antimicrobial showerheads do not contain the agent, which would violate Title 15 of the United States Code Section 1125 stating general provisions against false descriptions<sup>80</sup>, however without extensive material testing which was outside of the scope of this study, this explanation cannot be further explored. More likely, the reasoning for the lack of difference in DWPI abundance is due to too low of a concentration of the antimicrobial agent (silver and copper in the case of the silver-embedded and filter-based showerheads, respectively) to effectively inactivate microbes during a short exposure / contact time within a showerhead and shower hose (seconds to minutes). According to the manufacturer of the silver-embedded head, the active agent is tested in accordance with ISO 22196, which involves assessing the reduction of *Staphylococcus aureus* and *E. coli* on the antimicrobial material in nutrient abundant conditions after 24 h of incubation<sup>56</sup>. These conditions are vastly different from the shower water and showerhead environments and the organisms used are not commonly found in DW and don't represent the DWPI's claimed to be removed. Additionally, it is possible that the antimicrobial showerheads may be effective during a longer time of operation (after 84 days) or when DWPI concentrations are significantly higher.

The former explanation is unlikely since the manufacturer suggests replacing the silver-embedded showerhead after 60 days of use. It should, however, be stressed that none of the showerheads tested in this study have an National Sanitation Foundation (NSF) or the American National Standards Institute (ANSI) certifications for specific contaminant removal, so the manufacturers claims have not been tested to the voluntary standards used in the U.S.<sup>81</sup>. Furthermore, this study used molecular methods which detect both live and dead DWPIs, so it is possible differences may exist if culture-based approaches were solely used, however for the reasons mentioned previously (e.g., VBNC detection) molecular approaches were chosen.

Multivariate statistical analysis revealed that the most influential parameter to explain DWPI abundance was the showerhead age (days of use since installation) (Appendix A Table 5). The importance of showerhead age is unsurprising given biofilms develop in the virgin hose and fixtures and thus begin to influence the microorganisms in the shower water and aerosols<sup>45</sup>. According to the manufacturers of the silver-embedded and filter-based antimicrobial showerheads, both fixtures were to inhibit biofilm formation, and thus reduce the microbial load. However, DWPI and total bacteria concentrations were comparable regardless of head type, which further supports that these antimicrobial showerheads are no more effective than conventionally used ABS showerheads under real-use conditions (Appendix A Figures 2 and 3). The abundance trends observed over the course of the study in the water samples for each DWPI correlate with what little is known about DW biofilm dynamics: *L. pneumophila* and *P. aeruginosa* have different biofilm formation dynamics and thus may detach from the biofilm and enter the bulk water phase at different and transient times<sup>24,82</sup>. NTM is a known early colonizer of DW biofilms<sup>83,84</sup> and forms fairly consistent robust biofilms on common plumbing materials after as little as 7 days<sup>85</sup>, so it is

possible that the observed increase in water samples came from sloughing of the mature biofilm after day 42.

### **2.3.3 Aerosolization Behavior Of DWPIs Is Species-Specific**

Limited work has examined respirable bioaerosolization dynamics in full-scale DW systems, so characterizing bioaerosols generated as a function of time would yield insight into critical points of DWPI aerosolization in the lifespan of a showerhead. Regardless of showerhead type at the point of installation, respirable DWPIs that may be inhaled over the course of an average shower were found to be lower in abundance in this study (Figure 4) than in previous studies<sup>33,41</sup>. However, due to methodology differences in sampling time (60 minutes<sup>33</sup> compared to 20 minutes here), aerosol fraction collected (all sizes<sup>33</sup> compared to  $< 10 \mu\text{m}$  in this study) and aerosol collection instruments used it is not possible to compare these studies as truly equivalent, with the methodology of these other studies leading to higher bioaerosol counts inherently. Despite the low DWPI abundance, concentrations did vary by head type (Figure 4), with each DWPI exhibiting similar peaks in concentration at the same biofilm age across showerhead types. More specifically, NTM peaked in inhalable concentration at the time of installation (0-13 days), *P. aeruginosa* shows highest inhalable concentrations during early biofilm formation (14-42 days) and *L. pneumophila* displays consistent concentrations during both early and mature biofilm age (14-42 and 43-84 days, respectively). Collectively these results suggest that potential DWPI inhalation risk is DWPI specific and influenced by both the number of days of operation of the showerhead and the showerhead type.

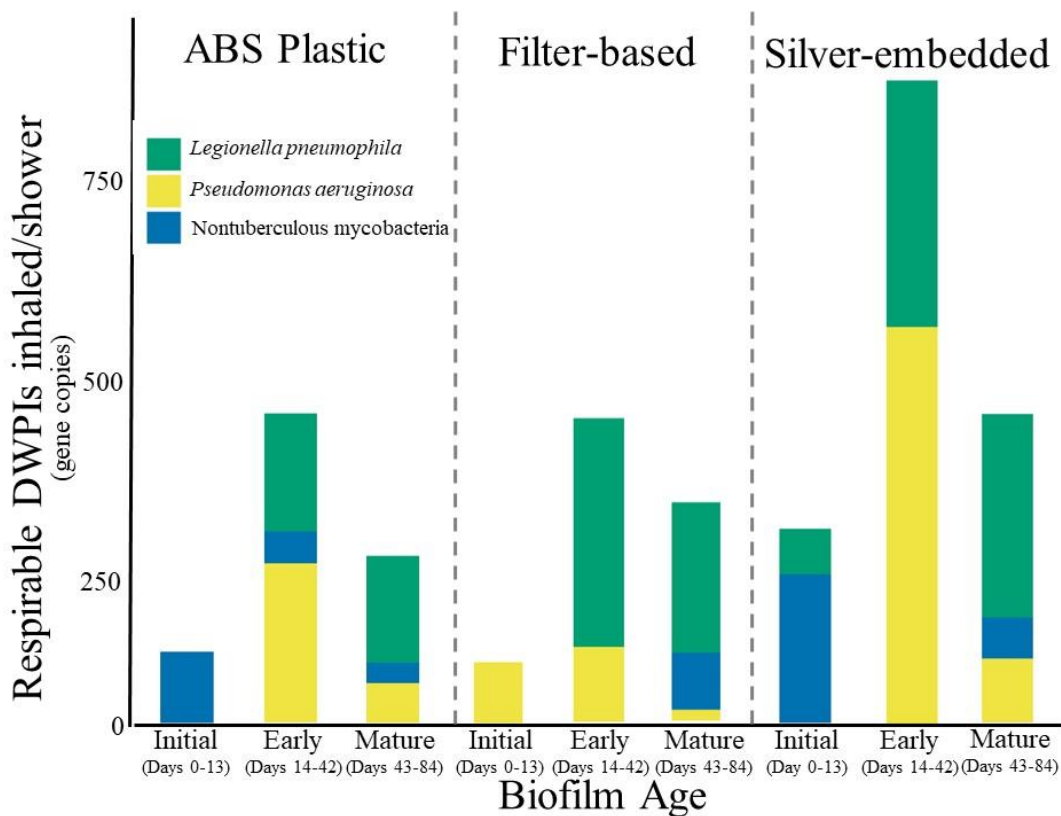


**Figure 4: Stacked barplots of the average absolute abundance of *Legionella pneumophila* (green), *Pseudomonas aeruginosa* (yellow), and nontuberculous mycobacteria (blue) within bio-respirable shower water-associated aerosols (<10  $\mu\text{m}$ ) produced during an 8-minute shower using ABS Plastic showerhead, Silver-embedded showerhead, and Filter-based showerhead. Averages are based on triplicates of each showerhead type.**

Looking at partitioning behavior (microbial concentration in the aerosol phase divided by the microbial concentration in the water phase), no statistically significant difference in DWPI behavior was observed between the showerhead types, however silver-embedded showerheads did have higher partitioning ratios and standard deviations than the other two showerheads (Table 1). Despite the lack of difference in DWPI partitioning between showerhead types, there were significant differences in individual DWPI partitioning behavior as a function of time (biofilm age) which was consistent across all showerhead types (Figure 5). Specifically, NTM appeared to partition at the highest frequency at time zero (Figure 5C) and then dissipated as the biofilm

established. Whereas *L. pneumophila* and *P. aeruginosa* show their highest partitioning behavior during early biofilm formation (Figure 4A and B). Within both phases *L. pneumophila* was very stochastic as it displayed large variation in absolute density (below the limit of detection – 308 gene copies/L) and was sporadically detected (Figure 4A). There are few studies that focus on aerosolization from DW, and those that do use vastly different methods than those used in this study in both aerosol collection and quantification methodology. Speaking very broadly, other studies have found *L. pneumophila*<sup>39</sup> and *P. aeruginosa*<sup>86</sup> present, but in low concentrations in shower water and even lower concentrations in shower aerosols when using culture-independent techniques, which yields comparable partitioning to that found in this study. Interestingly, these observations of NTM did not conform to the consensus within literature<sup>87</sup> that the genus is easily aerosolizable due to their hydrophobic cell membrane. This discrepancy could be attributed to the lack of size exclusion during aerosol collection in previous studies (i.e., collecting total NTM bioaerosols instead of respirable NTM bioaerosols), in addition other studies have collected samples from established plumbing sources of unknown ages, so it is conceivable that NTM aerosolizes better after more than 84 days.

Overall, considering both aerosolization and partitioning behavior data, antimicrobial showerheads did not significantly impact microbial aerosolization in the shower system, although the silver-embedded head had slightly higher ratios for all DWPIs and total bacteria (Figure 3 and Appendix A Table 4). Besides material type, there are many factors that contribute to showerhead aerosol generation such as number of water jets, orientation of jets on the showerhead, flow rate of shower water, and spray pattern<sup>37</sup>, all of which were controlled in this study. Although DWPI risk cannot be assessed due to the lack of viability data, these results demonstrate differing DWPI potential risk dynamics as a function of time. These differences need to be explored further using

both culture-based approaches and molecular methods targeting viable DWPIs as they suggest that quantitative microbial risk assessment for each DWPI should factor in the age of the showerhead.

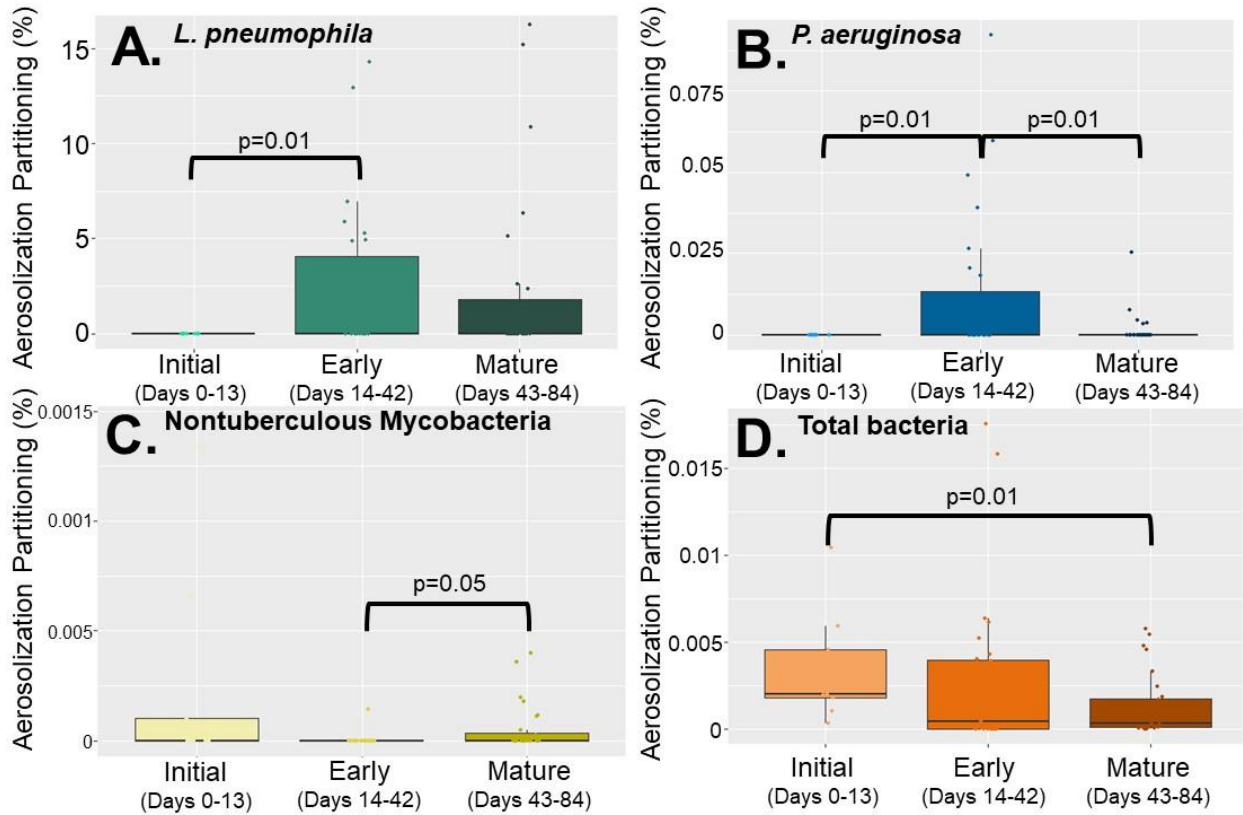


**Figure 5: Partitioning percentages of A *Legionella pneumophila*, B *Pseudomonas aeruginosa*, C nontuberculous mycobacteria, and D total bacteria based on biofilm growth stage; initial (0 -13 days), early (14-42 days) and mature (43-84 days) using all data collected from all showerhead types.**

**Table 1: Summary of generated linear models. In the model components column, ± indicates positive or negative association and the percent of the variance explained by each variable is superscripted.**

		<b>Overall Model</b>	
<b>Model (Transformation)</b>	<b>Model Components</b>	<b>Explained (%)</b>	<b>p-value</b>
<b><i>L. pneumophila</i></b>			
<b>Water (Square root)</b>	Showerhead Type <sup>27%</sup> + Showerhead Age <sup>2%</sup> + Total Chlorine <sup>25.6%</sup> + Total Calcium <sup>11.9%</sup> + Dissolved Copper <sup>2.3%</sup>	42.20	5.8 x 10 <sup>-6</sup>
<b>Aerosols (Square root)</b>	Total Chlorine <sup>21.9%</sup>	21.90	1.1 x 10 <sup>-4</sup>
<b>Partitioning ratio (Logarithmic)</b>	<i>L. pneumophila</i> in water <sup>29%</sup> – NTM emission <sup>0.5%</sup> – Total Chlorine <sup>5.2%</sup> + Total Iron <sup>7.1%</sup> – Dissolved Copper <sup>6.4%</sup>	49.10	3.2 x 10 <sup>-7</sup>
<b><i>P. aeruginosa</i></b>			
<b>Water (Square root)</b>	Showerhead Age <sup>33%</sup> + Free Chlorine <sup>18%</sup> + Dissolved Iron <sup>4.2%</sup> – Total Organic Carbon <sup>6.6%</sup>	61.7	1.5 x 10 <sup>-11</sup>
<b>Aerosols (Logarithmic)</b>	Temperature <sup>5.2%</sup> + Total Iron <sup>14.8%</sup> – Dissolved Organic Carbon <sup>5.2%</sup> + Total Bacteria in Water <sup>6.8%</sup>	32	1.4 x 10 <sup>-4</sup>
<b>Partitioning ratio (Logarithmic)</b>	Total Iron <sup>31.9%</sup> + Bacteria emission <sup>11.2%</sup> + Temperature <sup>6.4%</sup>	49.5	8.0 x 10 <sup>-9</sup>
<b>Nontuberculous mycobacteria (NTM)</b>			
<b>Water (Square root)</b>	Total Bacteria in water <sup>15.9%</sup> – Showerhead Type <sup>5%</sup> – Free Chlorine <sup>19%</sup>	39.9	1.3 x 10 <sup>-6</sup>
<b>Aerosols (Logarithmic)</b>	pH <sup>1.5%</sup> + Total Copper <sup>13.2%</sup> + Total Organic Carbon <sup>3.2%</sup> – Total Magnesium <sup>9.8%</sup>	27.8	7.3 x 10 <sup>-4</sup>
<b>Total Bacteria</b>			
<b>Water (Logarithmic)</b>	Total Iron <sup>23.4%</sup> + Temperature <sup>10.1%</sup> + Dissolved Copper <sup>4.8%</sup> + NTM in water <sup>16.2%</sup>	54.6	1.9 x 10 <sup>-9</sup>
<b>Aerosols (Square root)</b>	Total Bacteria in water <sup>24%</sup> – Total Iron <sup>0.01%</sup> + Total Magnesium <sup>10%</sup> + Dissolved Copper <sup>3.2%</sup> – Total Calcium <sup>8.6%</sup>	45.9	9.8 x 10 <sup>-7</sup>
<b>Partitioning ratio (Logarithmic)</b>	<i>P. aeruginosa</i> emission <sup>28.7%</sup> + Dissolved Silver <sup>8.8%</sup> – <i>P. aeruginosa</i> in water <sup>4.1%</sup>	41.6	5.3 x 10 <sup>-7</sup>

### 2.3.4 Microbial Community Dynamics Were Phase (Water And Aerosol) And Showerhead Age Dependent

RDA analysis revealed that the microbial community was significantly impacted by phase and age (days of operation), with phase explaining 7.2% of the variance observed. Between water and aerosol phases, the community structure and membership of dominant taxa were surprisingly comparable despite the bioaerosolization process being known to reduce overall microbial concentrations and cause damage to cell membranes (Figure 6)<sup>33</sup>. Alpha diversity analysis revealed that samples from either phase were similar in richness and diversity, but that water samples were less even than aerosol samples. Looking at the most abundant phyla (Figure 6A) in the water and aerosol samples, *Proteobacteria* were the dominant phyla in water (58%) and aerosol (61%) samples alongside other commonly reported DW phyla<sup>43,46</sup> such as *Firmicutes*, *Actinobacteria*, *Cyanobacteria*, and *Bacteroidetes*. However, at the more resolved genus level, there was much more variation in community composition between water and aerosol samples with only 40% of all genera being common between phases, with *Acidovorax*, *Sphingomonas*, and *Stenotrophomonas* being the most abundant which makes sense given their documented resistance to chlorine and ability to form DW biofilms (Figure 6B)<sup>88-90</sup>. Despite many similarities in the microbiome between the aerosol and water samples, there were distinctions in the beta diversity being driven by rare taxa which explains the distinct clustering of aerosol and water samples (Appendix A Figure 4).

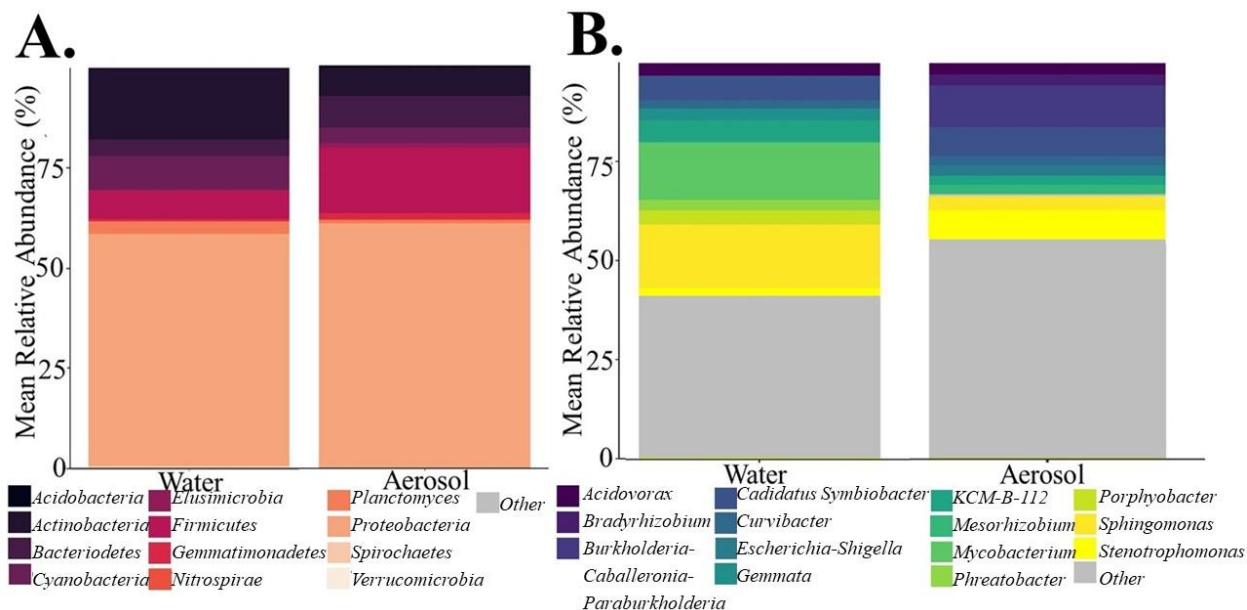


**Figure 6: Stacked barplots showing the top ten most abundance phyla A. and genera B. in shower water and shower water-associated aerosols. Data illustrate the average abundance observed across all showerhead types and all timepoints.**

Collectively, across all showerhead types 27% and 21% of genera were shared in water and aerosol samples, respectively, however ABS Plastic showerheads displayed the least number of genera (99 in water and 65 in aerosols) and filter-based showerhead had the most (148 in water and 74 in aerosols). The aforementioned DWPIs were among the top ten most abundant genera shared between showerhead types and phases, as well as *Mycobacteria*. *Mycobacteria* have been documented to make up large proportions of the DW microbial community<sup>48,83</sup>, and its presence as a major community member is in agreement with the absolute abundance data collected from these samples despite being detected in lower quantities than other studies<sup>33</sup>. These genera results suggest that the antimicrobial showerheads do not select for fewer taxa based on their material properties as expected, but in fact support different rare taxa compared to the commonly used plastic head (Figure 7A and 7B). The highest number of taxa being found in the filter-based showerheads makes sense as it has been documented that filters can be colonized by

microorganisms and support a large array of microbial growth on the unit process scale<sup>63,91</sup>, however understanding the material effects of the showerhead itself on microbial community must be further explored to determine if there are unintended consequences to using novel showerhead materials.

In addition to showerhead type and phase being known to impact the DW microbial community, the age of plumbing and associated fixtures has been shown to impact the microbiome<sup>43</sup> more than the showerhead type. NMDS analysis of the water samples from this study revealed that the microbial community structure was distinct during the different stages of biofilm formation, with tight clustering being observed on the day of showerhead installation and looser clustering in samples taken during early and mature biofilm development (Appendix A Figure 4). As the biofilm establishes, the microbiome in the water samples is influenced by the sessile community forming within the virgin fixture so the differences in the communities over time aligns with known biofilm processes. The membership in these samples also changes as showerhead age increases, which further suggests that biofilm formation in virgin plumbing fixtures impacts the composition of the microbiome in both water and aerosol samples (Figure 8). As the study progressed, samples significantly decreased in richness and diversity, but increased in evenness. Although biofilm formation kinetics and characterization in DW systems is an emerging area of research, these changes in alpha diversity may be influenced by the sessile community within the hose and showerhead sloughing into the water as the biofilm matures<sup>45</sup>. Such structural convergence has been documented in previous studies in DW distribution systems after different treatment processes<sup>92</sup>, and in a shower hose material study which initially saw differing microbial densities across material types but a convergence over time<sup>43</sup>.

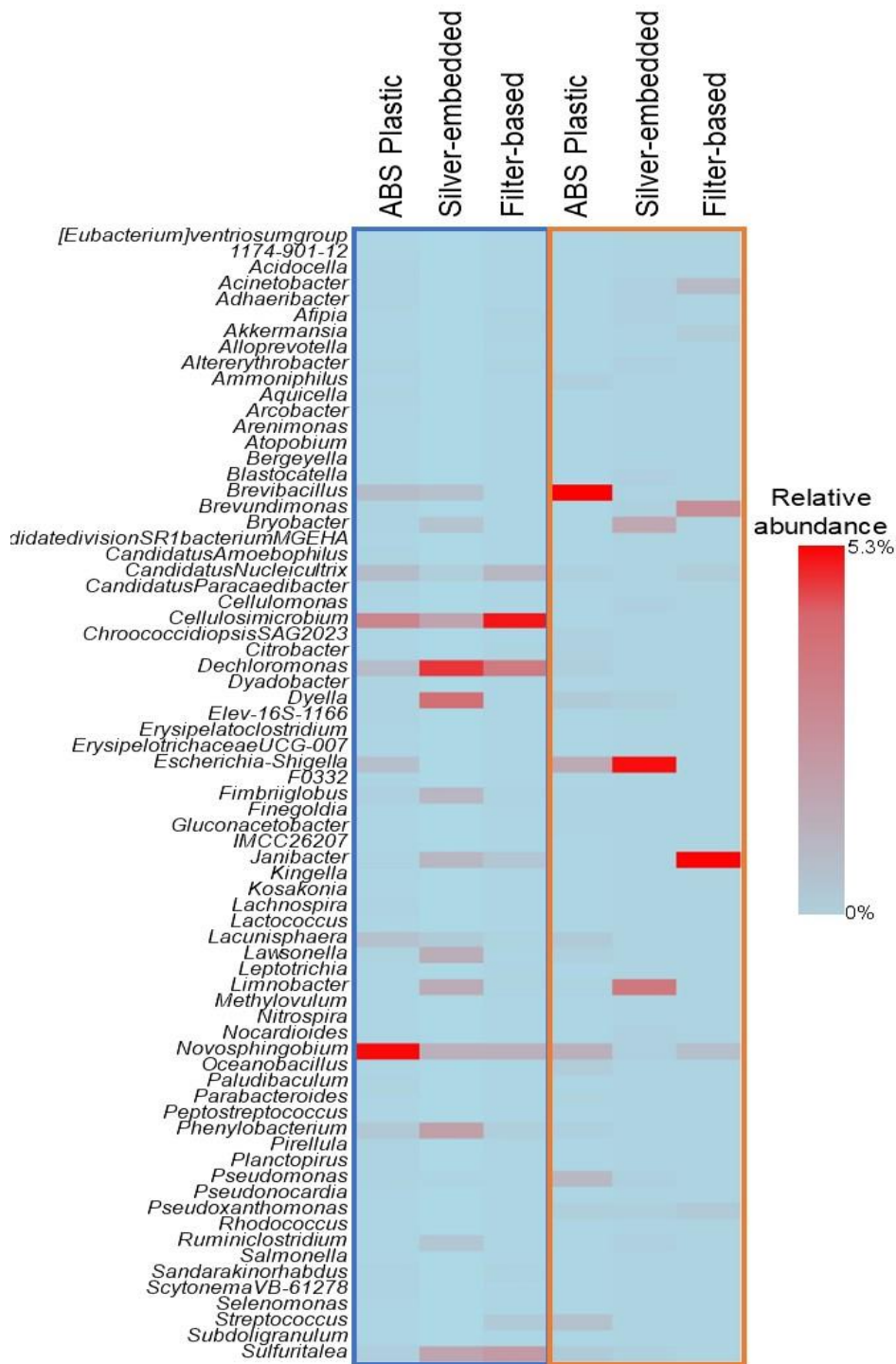
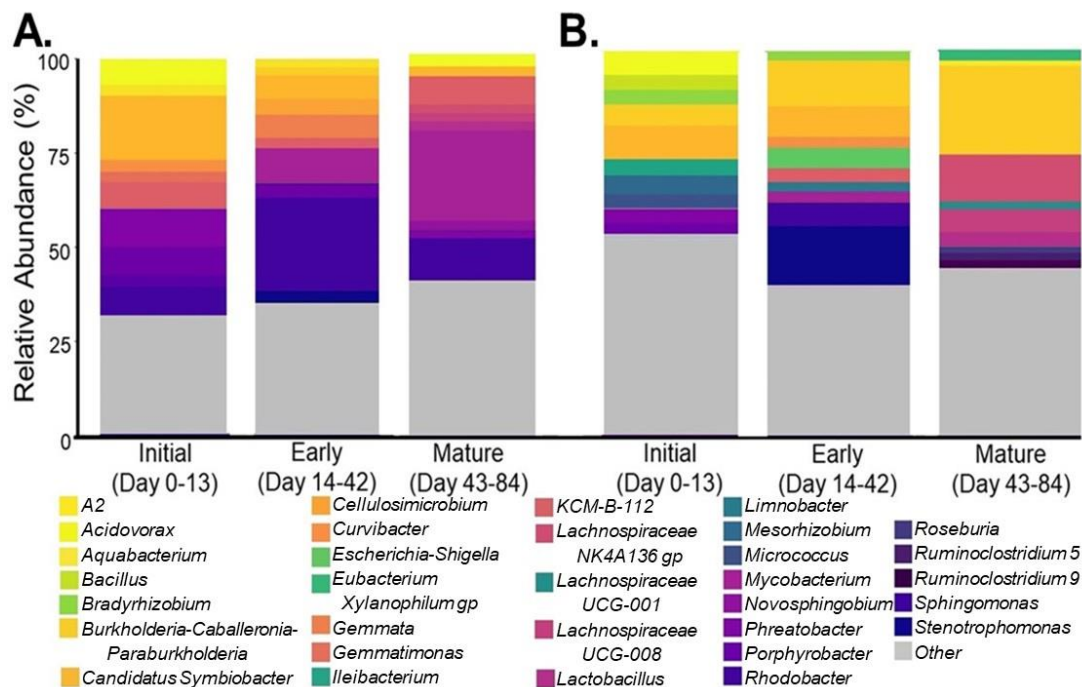


Figure 7: Heatmap showing the abundances of the fifteen least abundant genera produced in A. aerosol samples and B. water samples by each shower head type



**Figure 8: Top ten most abundant genera by biofilm establishment period for A. water and B. aerosol samples. Each bar represents an average across all showerhead types.**

## 2.4 Conclusions

Overall, antimicrobial showerheads did not produce significantly different water chemistry or DWPI abundances in shower water and shower water associated aerosols over the duration of the study. Despite not changing the absolute abundances of DWPIs or total bacteria, showerhead type impacted the microbial community of the water and aerosols which may indicate that there are material effects beyond the marketed antimicrobial properties that could be impacting microbial growth, establishment, and biofilm development. Aerosolization behavior of DWPIs was found to be the same across all showerhead types, however the proportion and time frame of maximum aerosolization varied for each DWPI studied. Although DWPI risk cannot be assessed

due to the lack of viability testing, these findings suggest that future quantitative microbial risk assessment for DWPIs should consider the showerhead age. There are many experimental considerations for this work, most notably that samples were analyzed for DNA and not RNA, so viability was not considered in this study, in addition to lacking the extensive materials and product design testing of these showerheads to confirm their marketed properties in the laboratory environment. Future work should also include in-depth materials testing of showerhead and hose material to independently assess and verify their antimicrobial properties in the DW environment. Additionally, temporal characterization of microbiome and DWPI abundance within the water, biofilm and aerosol phases in full-scale model studies like this one are required beyond the 84 days of this study to determine if the observed dynamics change, especially for NTM. The inclusion of a human analog (i.e. mannequin) should also be considered for subsequent studies to assess the changes in aerosolized DWPI deposition and to relate the findings more closely to consumer exposure. Based on the results of this study, a consumer choosing between a conventional or antimicrobial showerhead may want to install a cost-effective conventional showerhead which achieves similar chemical and microbial quality to the more expensive antimicrobial alternatives.

### 3.0 Specific Aim 2.0: Evaluate The Efficacy Of Silver In The Showering System

Specific Aim 2.0 was funded by The National Science Foundation (grant number: CBET- 1935378). This work was conducted with the help of Jamie Mastropietro, Daniel Huffman, and Krystolynn Harris during sample collection, Dr. Daniel Bain and Paige Moncure during ICP-MS analysis, Dr. David Malehorn during TOC analysis, Dr. Julianne Baron and the scientists at Special Pathogens Laboratory that performed culturing, and Dr. Esta Abelev for SEM and EDS analysis at the University of Pittsburgh's Nanoscale Fabrication and Characterization Facility. Daniel Huffman recovered, processed, and analyzed biofilm samples from shower hoses along with Yash Shah and Dr. Kira Lathrop for OCT analysis. The results of Specific Aim 2.0 are published in one journal publication with three other publications in preparation. In addition, results have been shared in 2 conference proceedings:

#### **Journal Articles**

1. Huffman, D.; **Pitell, S.**; Moncure, P.; Stout, J.; Millstone, J.; Haig, S.-J.; Gilbertson, L. **Moving beyond silver in point-of-use drinking water pathogen control.** *Environmental Science: Water Research and Technology* **2024**. <https://doi.org/10.1039/D3EW00564J>
2. **Pitell, S.**; Huffman, D.; Moncure, P.; Millstone, J.; Stout, J.; Gilbertson, L.; Haig, S.-J. **Not the silver bullet: assessing the effects of silver-containing antimicrobial showerheads on the drinking water microbiome.** *In preparation for submission to Frontiers in Microbiomes.*

3. **Pitell, S.**; Huffman, D.; Shah, Y.; Moncure, P.; Millstone, J.; Stout, J.; Lathrop, K.; Gilbertson, L.; Haig, S-J. **Characterizing the drinking water biofilm established in silver-containing showerheads.** *In preparation.*
4. **Pitell, S.**; Woo, C; Millstone, J.; Stout, J.; Gilbertson, L.; Haig, S-J. **The effects of ionic silver on *Mycobacterium abscessus* biofilms in a simulated drinking water environment.** *In preparation.*

### **Conference Proceedings**

1. **Pitell, S.**; Huffman, D.; Moncure, P.; Millstone, J.; Stout, J.; Gilbertson, L.; Haig, S.-J. **Assessing the impacts of silver-containing showerheads on the drinking water microbiome.** *Poster.* Association of Environmental Engineering and Science Professors (AEESP) Research and Education Conference (Boston, MA) 6/22/23.
2. Huffman, D.; **Pitell, S.**; Shah, Y.; Moncure, P.; Millstone, J.; Stout, J.; Lathrop, K.; Haig, S-J.; Gilbertson, L. **Flushing Out the Truth: Investigating the Impact of Silver on Biofilm Formation in Shower Fixtures.** *Poster.* Association of Environmental Engineering and Science Professors (AEESP) Research and Education Conference (Boston, MA) 6/21/23.

### 3.1 Introduction

The work in chapter 2 highlighted the shortcomings of POU antimicrobial showerheads, but the demand for antimicrobial showerheads continues to increase<sup>54,55</sup>. This trend may be driven by economic benefits as large-scale DWPI reduction intervention strategies such as thermal shock<sup>61</sup> or hyperchlorination<sup>62</sup> in plumbing are costly for building managers (\$4082 and \$8281 annually per 100 water outlets, respectively), are often only temporarily effective<sup>52,93</sup>, and are not suited for small domestic use. In addition, treating DW directly at the POU circumvents many of the complexities of addressing the entire building plumbing system. As discussed in [Chapter 2](#), POU devices can use many mechanisms to treat water (e.g., filtration through media or UV disinfection)<sup>53</sup>, however POU fixtures containing silver are readily being adopted in healthcare facilities<sup>94,95</sup>. Historically, solid silver (e.g., coins) was used as an antimicrobial agent to treat water<sup>96</sup>, whereas today it is more commonly used in an ionized form (e.g., copper-silver ionization<sup>97</sup>). Despite the popularity of copper-silver ionization systems for onsite water treatment in healthcare facilities; fueled by a need to reduce *Legionella*, DWPI abundances is often only temporarily reduced<sup>51,52</sup>. Given the recurrence of DWPIs after copper-silver ionization treatment there is concern about the development of antimicrobial resistance in both microbes present in the water and the biofilm growing within the plumbing system<sup>98</sup>. Silver inactivates microorganisms through a variety of different biochemical mechanisms such as destabilizing the thiol bonds in nucleic acids and proteins and creating reactive oxidative species intracellularly<sup>99</sup>, however the inactivation mechanism is likely a combination of many physiochemical processes<sup>99,100</sup>.

Many showerhead manufacturers are beginning to incorporate various types of silver into their showerhead designs as a way to reduce microorganisms in shower water or within the DW

biofilm. When testing the effectiveness of silver-containing POU devices, the same testing protocols such as ISO 22196:2011<sup>56</sup> are followed like with other antimicrobial materials, which do not accurately model the complex microbiota and oligotrophic environment of DW, and may give misleading results due to the induction of the VBNC<sup>101</sup> state many organisms enter when under stress. In fact, independent studies have found that silver-containing fixtures have minor effects when used on drinking water<sup>95,102</sup>, and may unintentionally select for antimicrobial resistance<sup>66,103</sup>.

Silver-containing showerheads that are marketed to reduce microbial load in shower water are an attractive option for building managers of high-risk facilities (e.g., hospitals or elderly care centers) or concerned consumers looking to reduce the risk of DWPI infection, however there is little data on how the incorporation of silver into a showerhead may impact the chemical and microbiological quality of DW and DW-associated biofilms under real-use conditions. To assess these potential impacts, this study evaluated the viable DW microbiota including DWPIs from shower water taken from three different silver-containing showerheads (silver ion-embedded polymer, copper-silver ion, and silver mesh) and were compared to samples from showerheads made with conventional fixture materials (ABS and metal). Additionally, two types of biofilm samples were collected, visualized, and analyzed for their microbial properties. Finally, CDC biofilm reactor experiments, operated to mimic the shower environment were conducted to characterize *M. abscessus* biofilms' response to ionic silver at variable silver doses to help close the gap on what silver concentration is required for optimal disinfection in DW POU applications.

## 3.2 Research Approach

### 3.2.1 INHALE Shower Laboratory Experimental Design And Sampling Regime

The INHALE shower laboratory as described in [Chapter 2](#) was used as the source location for all samples. Samples were collected across two sampling campaigns (C1 - March through May 2021 and C2 - February through April 2022) to account for temporal variations in water quality); all measurements were done identically between the campaigns, with the only experimental differences being the dates sampled and the showerheads tested. Both campaigns were conducted over a 12-week period, which was chosen based on one of the manufacturer’s guidelines of replacing the showerhead after 12 weeks of use.

Five different showerheads were used over the course of this study (Table 2), these were: (1) a commonly used ABS showerhead – used to simulate conventional showering dynamics; (2) a commonly used metal showerhead – used to simulate conventional shower dynamics; and (3) three different types of silver-containing showerheads - used to characterize a variety of antimicrobial technologies used in these fixtures. The first silver-containing showerhead, referred to from now on as “silver embedded” is composed of ABS plastic that is marketed to have silver nanoparticles embedded into the polymer. The second silver-containing showerhead, referred to from now on as “silver coated copper mesh” is composed of ABS plastic and contains a silver-coated copper mesh in both the showerhead and hose. The third silver-containing showerhead, referred to from now on as “silver mesh” was fabricated by the research team by adding silver mesh woven from 0.356 mm diameter pure silver wire (Thermofisher, Waltham, MA) to an ABS

plastic showerhead. All commercially available showerheads used in this study are de-identified. All showerheads were operated with the same spray pattern and flow rate.

**Table 2: Summary of showerheads used in Chapter 3.**

<b>Showerhead Type</b>	<b>Material</b>	<b>Commercial Availability</b>	<b>Campaign Used</b>	<b>Treatment Claims</b>
<b>ABS plastic</b>	acrylonitrile butadiene styrene (ABS) polymer	Yes	1, 2	None
<b>Metal</b>	Oiled bronze	Yes	1	None
<b>Silver-embedded composite</b>	Silver nanoparticles incorporated into polymer	Yes	1	Inactivate microorganisms
<b>Silver coated copper mesh</b>	Plastic housing with silver coated copper mesh in both the showerhead and hose	Yes	2	Inactivate microorganisms
<b>Silver mesh</b>	ABS plastic housing with silver mesh added	No	2	None

### 3.2.2 Showerhead Materials Testing

Because the previous results from [Chapter 2](#) saw no water chemistry or microbiological effects from the silver-embedded showerhead, materials testing on this showerhead was conducted to characterize the silver composition in the showerhead insert (the piece of the showerhead that claims to have silver in it as well as the piece that must be changed every 12 weeks in order for the showerhead to continue to treat water effectively). Three locations on two showerhead inserts from different manufacturing batches were isolated from the insert so that every location on the insert that has contact with the shower water was tested (Appendix B Figure 1). Scanning electron microscopy (SEM) using the Zeiss SIGMA 500VP SEM, and Energy-dispersive X-ray spectroscopy (EDS) analysis using an Oxford MAX80 EDS detector were performed on each of

the insert locations to visualize and assess the chemical composition of the samples, respectively. SEM imaging was performed using accelerated voltage of 20kV and a working distance of 10mm. Samples were coated with ~2 nm-thick coating of Pd/Au (80%/20%) for conductivity purposes on a Denton sputter coater. Both instruments are part of the University of Pittsburgh's Nanoscale Fabrication and Characterization Facility.

### **3.2.3 Water And Biofilm Sample Collection From Showerheads**

Water from each showerhead was sampled biweekly over the course of the 12-week campaigns (n= 6 sampling events per campaign). Briefly, water sampling entailed collecting the first 1.5 L for each head into a sterile Nalgene bottle. 1 L was immediately filtered through a 0.2  $\mu\text{m}$  polycarbonate filter (Millipore, Cork, Ireland) and the filter was stored at -80 °C within 20 minutes of collection to ensure the maximum amount of RNA was retained prior to extraction. The remaining water was used for water chemistry analysis and DWPI culturing.

Biofilms associated with the shower water samples were collected using two different methodologies. Each DW outlet was swabbed at the point where the copper supply pipe ends, and the showerhead hose was installed by swiping a sterile cotton swab around the entire interior diameter of the pipe three times. Swabbing was conducted immediately before showerhead installation for both sampling campaigns and immediately after the collection of the final water sample. Collected swabs were then placed in 10 mL PBS, vortexed until there was visible maceration of the swab itself (~5min), filter concentrated onto a 0.2  $\mu\text{m}$  polycarbonate filter (Millipore, Cork, Ireland), and stored at -80 °C within 20 minutes of collection to ensure RNA

integrity prior to extraction. Biofilms were also extracted from the shower hoses themselves after each sampling campaign was finished.

Biofilm recovery from the shower hoses was achieved by cutting two 5 cm-long segments from each hose; one segment was taken from either end of the hose (i.e., closest, and furthest away from the showerhead connection) with a sterile anvil lopper. Collected samples were placed in petri dishes, covered in foil and stored at -20 °C until optical coherence tomography (OCT) imaging was conducted. The remainder of the hose was used to extract the biofilm according to the procedure outlined in Proctor et. al., 2016<sup>43</sup> to allow molecular and chemical analysis of the biofilm to be performed. Briefly, each hose was filled with sterilized glass beads and deionized water, stoppered, sonicated at 42 kHz for 5 minutes, and the resulting biofilm-bead suspension was collected in a sterile Nalgene bottle. This sonication step was repeated three additional times for each shower hose, then the fifth and final sonication was performed using 0.05% v/v Tween20 in place of deionized water to encourage biofilm detachment. Each hose end was then swabbed with a sterile cotton swab and added to the biofilm suspension. The bottle containing the beads, solution, and swabs were then vortexed at maximum speed for 2 minutes. Aliquots from this homogenized solution were then taken for TOC and DOC analysis, total and dissolved metal analysis, and the remaining suspension was passed through a sterile Büchner funnel to remove the glass beads, then filtered onto a 0.2-µm polycarbonate membrane (Millipore, Cork, Ireland) as described in the previous [chapter](#). The filtered samples were stored at -20°C until molecular analysis was performed.

### 3.2.4 Water Quality Measurements

Ten water quality parameters (Appendix B Table 1) were measured in all collected water samples in accordance with standard methods. Temperature, pH, orthophosphate, free chlorine, total chlorine, total and dissolved organic carbon, and total and dissolved metals (iron, lead, copper, silver, calcium, and magnesium) were measured as described in [Chapter 2](#). Oxidation reduction potential was assessed at the time of collection using an ORP probe (Mettler-Toledo, Columbus, OH). All analyses, except pH, and temperature, were performed in triplicate and the coefficient of variation was at most 13%.

### 3.2.5 DWPI Culturing

Culturable DWPI abundances were quantified by the Special Pathogen Laboratory in Pittsburgh, PA. Water samples were quenched with sodium thiosulfate (enough to quench up to 20 ppm free chlorine in potable water) at the time of collection to prevent disinfection during transport. *Legionella sp.* were quantified using an in-house optimized ISO standard 11731:2017<sup>104</sup>, where the sample is spread onto buffered charcoal yeast extract agar and allowed to grow for 5 days at 36 °C. *P. aeruginosa* was quantified using a modified ASTM International Standard Test Method D5246<sup>105</sup>, where samples were filter-concentrated and then plated on M-PA-C selective media and incubated at 41 °C for 48 hr. NTM was quantified by filter concentrating and decontaminating the sample with 0.2 M KCL-HCL, pH 2.2 prior to plating on Middlebrook 7H10, Mitchison 7H11, and NTM elite and incubated at 30°C for 6 weeks. Only fast-growing NTM (*Mycobacterium gordonae* and *Mycobacterium mucogenicum/phocaicum*) were quantified due to the culturing time and competition.

### 3.2.6 DWPI Absolute Abundance Quantification

RNA from collected water and swab samples were extracted using the RNeasy Power Water kit (QIAGEN, Hilden, Germany), DNase-treated using the rigorous treatment of the TURBO DNA-free kit (Invitrogen, Waltham, MA), then converted to cDNA using the iScript cDNA Synthesis kit (Bio-Rad, Hercules, CA). Between each processing step, concentrations of the genetic material were obtained using the appropriate Qubit assay (Invitrogen, Waltham, MA). The extracted RNA and cDNA were then stored at -80 °C until further analysis. DNA was extracted from the biofilm samples using the Fast Spin DNA Extraction kit (MPBio, Irvine, CA) and was assessed to quantify the abundance of total bacteria, *L. pneumophila*, and NTM using the methodology described in [Chapter 2](#).

Absolute densities of total bacteria, *L. pneumophila*, *P. aeruginosa*, and NTM in the resulting cDNA water and swab samples were determined using ddPCR following a similar approach to that outlined in [Chapter 2](#). Due to the complex sample matrix caused by the RNA processing pipeline, RNA optimized ddPCR assays for each microbial target were developed (Appendix B Table 2).

### 3.2.7 Biofilm Imaging Using Optical Coherence Tomography

The 5 cm lengths of shower hose from the showerheads used in this study were further bisected, then transported on ice to the University of Pittsburgh Medical Center's Eye and Ear Institute for imaging via OCT on a Bioptigen Envisu R2210 instrument (Leica Microsystems, Wetzlar, Germany). Images were collected by conducting five volume sampling scans on

manually-located points of elevation that may be indicative of biofilm. The sampling scans with the least amount of feedback, water droplets, and clearest image were then rendered in FIJI 3D Viewer into three-dimensional models. These models were then manually edited to reduce background noise in the renderings and to clarify the biofilm.

### **3.2.8 16S rRNA Sequencing**

16S rRNA gene amplicon library preparation and sequencing were performed on cDNA from water and swab samples and DNA from biofilm samples at Argonne National Laboratory following the Illumina Earth Microbiome Protocol<sup>75</sup> and analyzed as described in [Chapter 2](#). A total of 8,818,427 reads with an average quality score of 38 were generated from these samples. In addition, functional abundances were predicted by PICRUSt2<sup>106</sup>.

### **3.2.9 Silver Nitrate Exposure To *M. abscessus* Biofilms In A CDC Biofilm Reactor**

#### **3.2.9.1 CDC Biofilm Reactor Experiments**

CDC Biofilm Reactors (BioSurface Technologies Corporation, Bozeman, MT, USA)<sup>107,108</sup> were employed to assess the impact of different silver ion exposures (silver nitrate) conditions on the viability, biofilm structure, and biofilm formation processes of different isolates of *M. abscessus* on ABS coupons. *M. abscessus* was assessed due to it being identified as a DWPI of major clinical<sup>109</sup> and DW biofilm<sup>48,85</sup> relevance. Furthermore, the antimicrobial activity of silver ions were assessed against NTM due to it being much more resistant to CSI than other DWPIs such as *Legionella*<sup>83,110</sup>, hence effective inactivation against NTM would translate to easier to kill

organisms. ABS coupons were used as this is the most common showerhead material and (Appendix B Figure 2) silver nitrate (Thermofisher, Waltham, MA) was chosen as the silver ion source due to its known effects on microorganisms<sup>96,111</sup> and precision of dosing in solution.

**Silver nitrate:** Two experimental silver nitrate concentrations were tested: 48 mg/L and 480 mg/L  $\text{Ag}^+$  as silver nitrate. These values were chosen to represent the silver ion dose used in CSI treatment<sup>110,112</sup> (48 mg/L) and an “extreme” treatment condition which was 10x CSI dosing.

***M. abscessus* Preparation And Adherence To Coupons:** Two strains of smooth *M. abscessus* were used in this study: one strain, referred to from now on as the environmental *M. abscessus* was isolated from a hot water system (provided by the Special Pathogens Laboratory). The other *M. abscessus* strain, referred to from now on as the clinical *M. abscessus*, was isolated from a patient with an NTM lung infection and was provided by the DePas lab at the University of Pittsburgh. Detailed information about the isolates, reactors, and general method development can be found in Appendix B Supplemental Procedure 1. Briefly, twenty ABS coupons (previously cleaned using soap and water) per isolate (n= 40) alongside controls were incubated in 24-well tissue culture plates (Corning Incorporated, Corning, NY), with one disk per well. Each disk was covered with 5 mL of each *M. abscessus* strain (early stationary phase) and incubated for 72h at 35°C with gentle shaking. Control disks were exposed to the same conditions as previously discussed except covered with 5 mL of growth media. At the end of the incubation time, loosely attached NTM were removed by dipping the coupon three times in diluted R2A solution, and a final average coupon density of  $5.1 \times 10^6$  cfu/cm<sup>2</sup> and  $1.9 \times 10^6$  cfu/cm<sup>2</sup> was achieved for the clinical and environmental *M. abscessus* strains respectively.

Five coupons per isolate were used for initial characterization (plate counts, microscopy, RT-ddPCR, and microscopy - Appendix B Supplemental Procedure 1). The remaining 30 NTM coupons and control coupons were carefully installed into the coupon holder (five NTM coupons per isolate per reactor) of each of the three CDC biofilm reactors (no silver nitrate, 48 mg Ag<sup>+</sup>/L feed solution, and 480 mg Ag<sup>+</sup>/L feed solution).

**CDC Biofilm Reactor Operation:** Reactors were operated daily as follows for 7 days to simulate the shower environment which is composed of a short continuous flow phase followed by a longer stagnation phase. Specifically, each day reactors were operated in continuous stirred tank reactor (CSTR) mode for 10 minutes where the effluent flow rate was equal to the influent flow rate and the stir baffle was operating at 100 rpm. Influent for CSTR phase for each reactor was 0.45 μm (ThermoFisher, Waltham, MA) filtered shower water that was warmed to 40 °C (the average showering temperature<sup>36</sup>) and contained either no silver nitrate, 48 mg Ag<sup>+</sup>/L, or 480 mg Ag<sup>+</sup>/L to get the contact times of 0 mg Ag<sup>+</sup>/L\*min, 480 mg Ag<sup>+</sup>/L\*min, and 4800 mg Ag<sup>+</sup>/L\*min. After 10 minutes of CSTR operation, each reactor was flushed for an additional 10 minutes (1 hydraulic retention time) with 0.45 μm filtered shower water to remove silver from the system and then allowed to stagnate for the remaining ~24 hours with no stirring (operate in batch reactor mode). Silver ions were measured every day in the influent and in the effluent at the end of the 10-minute exposure period. After seven days of operation all coupons were carefully removed for analysis with sterile forceps.

### 3.2.9.2 Characterization Of *M. abscessus* Before And After Silver Exposure

The biofilm coupons retrieved from the CDC biofilm reactors after the 7-day experiment alongside extra coupons that had biofilms attached to them, but not placed in the reactors (referred

to from here forward as initial biofilm) were assessed for biofilm density, silver accumulation, morphology characteristics, and biofilm kinetic behavior. One coupon per isolate per reactor was placed biofilm-side down in 4% paraformaldehyde for 4 hours then visualized using microscopy at the DePas laboratory. Biofilm imaging and quantification was done by staining the fixed biomass using FilmTracer™ FM™ 1-43 Green Biofilm Cell Stain (Invitrogen, Waltham, MA) and performing a 3x3 tile scan and z stack. The biofilms from the remaining 4 coupons per isolate per reactor were recovered by gently rinsing with diluted R2A before being placed in a 50 mL microcentrifuge tube (Thermofisher, Waltham, MA) along with a 1% Tween-diluted R2A solution and performing three rounds of 1-min sonication followed by 30s vortexing. Portions of the resulting biofilm suspension solution were used immediately for subsequent analysis.

Viability of culturable *M. abscessus* was assessed by performing plate counts on Middlebrook 7H11 media, ICP-MS analysis was performed to measure the concentration of silver within the biofilm, and the rest of the suspension was filter concentrated, extracted for RNA, and analyzed using ddPCR as described in [Chapter 3.2.5](#). After plate counts were finished, three representative colonies were chosen from each condition and used in aggregation assays to assess biofilm formation behavior as described in Spencer-Williams et al.<sup>113</sup>. Briefly, *M. abscessus* isolates were grown in R2A liquid media after being taken from the plate, reinoculated, then allowed to grow for 35 hours as this is the time of aggregate dispersal<sup>113,114</sup>. Samples were taken during this time period by passing the culture through a 5 µm cell strainer (Pluriselect, Leipzig, Germany) and the optical density (OD<sub>600</sub>) of both the planktonic fraction (i.e., cells that passed through the strainer) and the aggregates (i.e., cells that remained on the strainer) were recorded. The OD<sub>600</sub> value of the planktonic fraction was immediately recorded, while aggregates that collected on the strainer were resuspended in 6% Tween20 - PBS solution (Sigma-Aldrich, St.

Louis, MO, USA). This suspension was then sonicated to resuspend remaining aggregates before recording the OD<sub>600</sub> value. Both OD<sub>600</sub> readings were used to calculate the planktonic to aggregate ratios.

### **3.2.10 Statistical Analysis**

All data was visualized and analyzed using R statistical software (Version 4.0.5). Data analysis for all culturing, absolute quantification data, and water quality data followed the protocols described in [Chapter 2](#), with the addition of the analysis of the PICRUST2 results being conducted using the ggpicrust2 package<sup>115</sup>, with significance determined by differential abundance analysis conducted with LinDA<sup>116</sup> with a Benjamini-Hochberg correction. Significant differences in the dataset, linear mixed-effect models, alpha and beta diversity analysis, and redundancy analysis were all conducted as previously described. Significant differences in the biofilm densities were determined using paired Wilcoxon tests.

## **3.3 Results And Discussion**

### **3.3.1 Silver-Containing Showerheads Minimally Impacted Metal Composition In Shower Water**

Because of the different material types used in the showerheads, water quality was assessed to determine if there were any material effects of the showerheads themselves on observed water quality. It is important to note that the DW tested met all mandatory regulatory standards upon

treatment, so this DW was safe for direct potable use after treatment. While many commonly reported water quality parameters (e.g. pH, free and total chlorine, and organic carbon) were unchanged by showerhead type (Appendix B Supplementary Table 3), the concentrations of many metals were deemed to be significantly different, despite absolute concentrations being relatively comparable (Table 3). Magnesium, cadmium, and manganese were consistent regardless of showerhead type (Table 3). Low levels of both cadmium and manganese are often found in DW due to the contribution of natural deposits<sup>117,118</sup>, and the consistency of these values suggests that the showerhead type does not contribute to these overall concentrations. Stable magnesium concentrations in the water samples could be attributed to the magnesium sacrificial anode rod in the hot water heaters of the INHALE shower laboratory.

Zinc and iron concentrations were significantly less in the silver mesh and silver-coated copper mesh showerheads compared to the ABS plastic, metal, and silver-embedded showerheads (Table 3). While there may be contributions of these metals from specific showerheads, the large discrepancies are most likely attributed to the differences in metal levels based on time sampled: the metal and silver-embedded showerheads were installed and sampled in 2021, whereas the silver mesh and silver-coated copper mesh showerheads were installed and sampled in 2022 which allowed for possible water chemistry changes between the two sampling campaigns. Iron and zinc in DW are associated with pipe corrosion in the DW distribution system, so the decrease in concentrations seen in 2022 may be linked to the continued formation and subsequent effectiveness of orthophosphate corrosion control scale formation. Orthophosphate is a common corrosion inhibitor that was adopted by the city of Pittsburgh in 2019 to reduce lead levels in DW<sup>113</sup> by creating a protective coating within pipes, which may have provided the added benefit of also

reducing the concentrations of other pipe metals such as the zinc and iron from galvanized steel in the water<sup>119</sup>.

Copper and silver were also deemed to be significantly different by showerhead type (Table 3), which was expected due to the addition of silver to the silver-embedded, silver mesh, and silver-coated copper mesh showerheads and copper in the silver-coated copper mesh showerhead (Table 2). As expected, total copper concentrations were highest in the silver-coated copper mesh showerhead, however, only half of that was in the dissolved fraction where there was more consistency between absolute values. Silver also was slightly elevated in the silver containing showerheads compared to the conventional showerheads, however these differences are more likely artifacts of the limit of detection and detection frequency of the analytical method used. Silver was detected more consistently from the silver-containing showerheads, with detection frequencies of 100% for silver-coated copper mesh showerheads, 56% for silver mesh showerheads, 39% for silver embedded showerheads, 34% for ABS Plastic showerheads, and 6% for metal showerheads. Additionally, when silver was detected, it was often at the limit of quantification: silver was only detected above the limit of quantification 0% and 8% of the time for the conventional metal and ABS plastic, and 78%, 22%, and 33% for the silver-coated copper mesh, silver mesh, and silver-embedded showerheads, respectively. The lack of consistent silver detection in the DW samples was unexpected from the silver-containing showerheads since the silver component was hypothesized to contribute to water chemistry, but it is possible that the silver remained attached to the component and must have direct contact with the bulk water in order to provide additional disinfection.

**Table 3: Average and standard deviation of the total and dissolved metal concentrations recovered in shower water from different showerhead types in mg/L across all sample timepoints (n=18 for each antimicrobial showerhead and n=36 for ABS showerheads). Significance in analyte concentrations between head types were determined via one-way analysis of variants (ANOVA).**

Analyte	ABS Plastic	Metal	Silver Mesh	Silver-coated Copper Mesh	Silver-embedded	<i>p</i> -value from ANOVA
<b>Total Silver</b>	3.3 x 10 <sup>-3</sup> ± 0.01	5.6 x 10 <sup>-4</sup> ± 2.4 x 10 <sup>-3</sup>	8.9 x 10 <sup>-3</sup> ± 0.02	0.1 ± 0.2	0.01 ± 0.02	<b>&lt;0.001</b>
<b>Total Magnesium</b>	3.9 x 10 <sup>3</sup> ± 625.6	4.0 x 10 <sup>3</sup> ± 664.0	3.9 x 10 <sup>3</sup> ± 791.3	3.9 x 10 <sup>3</sup> ± 802.2	3.9 x 10 <sup>3</sup> ± 636.5	>0.05
<b>Total Copper</b>	59.1 ± 36.3	86.5 ± 36.1	45.7 ± 22.3	101.3 ± 78.6	88.7 ± 21.8	<b>&lt;0.001</b>
<b>Total Iron</b>	248.8 ± 463.2	440.1 ± 674.7	51.4 ± 14.2	52.7 ± 12.1	417.0 ± 599.5	<b>0.02</b>
<b>Total Lead</b>	0.2 ± 0.3	1.4 ± 1.0	0.3 ± 0.5	0.2 ± 0.2	0.4 ± 0.4	<b>&lt;0.001</b>
<b>Total Zinc</b>	77.9 ± 47.8	121.5 ± 27.4	55.8 ± 58.2	45.2 ± 38.8	118.6 ± 43.8	<b>&lt;0.001</b>
<b>Total Manganese</b>	5.0 ± 13.8	11.4 ± 24.0	0.7 ± 0.8	0.7 ± 0.8	5.7 ± 10.6	>0.05
<b>Total Cadmium</b>	0.02 ± 0.1	9.0 x 10 <sup>-3</sup> ± 7.4 x 10 <sup>-3</sup>	3.3 x 10 <sup>-3</sup> ± 0.02	5.0 x 10 <sup>-3</sup> ± 0.02	4.5 x 10 <sup>-3</sup> ± 7.9 x 10 <sup>-3</sup>	>0.05
<b>Dissolved Silver</b>	0 ± 0.01	0 ± 0	0.02 ± 0.07	0.1 ± 0.1	0.1 ± 0.4	<b>0.04</b>
<b>Dissolved Magnesium</b>	3.8 x 10 <sup>3</sup> ± 608.5	3.9 x 10 <sup>3</sup> ± 609.5	3.9 x 10 <sup>3</sup> ± 700.6	3.9 x 10 <sup>3</sup> ± 740.0	3.8 x 10 <sup>3</sup> ± 583.5	>0.05
<b>Dissolved Copper</b>	41.9 ± 31.7	63.2 ± 34.8	28.0 ± 14.0	56.5 ± 28.0	67.8 ± 27.0	<b>&lt;0.001</b>
<b>Dissolved Iron</b>	186.0 ± 385.6	320.8 ± 516.5	61.5 ± 50.0	86.7 ± 136.2	307.9 ± 513.2	>0.05
<b>Dissolved Lead</b>	0.02 ± 0.06	0.6 ± 0.5	0.2 ± 0.7	0 ± 0.06	0.1 ± 0.1	<b>&lt;0.001</b>
<b>Dissolved Zinc</b>	55.2 ± 41.6	99.0 ± 29.7	30.7 ± 30.0	25.4 ± 19.6	91.3 ± 31.9	<b>&lt;0.001</b>
<b>Dissolved Manganese</b>	5.3 ± 22.8	1.7 ± 3.0	0.6 ± 2.0	1.8 ± 5.3	0.6 ± 0.6	>0.05
<b>Dissolved Cadmium</b>	0 ± 0.01	0.09 ± 0.3	5.6 x 10 <sup>-3</sup> ± 0.02	0.01 ± 0.05	2.8 x 10 <sup>-3</sup> ± 4.6 x 10 <sup>-3</sup>	>0.05

### 3.3.2 Silver-Containing Showerheads Did Not Impact Viable DWPI Concentrations In Shower Water

This study quantified DWPIs using traditional culturing and culture-independent techniques. While culturing is used in many studies to determine viable concentrations of DWPIs, it can underestimate the density of microorganisms present due to the ability of DWPIs to enter a VBNC state<sup>26</sup>, which often occurs when DWPI are exposed to chemical stress such as silver ions<sup>102</sup>. Coupling culturing with a molecular absolute quantification method such as RT-ddPCR allows for VBNC microorganisms to be detected, and thus discounts potential differences in plate count results between conventional and silver-containing showerheads due to potential loss in cultivability. Regardless of methodology, there was no statistically significant difference ( $p > 0.05$ ) between DWPI densities recovered using culture or ddPCR by showerhead type (Figure 9). Furthermore, no water sample across both sampling campaigns was culture positive for *L. pneumophila* or *P. aeruginosa*, which was not necessarily surprising given that both DWPIs are often transiently detected in hot DW systems due to their preference for biofilm growth<sup>6,21,120</sup> as well as their ability to enter into a VBNC state<sup>25,26,101</sup>. NTM, specifically the rapid growing species (*Mycobacterium gordonae* and *Mycobacterium phocaicum/ mucogenicum*) were abundantly cultured from water samples sourced from every type of showerhead tested, with several samples exceeding the limit of quantification (Figure 9A). These results were largely in agreement with the absolute molecular quantification data (Figure 9B), however molecular NTM quantification was lower than expected likely due to the RNA extraction method not being rigorous enough to lyse NTM's notoriously resistant and thick cell membrane<sup>83</sup>. Interestingly, although *L. pneumophila* and *P. aeruginosa* were not culturable they were quantified at low density using the molecular

approach (RT-ddPCR) in all showerheads (Figure 9B) suggesting that the DWPIs are either in a VBNC state, not evenly distributed in the water or below the culturing detect limit.

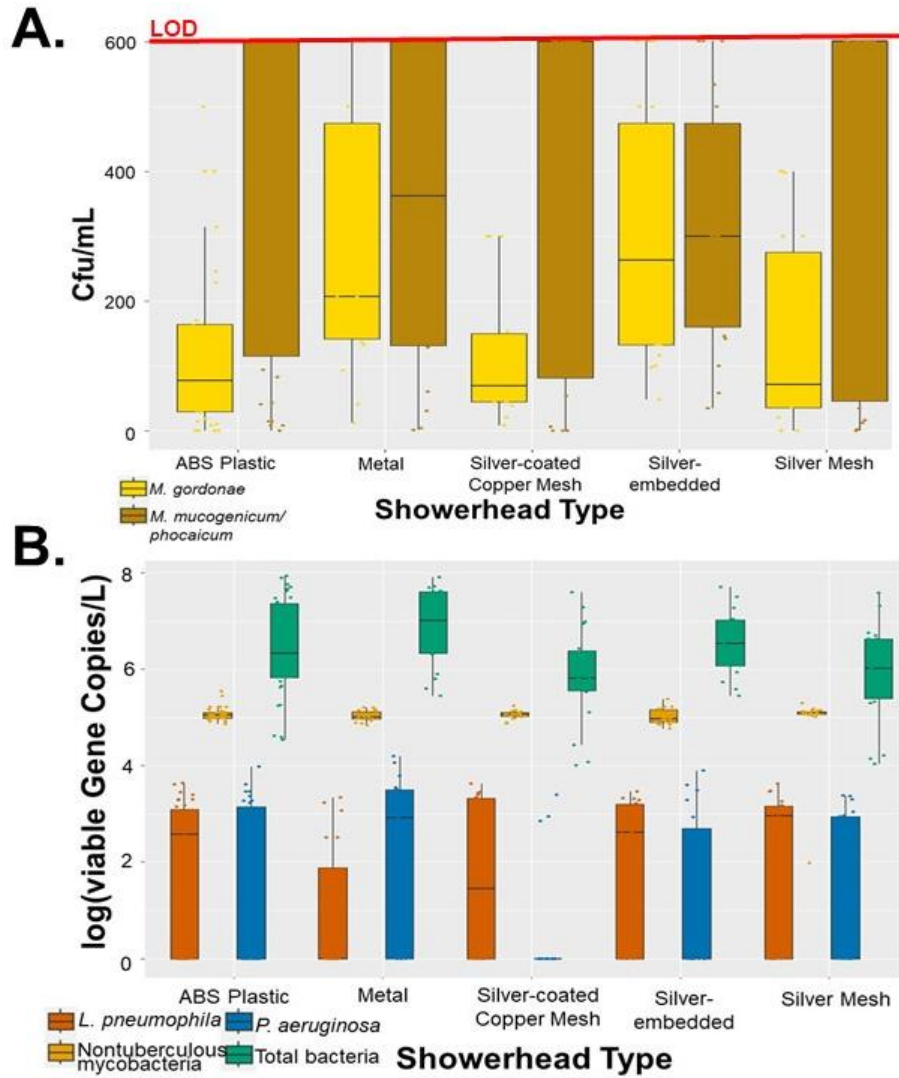


**Figure 9: Quantification of DWPIs by showerhead type. A. Enumeration of *Mycobacterium gordonae* (light yellow) and *Mycobacterium phocacium/mucogenicum* (light brown) in culture. The red line labeled “LOD” refers to the upper limit of detection of the culturing method. B. Microbial densities of *Legionella pneumophila* (dark orange), *Pseudomonas aeruginosa* (dark blue), nontuberculous mycobacteria (gold), and total bacteria (green).**

The microbial results from both culturing and ddPCR analysis suggest that these silver-containing showerheads do not decrease the viable DWPIs and total bacterial densities in shower water any more effectively than non-silver containing showerheads. A variety of factors such as insufficient silver concentration, silver source, or contact time can be responsible for these showerheads' lack of antimicrobial action. In the case of the silver-embedded head where there was no visible metal component, EDS and SEM analysis on two separate inserts failed to find any of the marketed antimicrobial silver materials (Appendix B Figure 1). Each of these inserts was tested in three different locations: on either side of where water passes through, and in the center of the insert to maximize the potential to locate the silver in the showerhead. This finding challenges the marketing claims of this showerhead, but it is possible that all the sites on both inserts received inconsistent dosing of silver nanoparticles during polymer formation or that there is silver in other components of this showerhead, however regardless of if this is the case the result is insufficient disinfection.

To further isolate the effects of pure silver without the potential shortcomings of commercially available showerheads, showerheads containing pure silver mesh were created in-house and tested, and even these showerheads did not reduce microbial loads. Because of these findings, it is likely that the effectiveness of silver-containing showerheads in standardized ISO tests but not in real-world application can be attributed to materials testing methodology: the silver-embedded showerhead was tested using ISO 22196:2011 which measured pure culture solutions exposed to the silver-containing material after 24 hours of exposure<sup>56</sup>, and the silver-coated copper mesh showerhead was tested using ASTM E 2149 which measured pure culture solutions only exposed to the mesh after 16 hours of exposure<sup>121</sup>. Although both methods showed >2 log removal

of relevant microorganisms such as *L. pneumophila* and *P. aeruginosa*, the methodology itself is a poor proxy to the showering environment.

The microbial community in shower water and the biofilms they form are complex and intertwined<sup>18</sup>. They often display functional characteristics such as antimicrobial resistance that vary greatly from laboratory strains<sup>122</sup>. Therefore, reducing these community complexities by using microorganisms that are not commonly found in DW to test antimicrobial materials may yield results that may appear that the antimicrobial treatment is more effective than it is for application in DW. Another crucial factor to consider is the contact time (amount of antimicrobial material and the duration of treatment) used in these tests; testing the antimicrobial properties over multiple hours may show that it is effective at achieving log removals of microorganisms, but water flowing through the showerhead and hose under use conditions would only be exposed to the antimicrobial material for a brief amount of time before exiting the showerhead. If the antimicrobial silver showerheads exhibited poor performance due to insufficient contact time, then at the very least the initial stagnant water plug within the showerhead and hose would be adequately treated. Although this particular water fraction wasn't singled out in our study, any resulting impact should still have been observable given the first plug of water after stagnation contains the highest microbial loads<sup>1,48,77</sup>. Overall, this study has shown that the standardized methods used to evaluate antimicrobial materials must consider the application to appropriately test their effectiveness and thus generate market claims that are applicable to consumer use.

### 3.3.3 Microbial Community Membership Varied Between Showerhead Type In Shower

#### Water

Although the anti-microbial silver-containing showerheads did not effectively reduce absolute or culturable numbers of DWPIs or total bacteria, there was potential for the presence of silver to affect the greater microbial community. It is known that materials used in DW plumbing can affect microorganism growth<sup>44,85,123,124</sup>, so it is reasonable to consider that the materials in the showerheads tested will likewise influence the microbiome. Silver's effects on the DW microbial community when used as a plumbing material have not been explored to the authors' knowledge. However, sublethal exposure to antimicrobial substances like silver have been shown to select for increased resistance to antimicrobial metals in the microbial community<sup>98,102,103</sup> in addition to co-selecting for antibiotic resistance genes<sup>125</sup> that may cause unintended public health consequences.

Sequencing analysis on the water samples revealed significant variations in community structure among samples obtained from different showerhead types, evident in distinct clustering observed in NMDS plots (see Appendix B Figure 3). Subsequent redundancy analysis on the microbial community showed that showerhead type was a statistically significant factor explaining 10.2% of the variance in community composition ( $p = <0.001$ ). Furthermore, showerhead type significantly impacted alpha diversity (Appendix B Table 6).

Assessing the membership of the shower water microbiome in the different showerheads there were clear differences; metal showerheads had the lowest absolute number of total taxa present in samples (genera=74, OTU=121), followed by the silver-embedded (genera=102, OTU=203), silver mesh (genera=142, OTU=239), ABS plastic showerheads (genera=144, OTU=293), and the silver-coated copper mesh showerhead (genera=270, OTU=802) had the

greatest number of genera (Figure 10A). Interestingly, two-thirds of the genera present within silver-containing showerheads were unique / not shared with the other showerhead types (Figure 10A). When compared to the conventionally used ABS showerhead, the heterogeneity of the microbial community recovered from the silver-containing showerheads both in number of genera present and the minimal overlap in the specific taxa suggests that the actual form of the silver in the showerhead more closely influenced the viable microbial community more so than simply the presence or absence of silver.

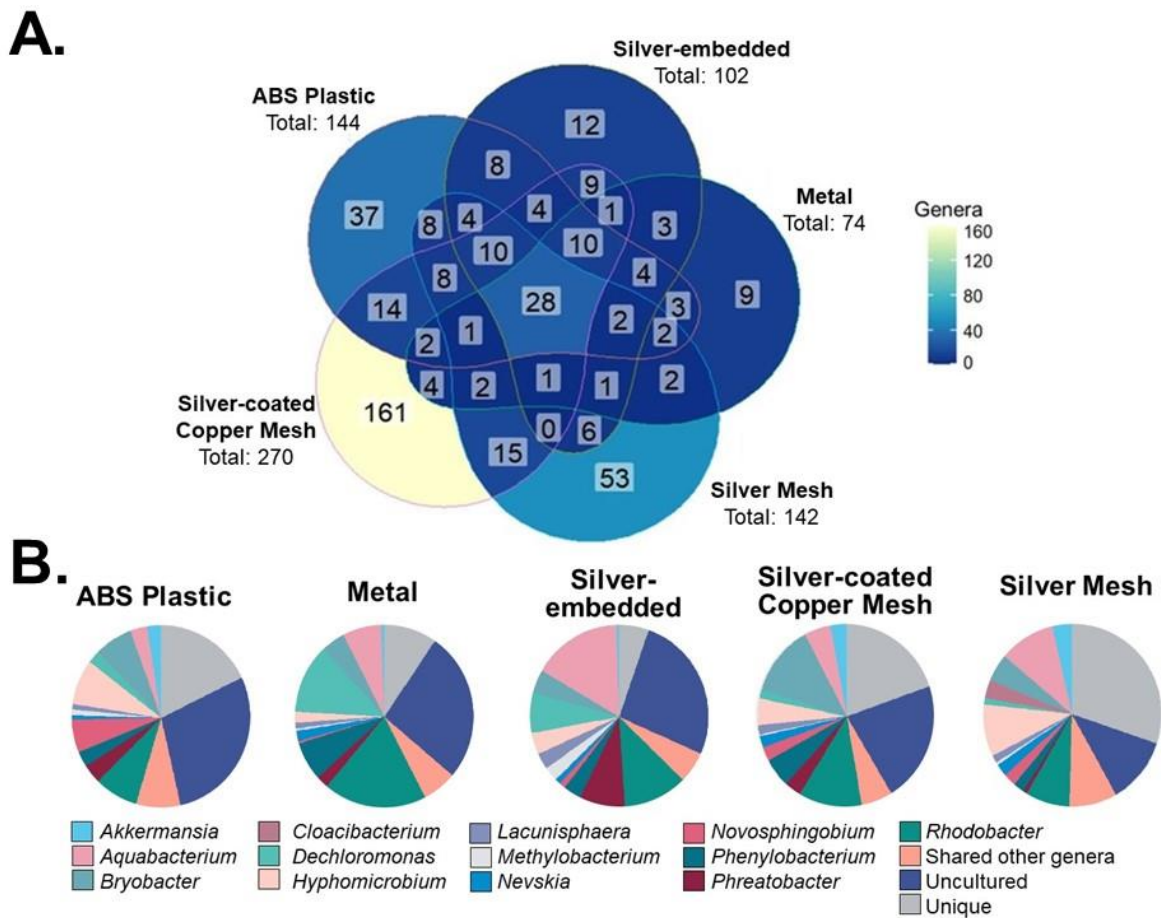


**Figure 10: The overlap and proportion of core genera (84% relative abundance on average) in each showerhead type. A. Venn diagram illustrating the shared and unique genera between different showerhead types, and B. Pie charts showing the relative abundance of core genera in each showerhead type. All other shared genera**

**constituting <30% relative abundance each were combined in the “shared other genera” category, and all genera not present in all showerhead types were combined in the “unique” category.**

Assessing the common shared or core microbiome across all samples (Figure 10), only 28 genera were found, which is surprising given all the samples were sourced from the same system. In this core community, genera associated with DWPIs were present (e.g., *Legionella* and *Pseudomonas*), which was in agreement with the quantification data, as well as *Burkholderia-Caballeronia-Paraburkholderia*, another emerging DWPI<sup>1</sup> that was not targeted for direct quantification in this study. These DWPIs, while ubiquitous, were not in the top ten most abundant genera in the water samples. In addition, sequencing data revealed that *Mycobacteria* was not detected in every sample which corroborates the poor NTM recovery reflected in the absolute quantification data.

Assessing the 28 dominant and core microbiome shared across all showerhead types *Pseudomonadota / Proteobacteria* was the dominant phylum accounting for on average 57% of the community, with 58% of these organisms being members of the *Alphaproteobacteria* class. *Pseudomonadota / Proteobacteria* dominance is consistent with many other DW microbiome studies<sup>18,126–129</sup>, and likely is explained by their ability to thrive in chlorinated systems in both the bulk water and biofilms<sup>18,129</sup>. Further, the phylum contains many of the Gram-negative DWPIs that have been identified to be of public health concern<sup>1</sup>, as well as being a known reservoir for antimicrobial resistance genes<sup>126</sup>. Furthermore the other 27 major genera found in this study are consistently found in high relative abundance in previous DW studies<sup>88,90</sup>, although interestingly there were differences in the specific relative abundances between the showerheads. For example the conventional ABS plastic showerhead had higher relative abundances associated with *Novosphingobium* than the other showerheads which has been observed in other water systems

using conventional materials<sup>130-132</sup>. *Dechloromonas* was found in higher abundances in the metal showerheads. This genus were found to dominate a model distribution system constructed of steel likely due to it supporting various redox reactions<sup>132</sup>. Given its dominance in metal showerhead samples, it can be assumed that distinct environmental conditions have been formed to favor for the proliferation of facultative anaerobes like *Dechloromonas*. Regardless of only 28 core taxa being shared across all samples, these genera accounted for 70-95% of the relative abundance in the samples, suggesting that the significant differences in community composition observed are due to rare taxa (Figure 10B).

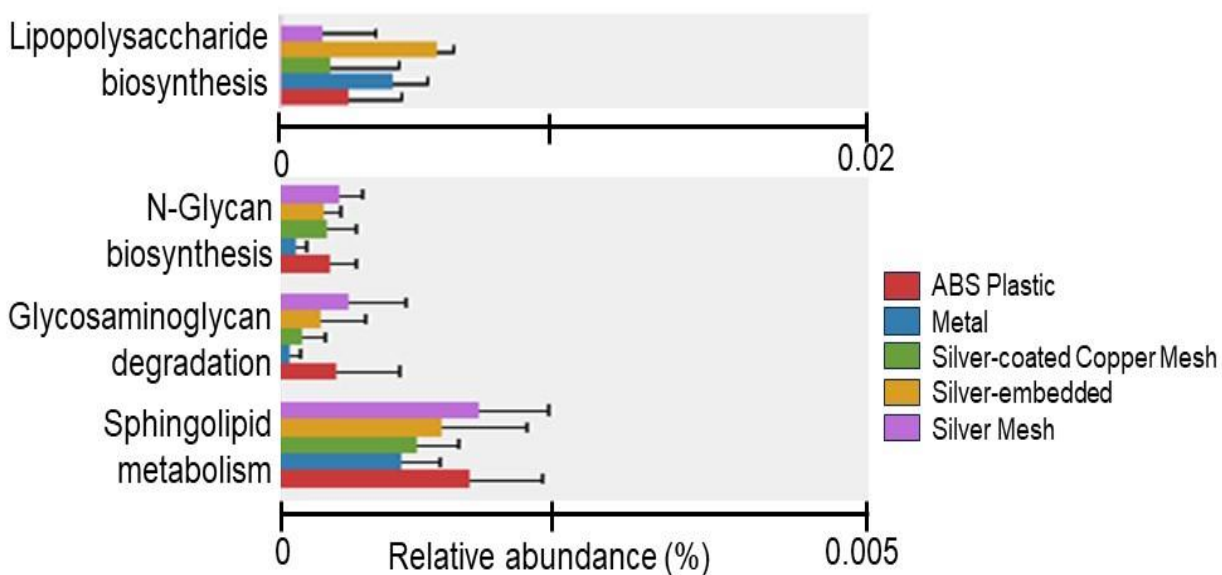


**Figure 11: Average relative abundance and standard deviation of statistically significant functional traits in water samples by showerhead type obtained from PICRUSt analysis.**

Although >70% of the genera and 52.5% of OTU relative abundances were shared between all showerhead types, there were distinct differences in predicted community functionality traits (Figure 11). Particularly, important functional differences that impact biofilm development and

possible pathogenicity were significantly affected, such as the synthesis of lipopolysaccharides and N-glycans and the metabolism of glycosaminoglycans and sphingolipids. Lipopolysaccharides are known to be essential components of the Gram-negative bacterial cell membranes, and can elicit a response to the human immune system<sup>32</sup>. Although lipopolysaccharides may reduce biofilm-forming capabilities of microorganisms<sup>133</sup>, their presence indicates higher levels of Gram-negative microorganisms and as a consequence, greater potential pathogenicity<sup>134</sup>. Interestingly, the known silver-containing showerheads (the silver-coated copper mesh and silver mesh) had lower relative abundances of lipopolysaccharide synthesis than the conventional material showerheads, which suggests that the silver-containing showerheads may select for microorganisms that have better biofilm-forming characteristics. This hypothesis is supported in other possible traits identified to be significantly different from the conventional ABS showerhead. Silver mesh showerheads were observed to have the highest levels of N-Glycan biosynthesis and degradation of glycosaminoglycans and sphingolipids- traits crucial for biofilm formation and stress tolerance<sup>135,136,136,137</sup>. Therefore, it is not surprising that microorganisms in direct contact with pure silver would display heightened functional traits for stress management, with the formation of biofilms representing a well-documented microbial strategy for surviving physical, chemical, and biological stress<sup>138,139</sup>. Since there is limited understanding of these particular pathways and characteristics in the DW microbiome, additional research is necessary to fully understand the functionality of these specific traits within the microbial community. Moreover, further investigation into gene expression is warranted to validate whether these traits are being upregulated in response to silver.

Though the non-lethal effects of silver on the DW microbiome have not been extensively researched, what work that has been published surrounding the effects of silver have corroborated

trends in this dataset<sup>99,140-145</sup>. The microbial community of water treated with CSI have been reported to increase the number of rare taxa in the treated water, but did not significantly alter the dominant microbiome<sup>140</sup>. In addition, silver amendment to stainless steel pipes did not impact biofilm formation but increased the number of rare taxa present compared to plain stainless steel<sup>141</sup>. Looking holistically at the use of silver as an antimicrobial in other environmental matrices its impacts on the microbiome seem to vary based on the state of silver used (e.g., nanoparticle or ion<sup>99,142</sup>), what other chemicals are present as either surface stabilizers or anions<sup>143,145</sup>, and whether the exposure is continuous or an isolated event<sup>143-145</sup>. Because of this, it is essential for collaboration between engineering and materials science to fully characterize how materials influence the microbial community and to optimize disinfection strategies using silver and other intrinsic antimicrobials.

### **3.3.4 Showerhead Age Influenced The Microbiota In Water Samples**

The showerhead age (days of use), or the amount of time of daily use of the showerhead, was the second most important parameter in explaining the variance in the microbial community (explaining 5.2%,  $p > 0.001$  - Appendix B Table 6). Plumbing age has been identified to influence the microbiome due to material degradation and subsequent release into water as well as the opportunity to allow biofilms to develop<sup>146-148</sup>, which is expected to influence the microbiome of the resulting shower water due to the dynamic nature of biofilm growth<sup>45</sup>. Concentrations of viable DWPIs in shower water that were quantified using RT-ddPCR analysis showed no clear trends across all showerhead types (Appendix B Figure 5), but trends in cultured NTM emerged (Figure 12).

*M. gordonae* concentrations in shower water were most abundant in the initial (first incidence of sampling) and early (the first 30 days of use) biofilm growth periods, but then significantly decreased by the mature (after 30 days of use) biofilm growth period for the ABS plastic, metal, silver-embedded, and silver mesh showerheads (Figure 12A). Conversely, *M. mucogenicum* / *phocaicum* concentrations significantly increased by the mature biofilm growth period for the ABS plastic, metal, silver-coated copper mesh, and the silver mesh showerheads (Figure 12B).

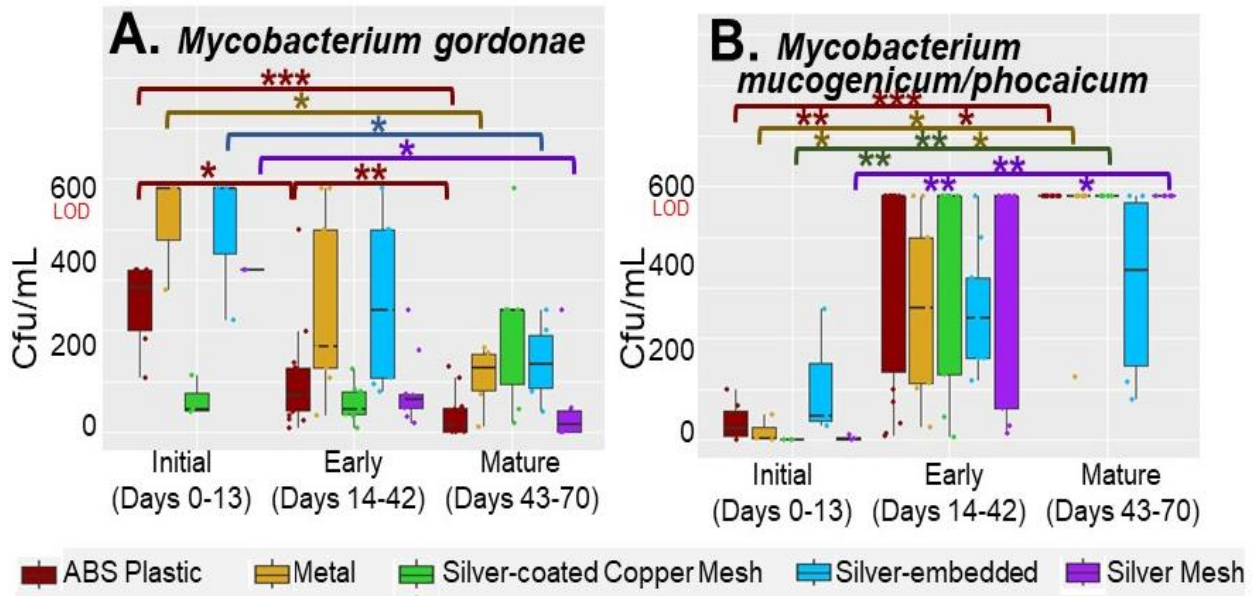


**Figure 12: Viable concentrations of A. *Mycobacterium gordonae* and B. *Mycobacterium mucogenicum* / *phocaicum* for ABS plastic (red), metal (yellow), silver-coated copper mesh (green), silver-embedded (blue), and silver mesh (purple) showerheads by biofilm formation stage. Significant differences at p-values <0.05, <0.01 and <0.001 are denoted by \*, \*\*, and \*\*\* respectively.**

This inverse relationship between NTM species observed in this study is interesting since it is known that *Mycobacterium sp.* can be cooperative across species in clinical infection<sup>149</sup> and many genera are often present in environmental samples<sup>48</sup>, so there are likely other factors at play

for the apparent genus succession seen in the culture results. *M. gordonae* is classified as a slow-growing NTM, whereas *M. mucogenicum* / *phocaicum* is a fast-growing NTM<sup>150,151</sup>: because NTM are known biofilm colonizers<sup>43,46</sup> and are relatively hydrophobic due to their unique cell membranes<sup>83</sup>, it is possible that *M. gordonae* did not assimilate to the biofilm until after weeks of continuous use and consequently was found in the water fraction in early weeks. *M. mucogenicum* / *phocaicum*, on the other hand, may have established biofilm growth earlier due to their faster growth rate, then thus experienced accelerated biofilm dynamics so that sloughing could occur. These trends in NTM data after initial colonization were also observed in a study conducted by Yang et al.<sup>152</sup> in established DW distribution systems and building plumbing, where *M. gordonae* was more abundant in biofilm swab samples and *M. mucogenicum* was more abundant in water samples<sup>152</sup>. The culture-independent quantification data showed that NTM as a genus did not significantly change as a function of time, so monitoring species distributions within a genus can help better assess potential risk since each species of NTM has a different infection incidence<sup>151</sup>.

Other viable DWPIs assessed in this study followed trends in the water samples that have been previously described in Chapter 2, where *L. pneumophila* and *P. aeruginosa* were variable and transient throughout the system regardless of biofilm age, and total bacteria concentration was variable, with the higher concentration in the silver mesh showerheads and lowest concentration in the metal showerheads (Appendix B Figure 5). It is possible that contact with the pure silver mesh in the showerhead provided some disinfection, which may have lessened over time as the material itself aged or was covered by scale or silver-resistant biofilms. The microbial densities in the water taken from the metal showerheads, conversely, may be equally influenced by the showerhead material type: while there is little literature surrounding the impacts of oiled bronze specifically on microbial growth, metals in general support formation of more robust biofilms that

can grow thicker compared to other materials due to microscopic corrosion that occurs and creates a better environment for microbial adhesion<sup>85,147</sup>.

There were no statistically significant differences in beta diversity by biofilm development age in the water samples. However, there were some differences in alpha diversity. When all water samples were pooled regardless of showerhead type, evenness significantly decreased as a function of biofilm development age and diversity subsequently increased (Appendix B Table 6). These significant changes in diversity and evenness with fixture age point towards the showerhead hosting a dynamically changing environment (e.g., temporal chemical gradients, changing surface topology due to biofilm formation and changing biofilm membership) which selects for different organisms. Moving forward it is important that future risk assessment tools consider showerhead age as this will likely influence the concentration and types of organisms exiting in shower water.

### **3.3.5 Shower-Associated Biofilms Contained Complex Microbial Communities**

The results of this chapter highlight how important temporal dynamics of biofilm development are in helping explain the microbial trends in the water samples. Two types of biofilm samples were taken in this study that provide different insights into the sessile microbial fraction: swab samples were taken of the biofilm at the outlet of the building plumbing before and after 12 weeks of continuous fixture use and analyzed for RNA (the living community), and the entire biofilm grown in the showerhead hose over the 12 weeks was recovered and analyzed for DNA. The outlet swabs, which will be referred to as ‘swab’ samples in this section, illustrated the microbial characteristics of the plumbing system prior to material type being introduced as a variable, and help elucidate how consistent use over time impacts the viable microorganisms in

the plumbing system. The biofilm recovered from the hoses, which will be referred to as the ‘hose’ samples in this section, offered insights into how the biofilms were influenced by showerhead and hose material type. While these two types of samples are both of biofilms, their results cannot be directly compared to each other because of the different extraction methodology which may introduce recovery bias for certain organisms<sup>32</sup> and nucleic acids assessed as hose samples will represent both the viable and dead microbial community.

DWPI densities in the swab and biofilm samples followed abundance trends seen in the water samples in this body of work and samples described in the previous chapter<sup>153</sup>, where *L. pneumophila* and *P. aeruginosa* were present inconsistently and in low quantities when detected, and NTM were detected in greater quantities with more consistency (Figure 13). The swab samples taken before and after the 12 week-long sampling period showed consistent DWPI densities between individual samples as well as when compared to sampling time (Figure 13A). There was a significant increase in *L. pneumophila* after the sampling campaign was concluded, which inversely correlates to the trends seen in the water samples. Although *L. pneumophila* was not elevated in the shower water, the higher density in the biofilm may lead to sloughing events beyond the 12-week sampling period. Because shower systems often are used for more than 12 weeks at a time, longer periods of use must be evaluated to determine if this change could have adverse outcomes in microbial water quality.

The hose samples taken from the silver-embedded and metal showerheads had very little genetic material recovered during extraction likely due to unoptimized recovery procedures, but samples from the ABS plastic, silver mesh, and silver-coated copper mesh showerheads were processed with additional detachment steps which improved recovery. Because of this, comparison

of absolute microbial densities for these the silver-embedded and metal showerheads cannot be conducted. Comparing the ABS plastic, silver mesh, and silver-coated copper mesh showerheads, there were no statistically significant differences in microbial densities, so it is likely that the silver-containing showerheads and hoses do not act as an effective bacteriostatic material over the course of 12 weeks (Figure 13B).

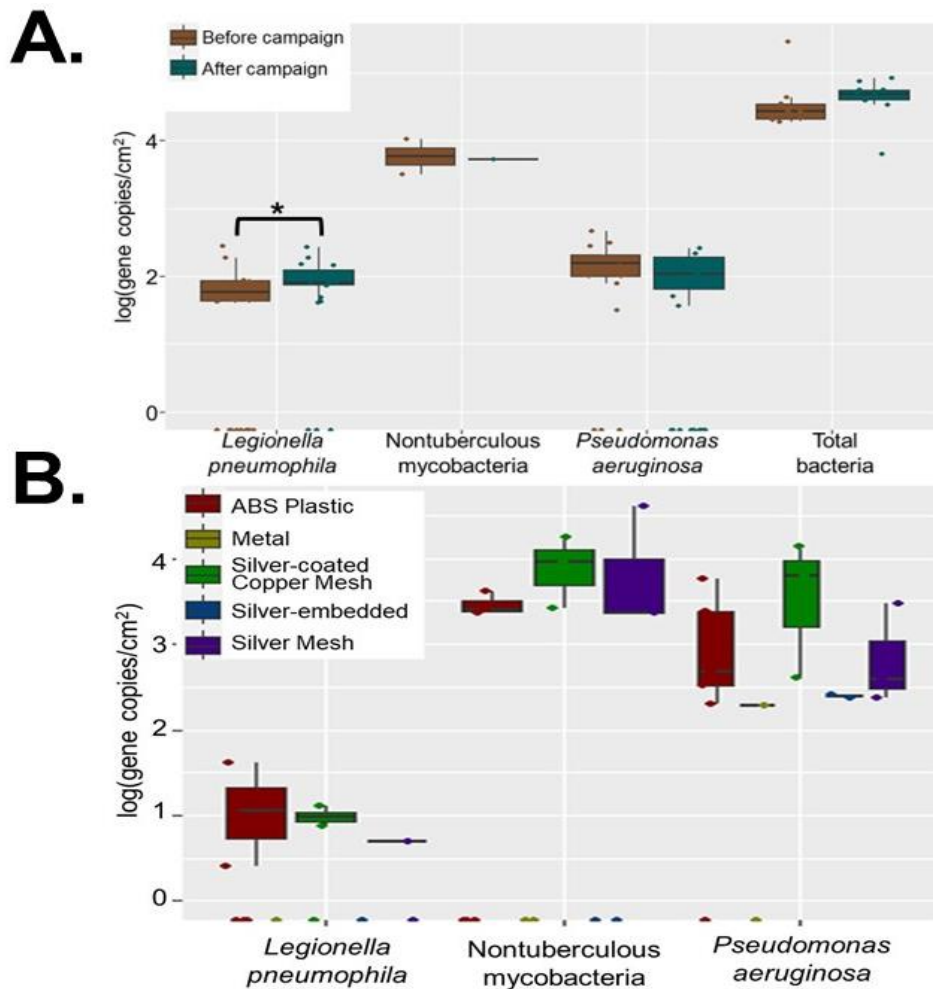


**Figure 13: Absolute quantification of DWPI biofilm densities in A. swab samples before (n=18) and after (n=18) the 12 week long sampling campaign and B. hose samples of different showerhead types (n=3) after 12 weeks of daily use.**

Looking at the microbiomes, the alpha and beta diversity metrics of the hose and swab biofilm communities were not significantly different between the showerhead types and time sampled (Appendix B Table 6). This structural similarity echoes the absolute quantification data, where there were no large differences in magnitude for any of the DWPIs. However, there were marked changes in the dominant community membership for both sample types (Figure 14). Overall, there were 233 and 217 genera present in the swab and hose samples, respectively, with 37% and 29% of core microbiome shared at the beginning and end of the study in the swab and between the different showerhead types in hose samples, respectively. Despite the large number of genera present that were unique to each shower hose type as well as the before and after swab samples, the relative abundances of the shared genera for each sample type were 85% on average in the swab samples and 92% on average in the hose samples. Interestingly, despite the similar relative abundance of taxa in the core biofilm and swab microbiomes differences were present in which taxa dominated in different showerheads.

Swab samples were dominated by uncultured bacteria regardless of time sampled, and many of the identifiable microorganisms such as *Pseudomonas* are known biofilm formers<sup>82</sup>. The relative abundances of *Bradyrhizobium*, *Bryobacter*, *Nevskia*, and *Novosphingobium* decreased as a function of shower use, and conversely, the relative abundances of *Bacillus*, *Rhodobacter*, and *Ruminoclostridium* 9 were higher in the samples taken at the conclusion of the sampling campaign (Figure 14A). These dominant taxa have been previously recovered from shower-associated biofilms as major community members<sup>6,42</sup>, but there has been little biofilm work in full-scale systems that monitor how biofilms change over time to compare this data to since most DW biofilm studies use biofilm reactors with small coupons of pipe material to monitor growth dynamics<sup>85,108,154</sup>.

The hose biofilm community demonstrated high variation in major taxa by shower hose type, with marked differences in all taxa present (Figure 14B). The biofilms recovered from the silver-containing showerheads had fewer total number of genera present and lower relative abundances of rare taxa than the non-silver showerheads and hoses, which corroborates the findings of Chapter 2<sup>153</sup> that silver used in fixtures functions less like an antimicrobial (since the DWPI densities were fairly consistent) and more like a microbial selector.

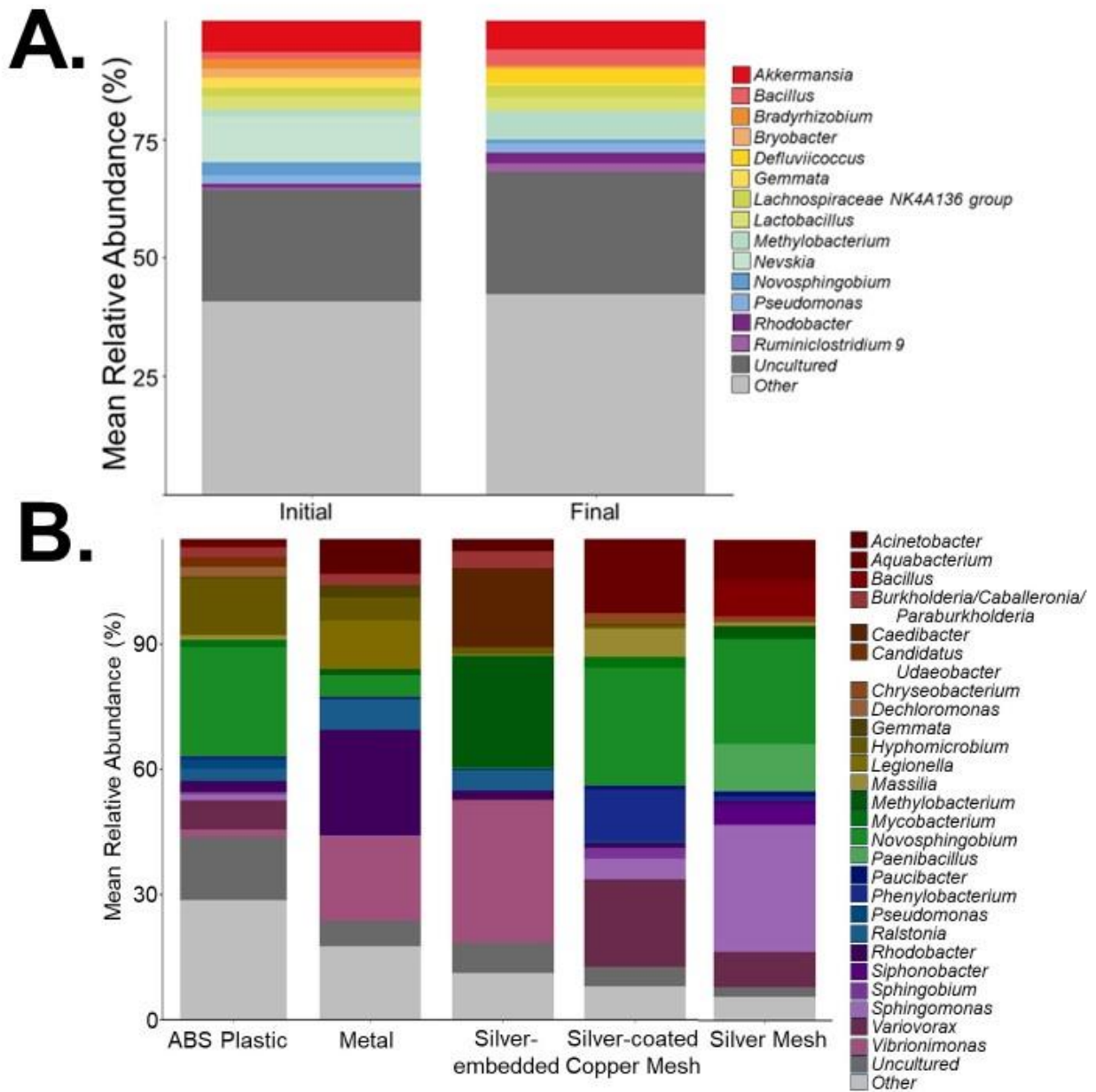
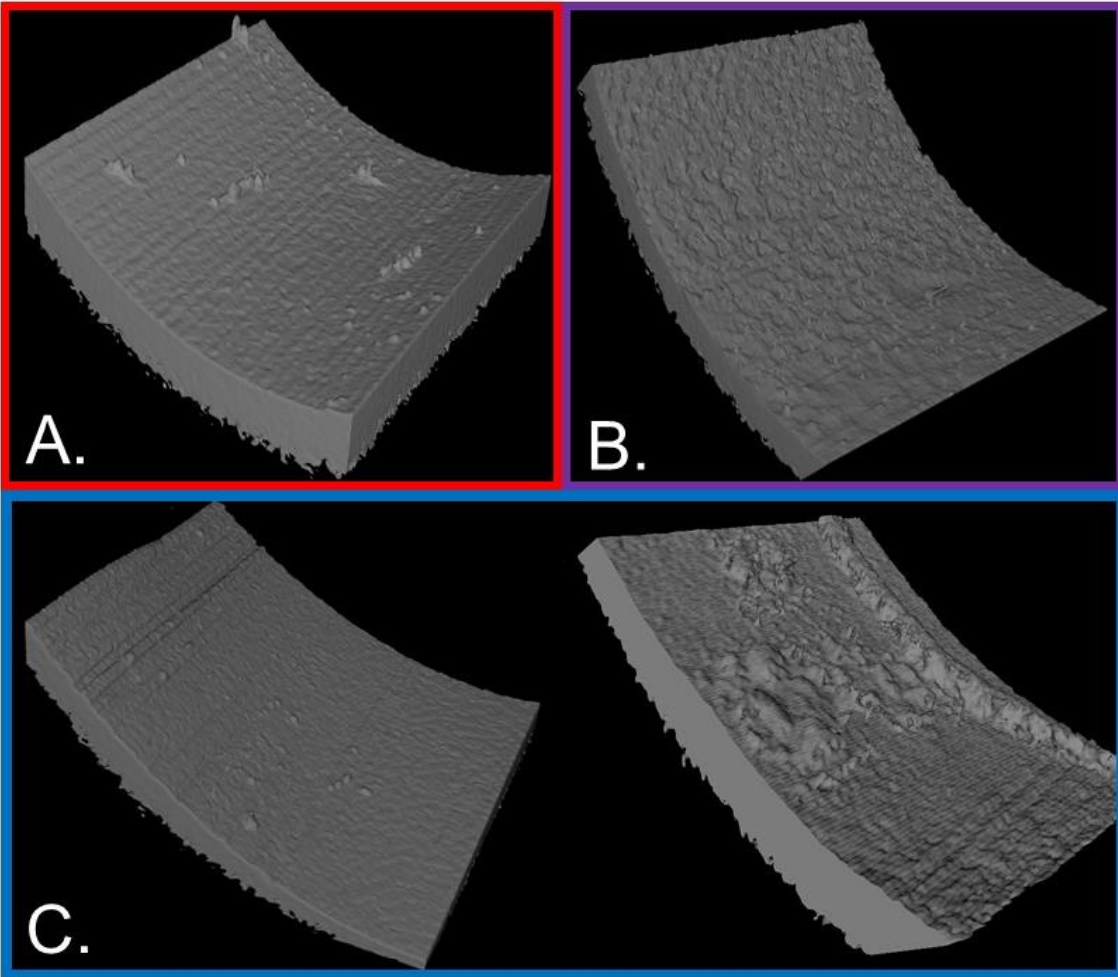


Figure 14: Ten most abundant genera from A. swab samples taken from the plumbing outlet before the shower hose before (n=18) and after (n=18) the 12 week long sampling campaign and B. hose samples of different showerhead types (n=3) taken from the hose to the showerhead after 12 weeks of daily use.

### 3.3.6 Shower Hose Biofilm Topography Was Influenced By Material Type

Biofilms imaged from the showerhead hoses had similar quantities of overall biofilm development regardless of showerhead type, but the overall morphology of the biofilm differed (Figure 15). The biofilm grown on ABS plastic showerheads tended to form small clumps of varying depth, shape, and roughness unevenly across the sample surface (Figure 15A) consistent with findings from a study conducted in plasticized poly-vinyl chloride showerheads<sup>155</sup>. The inconsistent biofilm formation in the ABS showerheads could be attributed to the variable amounts of organic carbon leaching from the hose itself: both plasticizers and the materials have been identified as potential carbon sources and influence growth in DW<sup>44,124</sup>. The silver-coated copper mesh hoses grew biofilms that covered the hose samples more evenly, but had large rough protrusions and depressions resembling hills and valleys all over the interior surface (Figure 15B). The silver mesh hoses showed much greater biofilm morphology variation, with some samples presenting with modest biofilm growth (a few small clusters), and other samples had large, tall clusters of microbial growth in specific portions of the hose, with little growth on other sections (Figure 15C). The differences seen between the silver shower hoses may be due to material effects or from the actual implementation of the material in the shower hose. It is known that there are additive antimicrobial benefits to combining copper and silver<sup>102,112</sup>, so this could contribute to the overall lower biomass observed in the silver-coated copper mesh hoses (Figure 15C) compared to the silver mesh hoses (Figure 15B). An alternative explanation could be that the way the silver agent was incorporated: the silver-coated copper mesh was implemented by the manufacturer, and was in a cylindrical shape, whereas the silver mesh was installed by the research team in the showerhead alone, and may have been resting on the wall of the hose at some points due to the sheet-like nature of the

silver mesh used. Subsequently, these material shapes could impact flow within the hose, explaining the ridge seen in one of the OCT images.



**Figure 15: Representative 3D renderings generated from OCT images taken from A. ABS plastic shower hoses, B. hoses containing pure silver mesh, and C. shower hoses with the addition of silver-coated copper mesh in the hose.**

OCT has been used as a valuable visualization tool to study biofilm formation<sup>42,156–160</sup>, however there have been no studies to the author’s knowledge utilizing OCT to study the impacts of silver materials on the resulting biofilm structure. OCT analysis of DW biofilms formed on common plumbing materials observed compaction after 30 days of flow, which is consistent with

the observations of this study, where all biofilms were tightly compressed at the time of analysis<sup>159</sup>. Additionally, OCT analysis conducted in other hoses collected from chlorinated DW systems also reported similar biofilm structures to what was seen in this study<sup>42</sup>. OCT methodology for *in-situ* analysis of DW biofilms is an emerging topic of research<sup>158</sup>, and this preliminary analysis of shower hoses using OCT demonstrated that the DW biofilms formed in shower hoses are a reasonable candidate for imaging using this technique.

There has been little mechanistic work that has focused on the non-lethal impact of silver on the DW biofilm since much of the literature focuses on silver-containing treatments for the planktonic DW microbiome<sup>50,97,102,110</sup> or a material's ability to inhibit DW biofilm growth altogether<sup>161</sup>. The work on sub-lethal exposure of biofilms to silver has been done primarily in monoculture with *P. aeruginosa*, and has found that silver in either form (ion or nanoparticle) to be deleterious to overall growth<sup>162-164</sup>. However, some of these studies which have reported lower cell densities in biofilms exposed to silver<sup>100,162</sup> have suggested this may be due to VBNC state induction<sup>164</sup>. Additionally, silver exposure in either form has been shown in both gene expression and proteomics studies to change *P. aeruginosa*'s adhesion and dispersal behavior, ability to quorum sense, synthesize virulence factors, polysaccharides, and extracellular polymeric substance, the latter being integral to biofilm formation<sup>100,162,163</sup>. Collectively, these studies suggest that silver as an anti-biofilm forming material may be less effective than widely accepted, and additionally corroborates the results seen in the OCT images taken in this study.

### 3.3.7 Response To Silver Nitrate By *M. abscessus* Biofilms Was Dose-Dependent

Given the number of silver-containing showerheads on the market and the limited antimicrobial impact observed by these showerheads earlier in the chapter, it was important to assess whether contact time was the factor preventing inactivation. Operating CDC biofilm reactors containing ABS coupons seeded with an environmental or clinical *M. abscessus* biofilm the impacts of two different silver contact times (480 mg Ag<sup>+</sup>/L\*min, and 4800 mg Ag<sup>+</sup>/L\*min) were explored. Biofilm density measurements from either *M. abscessus* strain recovered from coupons taken from the control reactor (0mg Ag<sup>+</sup>/L\*min) after 7 days of operation were not statistically different ( $p > 0.05$ ) from measurements take from the coupons prior to being placed in the reactors (i.e., initial biofilm). Regardless of quantification method (microscopy, culture, or rt-ddPCR) there were no statistically significant reductions in *M. abscessus* biofilm densities between the control reactor and the 480 mg/L\*min Ag<sup>+</sup> reactor, meant to simulate the silver-only component of CSI<sup>110,112</sup>. However, there were decreases in both viable absolute abundances (6-6.9 log reduction) and culturable concentration (~3 log reduction) of *M. abscessus* in the 4800 mg/L\*min Ag<sup>+</sup> reactor meant to operate as an extreme exposure scenario (Figure 16). However, there were no significant differences in the reduction concentration between the clinical and environmental strains. These trends were also seen in the microscopy done on the biofilm (Figure 17). It should however be noted that the order of magnitude decrease between the 480 mg/L\*min Ag<sup>+</sup> reactor and the 4800 mg/L\*min Ag<sup>+</sup> reactor observed by viable absolute and culturing methods was not observed by microscopy, but this is likely due to dead cells remaining part of the biovolume adhered to the imaged coupon (Figure 17).

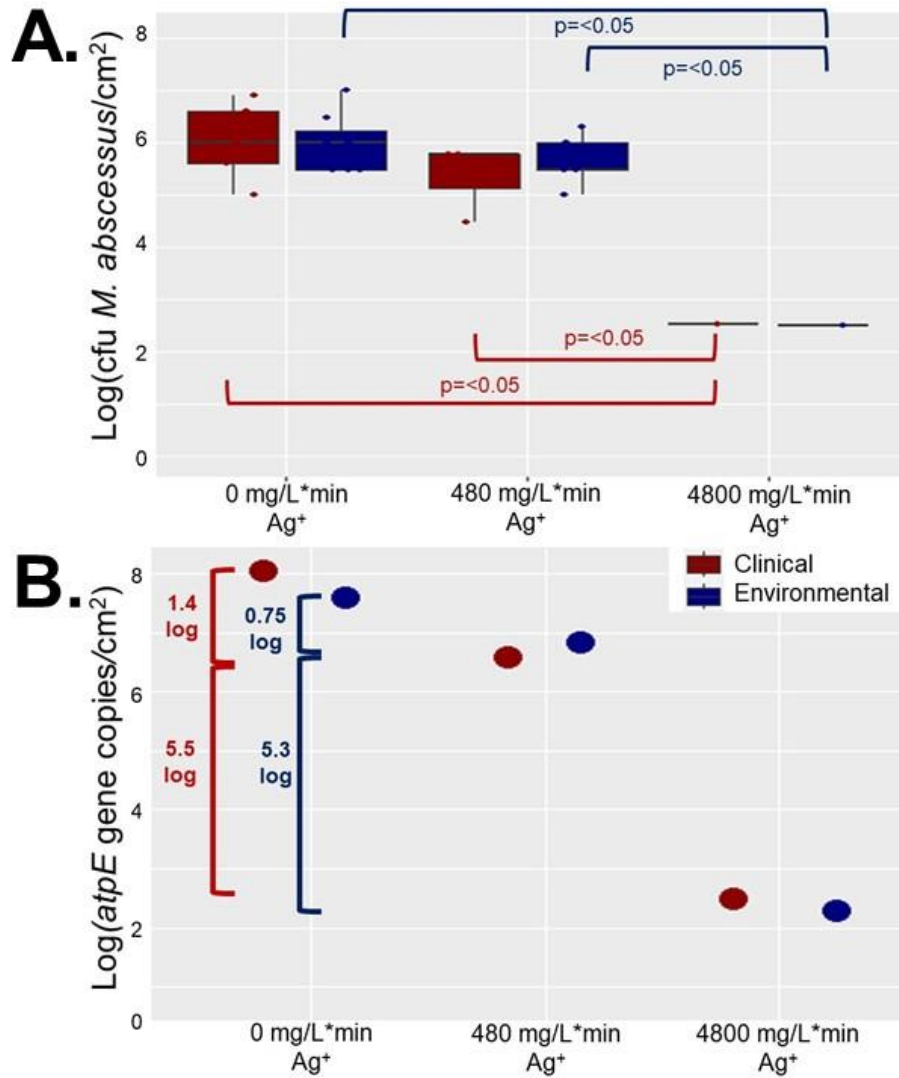


**Figure 16: Recovered *M. abscessus* biofilms after reactor operation for clinical (red) and environmental (blue) isolates quantified using A. plate counts (n=8), and B. ddPCR results (n=1). Significance in A. is denoted by brackets, but there were not enough samples to determine significance for B.**

Like discussed in [Chapter 3.3.5](#), studies on the effects of silver have focused on biofilm prevention in laboratory conditions, using *P. aeruginosa* as the model biofilm forming organism<sup>100,161–163</sup>. *Mycobacterium* as a genus is known to be more resistant to silver than other DWPIs<sup>103,110,165</sup>, and has been cited as a robust biofilm grower<sup>83–85</sup>, which increases microorganisms’ resistance to antimicrobial substances<sup>45</sup>. Therefore, it is unsurprising that *M.*

*abscessus* biofilms survived regardless of silver ion dose or number of repeated exposures. The lack of significant differences between the control reactor biofilms and the 480 mg/L\*min Ag<sup>+</sup> reactor (Figure 16) may also be, in part, explained by the fundamental utilization of CSI, where this silver dose was modelled after. CSI is usually implemented in buildings where there is risk of DWPI infection, and is a technology where both copper and silver ions are being continually released into the DW conveyed in the building plumbing<sup>50,97</sup>, allowing for relatively long contact times to occur. Additionally, studies on the long-term efficacy of CSI show that initial treatment is often effective for combatting the target microorganism (often *L. pneumophila*), but regrowth occurs after the initial period of treatment<sup>49–52,97</sup>. This experiment aimed to isolate the necessary silver ion concentration needed for an effective antimicrobial POU device, where the contact time is much briefer, and only silver is used, so it is possible that these differences caused less effective microbial inactivation. Bench-scale evaluations have demonstrated that there are additive antimicrobial effects when both copper and silver ions are present in a solution<sup>102</sup> so perhaps future antimicrobial silver showerheads should incorporate both ions.

The ~ 3 log decreases seen in the highest dosed reactor (4800 mg/L\*min Ag<sup>+</sup>) were significantly lower than the other two reactors (Figure 16), however the concentration of silver nitrate that was added to the reactor was so high that it created DW that was no longer potable: there was significant discoloration of the feed and extensive visual silver deposition in all parts of the glassware used (Appendix B Figure 6). This infeasibility suggests that silver ion exposure at this concentration is not appropriate for DW, and even then, the *M. abscessus* biofilm was not fully eliminated. Preliminary experiments for this study determined that the driving parameter for disinfection was time, not silver concentration, which contextualizes why some silver-containing technologies report greater microbial reduction during implementation than seen in this work,

since these applications have longer exposure time (Appendix B Figure 7). Based on these results, ionic silver is not a reasonable antimicrobial for eradicating *M. abscessus* biofilms in situations where exposure only occurs for a short period of time like with POU applications.

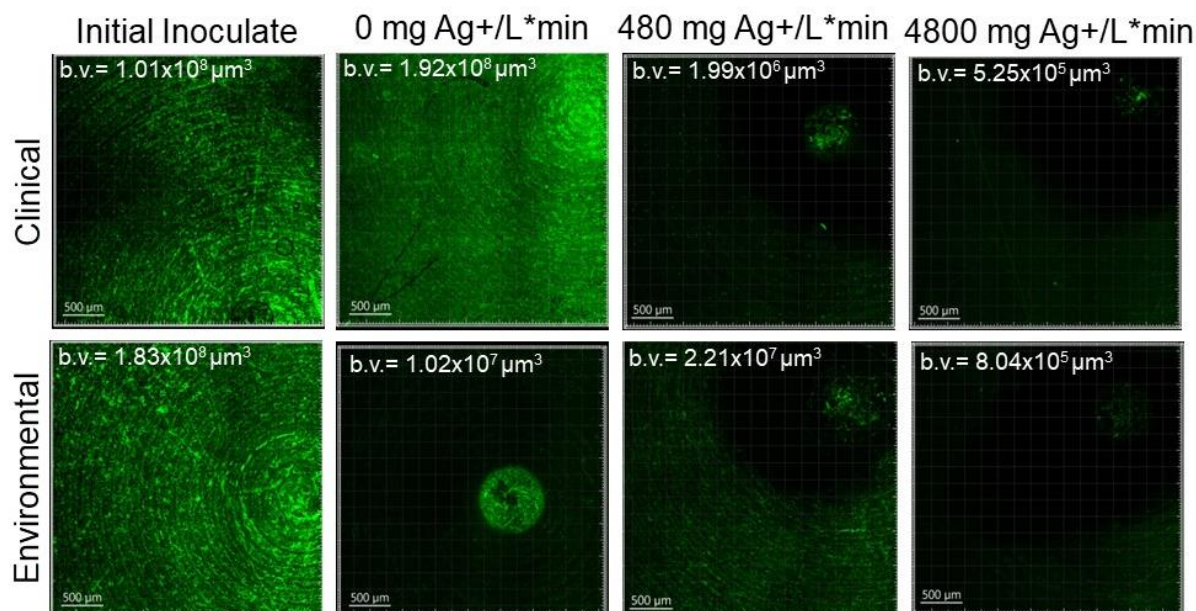


**Figure 17: Fluorescent microscopy results of representative sections of *M. abscessus* biofilms recovered after 7 days of reactor operation by isolate (row) and exposure condition (column). Green indicates the presence of biomass, and total biovolume (abbreviated b.v.) was included on each image that was quantified from zstack data.**

Although significant inactivation was achieved in the high exposure reactor (4800 mg/L\*min Ag<sup>+</sup>) at least 1600 *M. abscessus* cfu/cm<sup>2</sup> remained after 7 days of chronic silver exposure which may have led to non-lethal effects such as behavioral modification, or changes in morphology which can have important consequences for public health. Aggregation assays conducted on isolates recovered from the reactors revealed that the aggregation behavior, or tendency for microorganisms to form a biofilm instead of being planktonic (dispersed in solution), changed with silver exposure (Figure 18). Based on ratios of planktonic to aggregated cells for the

environmental and clinical *M. abscessus* isolates obtained from coupons not placed in the CDC bioreactors, peak dispersal occurred between 24 and 33 hours, after which time they returned to a predominately biofilm phase (Appendix B Figure 8). Given that biofilm dispersal and formation behavior followed the same trends in the control reactor to those from coupons not placed in a reactor any observed differences in the silver reactors must be due to the different silver exposure conditions. Silver itself is thought to cause microbial inactivation on a variety of different mechanisms from causing cell membrane disruption<sup>111</sup> to interrupting essential cellular functionality such as protein synthesis, cellular respiration, and DNA stability<sup>102,111</sup>. While the major antimicrobial mechanism of silver and its behavior within a biofilm is unknown, previous work on biocidal copper reported that cell death is only achieved if copper adheres to the surface of the cells<sup>112</sup>, so further research is needed to determine fate and transport of silver and other metals in biofilms. Additionally, water chemistry factors such as pH<sup>102,166,167</sup>, organic matter<sup>102,168</sup>, and other compounds such as orthophosphate<sup>168</sup> that are present in the DW matrix can reduce the efficacy of silver as an antimicrobial by making it no longer reactive to microorganisms, so correcting doses based on treatment conditions must also be further considered.

Overall, there were interesting differences in biofilm behavior between the strains and the different silver doses. A greater proportion of clinical *M. abscessus* strains isolated from the 480 mg/L\*min Ag<sup>+</sup> reactor entered a planktonic phase earlier than those isolated from the control reactor (peak disaggregation occurring at 24h, instead of between 24-33h in the control reactor (Figure 18)). Interestingly, the environmental *M. abscessus* strains isolated from the lower dose silver reactor dispersed (entered a planktonic phase) later than those isolated from the control reactor (peak disaggregation occurring at 33h, instead of between 24-33h in the control reactor, (Figure 18)). This shift in when peak disaggregation occurred was likewise seen in strains isolated

from the 4800 mg/L\*min Ag<sup>+</sup> reactor but were more pronounced (Figure 18C). These results are fairly consistent with the biofilm work conducted in *Pseudomonas*<sup>162,169</sup> as well as conventional knowledge about antimicrobial exposure: microorganisms contained in biofilms exposed to biocide tend to develop resistance to both the initial biocide, but also other antimicrobial substances due to the altered regulation of virulence proteins, quorum sensing, synthesis of polysaccharides and proteins essential for cellular adhesion and biofilm formation, and horizontally transferred gene components<sup>162,163,170</sup>.

Finally, the clinical *M. abscessus* strains isolated from the 4800 mg/L\*min Ag<sup>+</sup> reactor exhibited very different biofilm behavior, as the majority of the community stayed in a biofilm / aggregated phase throughout the times sampled (Figure 18C). Reasoning for the lack of disaggregation could be attributed to priming caused by in-situ survival from the human immune system and antibiotics, which may improve biofilm formation and robustness in this assay<sup>171</sup>. Overall, these results suggest that clinical *M. abscessus* isolates which survive chronic repeated exposure to silver adapt to form a biofilm either as a defense or virulence mechanism similar to what is observed during active infection<sup>109,172,173</sup>. Future transcriptomic and proteomic work should be carried out to properly characterize and understand the biofilm forming behavior and mechanisms used by DWPIs after exposure to biocides such as silver.

### 3.4 6 Conclusions

The results of the work outlined in this chapter demonstrated that silver-containing showerheads did not produce significantly different viable DWPI abundances in shower water or

associated biofilms over the duration of 12 weeks. Although the absolute abundances of culturable or molecularly detected DWPIs remained unchanged, the incorporation of silver, along with the specific type of silver utilized in the showerhead, influenced the microbial community of both water and associated biofilms, as well as the structure of the biofilms themselves. These findings suggest material effects beyond the marketed antimicrobial properties, potentially influencing microbial growth, establishment, and biofilm development. Instead, as observed in Chapter 2, showerhead age was an important parameter in explaining microbial trends in the water samples, however in this chapter this conclusion is true for the viable microbiome, instead of both the dead and alive community assessed in chapter 2 and thus should be considered when doing future quantitative microbial risk assessment.

CDC biofilm reactors operated to mimic as a shower environment were used to assess the effects of silver on *M. abscessus* biofilms and ultimately showed that ionic silver, even at extremely high and non-practical concentrations is insufficient to eradicate *M. abscessus* biofilms when contact time is relegated to the average shower duration. Furthermore, and possibly most concerning, increased biofilm formation and changes in growth kinetics were observed in clinical *M. abscessus* strains surviving from the highest silver condition studied. This implies that prior host infection could enhance tolerance to disinfectants. However, to truly understand if such a link exists, further CDC biofilm experiments assessing the same endpoints measured in this study, alongside gene expression assays in more NTM species and morphologies are required.

Collectively, the results of this chapter, like the previous, suggest that choosing a conventional showerhead over a silver-containing antimicrobial showerhead may be more cost-effective and achieves similar relevant microbial quality to the more expensive silver alternatives. However, future work must account for the viable bioaerosol loads that are generated during

showering since that is the hypothesized route of exposure to DWPIs. Additionally, temporal characterization of the microbiome and DWPI abundance within the water, biofilm and aerosol phases in full-scale model studies like this one are required beyond the 12 weeks of this study to determine if the observed dynamics change, since showerheads are not often replaced that frequently.

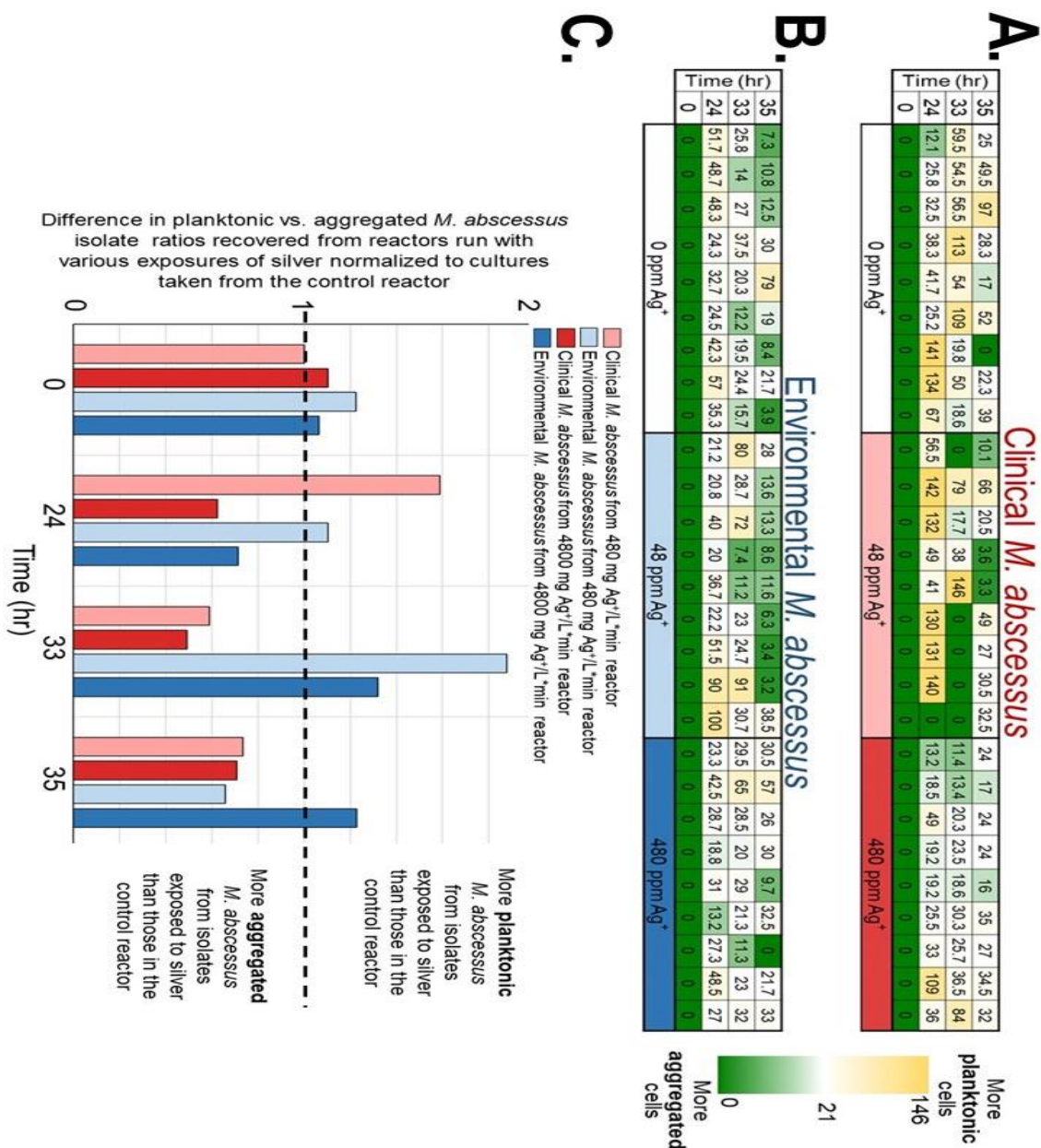


Figure 18: Planktonic vs. aggregate *M. abscessus* ratios (ranges in parentheses) for A. clinical (0–163) and B. environmental (0–100) isolates for the initial inoculates and after silver exposure (each tile is one technical replicate (n = 9 per isolate × condition × time)). Blue cells represent a smaller ratio, signifying a larger proportion of aggregated *M. abscessus* cells, while white/red cells represent a higher ratio (larger proportion of planktonic *M. abscessus* cells). The white cells represent the 50th percentile. The ratios were obtained by

**dividing the planktonic OD600 measurements by the aggregate OD600 measurements. C. The values from A. and B. were normalized to the results of the isolates taken from the reactor with no added silver.**

#### 4.0 Specific Aim 3.0: Examining The Impacts Of Shower Use Patterns On DWPIs And The Microbiome

Specific Aim 3.0 was funded in part by the Mascaro Center for Sustainable Innovation, and IDEXX Laboratories provided the Legiolert culturing assays but had no part in the analysis or interpretation of this study. For the low flow portion of this chapter, Evan Trump performed sample collection and ddPCR data acquisition, Isaiah Spencer-Williams and Dr. Daniel Bain facilitated ICP-MS analysis, and Dr. Cheolwoon Woo aided in 16S rRNA amplicon sequencing analysis. The results of Specific Aim 3.0 will be published in two publications: the work conducted in response to the COVID-19 shutdown contributed to a greater body of work and is published, and the work focusing on water-conserving showerheads has been submitted for review in *Frontiers in Microbiology*. Results were shared in 2 conference proceedings:

##### **Journal Articles**

1. K. Dowdell, S.; Greenwald Healy, H.; Joshi, S.; Grimard-Conea, M.; **Pitell, S.**; Song, Y.; Ley, C.; C. Kennedy, L.; Vosloo, S.; Huo, L.; Haig, S.-J.; A. Hamilton, K.; L. Nelson, K.; Pinto, A.; Prévost, M.; R. Proctor, C.; Raskin, L.; J. Whelton, A.; Garner, E.; J. Pieper, K.; J. Rhoads, W. *Legionella Pneumophila* Occurrence in Reduced-Occupancy Buildings in 11 Cities during the COVID-19 Pandemic. *Environmental Science: Water Research & Technology* **2023**. <https://doi.org/10.1039/D3EW00278K>.
2. Woo, C.; **Pitell, S.**; Trump, E.; Haig, S.-J. Balancing Water Conservation and Health: Do water-saving showerheads impact the microbes we breathe in during showering?  
*Submitted to Frontiers in Microbiology*

## **Conference Proceedings**

1. **Pitell, S.**; Trump, E.; Haig, S.-J. Observing drinking water-associated opportunistic pathogen abundance from a model shower system after the Covid-19 shutdown. *Presentation*. Building Water SLAM (Stagnation, *Legionella*, and Metals) Symposium (virtual) 7/7/21
2. Trump, E.; Haig, S.-J. (presented by **Pitell, S.**) Save It, Don't Spray It: Do water saving showerheads impact the microbes we breathe in during showering? *Presentation*. Mascaro Center for Sustainable Innovation's Undergraduate Research Symposium (Pittsburgh, PA) 7/25/22

## 4.1 Introduction

Chapters 2 and 3 were focused on how antimicrobial showerheads impact the microbial community of shower water, but the majority of the general public may not consider implementing these technologies. Instead, consumers may make decisions about what kind of fixtures they use based on other factors such as aesthetics and personal preferences, immediate and lifecycle cost, and environmental and water-saving potential<sup>174</sup>, without considering the potential effects on microbial load. People that use municipal DW may also experience changes in their DW microbial risk profile based on conditions outside an individual's control, such as stay-at-home orders.

These types of circumstances have already occurred over the course of the work included in the thesis: the water quality impacts of the COVID-19 shutdowns<sup>175,176</sup> and the increasingly dire water scarcity crisis<sup>177,178</sup>. While wildly different, these two situations exemplify how novel global challenges can directly impact consumers' access to quality DW. Current DW water quality in the US relies on minimizing the water age, or the time between the DW leaving the plant to POU, so that there is still a measurable disinfectant residual and reduced potential for the distribution system and plumbing to affect the water characteristics<sup>48,179</sup>. When water isn't used at the outlet, treated DW stagnates in the building plumbing. This extended water age allows for the disinfectant to decay and for plumbing materials to leach into the water. These phenomena have been documented in DW that has stagnated overnight<sup>180,181</sup> or in the short-term<sup>182</sup>, but the effects of prolonged stagnation in buildings with previously consistent water demand was not extensively studied due to logistical issues until 2020. Conversely, because the DW distribution system relies on demand to maintain water quality, overall decreases in water availability in many parts of the world are creating pressures to reduce water use at the tap, which may ultimately also cause

decreases in water quality. In order to create resilient DW systems that can adapt to these and other types of circumstances that may occur in the future, there must be robust characterization of how these novel global events impact DW quality for all consumers, not just those at risk for DWPI infection.

During the early months of 2020, many buildings dramatically reduced their occupancy or completely shut down in response to the stay-at-home orders put in place to mitigate viral transmission<sup>183</sup>. While these public health interventions decidedly helped reduce the proliferation of COVID-19 to varying degrees<sup>184</sup>, reducing water demand in an unprecedented number of buildings with little official guidance for building operators led to decreases in microbial and chemical water quality<sup>175,181,185,186</sup>. Some of the first guidelines to emerge for those responsible for maintaining these now vacant buildings included flushing, where certain DW outlets are turned on and are allowed to flow for a certain amount of time or for a certain volume of water, causing stagnated water to be removed from system, and water quality to return to pre-stagnated levels<sup>187,188</sup>. However, there were no clear and concrete specifics on how to effectively flush (e.g., how long or how much, how frequently, or which water outlets)<sup>189,190</sup>, and flushing demonstrated varying degrees of effectiveness that was highly building specific<sup>128,185,186,191,192</sup>. While the response to characterize the effects of extended stagnation in these low-occupancy buildings was multi-faceted and robust<sup>186</sup>, many questions surrounding the building history, pre-established plumbing features, DW quality during normal use patterns, and other confounding variables remained. To address both the ambiguity in prescribed flushing regimes as well as isolating flushing as a remediation strategy in a controlled environment, water samples were taken from the INHALE lab (stagnated for 95 consecutive days due to COVID-19 shutdown) before and after performing flushing over the course of 7 days. These samples were analyzed for conventional

water quality parameters and microbial abundances of total bacteria, NTM, and *L. pneumophila* to assess if flushing as an intervention strategy for buildings with extended reduced occupancy was effective at reducing microorganisms in water and re-establishing the standard water chemistry for a system that has been extensively characterized.

Although the response to water scarcity has not happened with as much immediacy as the response to the water quality issues brought on by COVID-19, it is expected that the adoption of water conservation behaviors will be essential to meeting increasing global water demand<sup>193</sup>. There are many large-scale intervention strategies that can help reduce overall DW usage across sectors such as the adoption of efficient crop irrigation, landscaping practices<sup>194,195</sup> or instituting industry-specific systems that reduce overall water use in their respective sectors<sup>195</sup>, however there is a push by the US EPA<sup>59</sup> to improve water conservation on an individual level. One of the most common intervention strategies to reduce household water use is the use of water-conserving DW fixtures such as showerheads due to the ease of adoption and economic benefits<sup>196</sup>. According to the US EPA's WaterSense program, low flow showerheads are any showerhead with a flow rate that is less than 7.6 L/min (2 gal/min)<sup>59</sup>, and the lower the flow rate, the less water and energy are ultimately used. Low-flow fixtures not only save the average American home 2,700 gallons of DW a year, but also 330 kWh of electricity that is used to heat the DW<sup>59</sup>. Low-flow showerheads work by employing atomization technology, which produces smaller water droplet sizes that aerosolize more readily and evaporate more quickly than droplets generated by conventional showerheads<sup>197</sup>. As a result, low flow showerheads have a greater potential to generate more respirable (aerosols less than 5  $\mu\text{m}$  in diameter) and bio-respirable (aerosols between 2  $\mu\text{m}$ - 5  $\mu\text{m}$  that are still respirable, but large enough to fit a microorganism within it) aerosols. Although low-flow showerheads have been tested extensively to ascertain water saving metrics and validate consumer

happiness<sup>198,199</sup>, very little research has been conducted regarding how low-flow showerheads may impact the microbial loads in both DW and DW-associated aerosols. This study isolated the impact of flow rate on water and aerosol samples taken from the INHALE shower laboratory to assess if the use of water saving showerheads have unintended effects on DWPI abundances and the greater microbiome in the shower system.

## **4.2 Research Approach**

### **4.2.1 Methodology Used After The COVID-19 Shutdown**

#### **4.2.1.1 INHALE Shower Laboratory Setup And Sampling Regime**

The INHALE shower lab stagnated for 95 consecutive days prior to sample collection over the course of the building shutdown. During the shutdown and for the course of this sampling, each outlet had an ABS plastic showerhead installed (Amazon, Seattle, WA). Each showerhead was sampled twice a day: the first 1.3 L to come out of the shower (referred to as the “first draw” samples in this chapter) and another 1.3 L after allowing water to flow for 5 minutes (referred to as the “flushed” samples in this chapter). These samples were taken over the course of 7 days: sampling was done for three consecutive days, then again on day 7 after daily 5-minute flushing.

#### **4.2.1.2 Water Sample Processing**

A portion of the collected water was dedicated to water chemistry analysis. Free and total chlorine concentrations were determined at the time of collection for both first draw and flushed

samples with the DPD method<sup>73</sup> using a portable DR900 spectrophotometer (Hach, Loveland, CO, USA). Temperature and pH were monitored onsite using a portable pH and temperature meter (HANNA Instruments, Woonsocket, RI). The concentration of culturable *L. pneumophila* was assessed in all samples using the Legiolert detection system (IDEXX Laboratories, Westbrook, ME) following standard procedures<sup>200</sup>. The rest of the water was filter concentrated for microbial analysis as described in [Chapter 2](#).

## **4.2.2 Methodology Used To Assess Water-Conserving Showerheads**

### **4.2.2.1 INHALE Shower Laboratory Setup, Sampling Regime, And Sample Processing**

For this work, the INHALE laboratory was installed with ABS showerheads with flow rates of 1, 1.5, and 1.8 gallons per minute in each stall. Water, aerosol, and particle sample collection was conducted from each showerhead over the course of eight weeks where sampling events occurred weekly with a two-week hiatus during the fourth and fifth weeks to simulate longer stagnation.

Three different types of samples were collected for each showerhead over the six sampling events. Aerosol particle number and diameter were collected with the AeroTrak Handheld Particle Counter 9306 (TSI, Inc., Shoreview, MN, USA) in bins of 0.3–0.5, 0.5–0.7, 0.7–1, 1.0–2.0, and 2.0–5.0  $\mu\text{m}$ . The particle counter was programmed to take a reading once every 3 seconds at a flow rate of 2.83 liters per minute. The particle counter was run for 30 minutes for each showerhead: 5 minutes before turning on the showerhead to assess background particulates, 20 minutes while the shower was running, and 5 minutes after turning it off to monitor particle dissipation. A pause of 20 minutes was implemented between the measurements from different

showerheads, permitting the laboratory conditions to revert to the initial temperature, relative humidity and allow particle concentrations to reach room baseline values.

Airborne bacterial particles were collected with the Series 110A Spot Sampler<sup>TM</sup> aerosol particle collector (Aerosol Devices, Inc., Fort Collins, CO, USA) with the addition of a SCC1.829 cyclone (Mesa Labs, Lakewood, CO) that allowed for collection of respirable aerosols (<10 µm in diameter). The aerosol collector was run for 40 minutes while each showerhead was running at an aerosol collection flow rate of 1.5 liters per minute and the aerosols were collected in 0.5 mL of phosphate-buffered saline (PBS) as highlighted in [Chapter 2](#). Additionally, controls were conducted in the form of one background control per week where the collector was run without the shower turned on, and one HEPA control where the collector was fed air that had already passed through a HEPA filter. After sampling, PBS was transferred to a sterilized 2 mL tube and the tube was stored at -20°C until subsequent analysis.

Composite water samples from each showerhead were collected over the course of 8 minutes, totaling 1.3 L of shower water in a sterile Nalgene bottle. 1 L of the water was filter concentrated onto a 0.2 µm polycarbonate filter (Millipore, Cork, Ireland) and preserved at -20°C until subsequent molecular analysis. Additionally, field and filters negative controls were ran during each sampling event. The remaining water was used to assess the shower water quality. Temperature, pH, free chlorine, total chlorine, and total and dissolved metals were measured as described in [Chapter 2](#).

### **4.2.3 Methodology Used In Both Studies**

#### **4.2.3.1 DWPI Absolute Abundance Quantification**

DNA was extracted using the Fast Spin DNA Extraction kit (MPBio, Irvine, CA), as described in [Chapter 2](#). Absolute densities of total bacteria, *L .pneumophila*, and NTM were determined using ddPCR (QX200, Bio-Rad, Hercules, CA), using the same reagents and procedures highlighted in [Chapter 2](#) and Appendix 2.

#### **4.2.4 16S rRNA Sequencing**

The overall microbial community in each sample was assessed by 16S rRNA gene amplicon sequencing conducted at Argonne National Laboratory (Lemont, IL, USA) using the same methodology as outlined in [Chapter 2](#).

#### **4.2.5 Statistical Analysis**

All data was visualized and analyzed using R statistical software (Version 4.0.5). Data analysis for all sequencing, absolute quantification data, water quality data, and aerosol particle data followed the protocols described in [Chapter 2](#), with the addition of the analysis of the PICRUS2 described in [Chapter 3](#).

## 4.3 Results And Discussion

### 4.3.1 Microbial Water Quality Was Severely Impacted By Prolonged Stagnation

After the extended building shutdown (95 days of no water operation) the microbial densities were approximately 2 orders of magnitude higher than seen during regular use conditions ([Chapter 2](#)). After flushing for 5 minutes (a standard practice used by building managers to alleviate water quality issues after periods of stagnation) a significant 2-log reduction in total bacterial density was observed, with a steady decrease in density observed in the first draw samples resulting in system baseline/ pre-shutdown concentration after 7 days of flushing (Figure 19D). Interestingly, the reductive performance of flushing shown for total bacterial density was not observed for DWPIs (Figure 19). *L. pneumophila* quantified using either culture or molecular methods were both detected in relatively the same concentrations regardless of detection method, and were present in higher quantities than described in Chapters [2](#) and [3](#). Culturable *L. pneumophila* results revealed that first flush concentrations only significantly decreased after 7 days of daily flushing and that concentration in the 5-minute flush samples were significantly higher than the first draw samples after 3 and 7 days of flushing (Figure 19A). NTM exhibited significant 2 log decreases in paired first draw and flushed samples over the course of 1 week of daily flushing, however, the NTM concentration exiting the showerhead water did significantly increase by 2.5 logs after the first day of flushing and did not return to initial concentration seen on day 1 (Figure 19C). The increase of NTM in the water samples after the first flush may be caused by the change in the hydraulic environment of the pipes: due to the change in flow, the next flushes may have dislodged areas of the biofilm where NTM was more prevalent, leading to larger densities in the water.

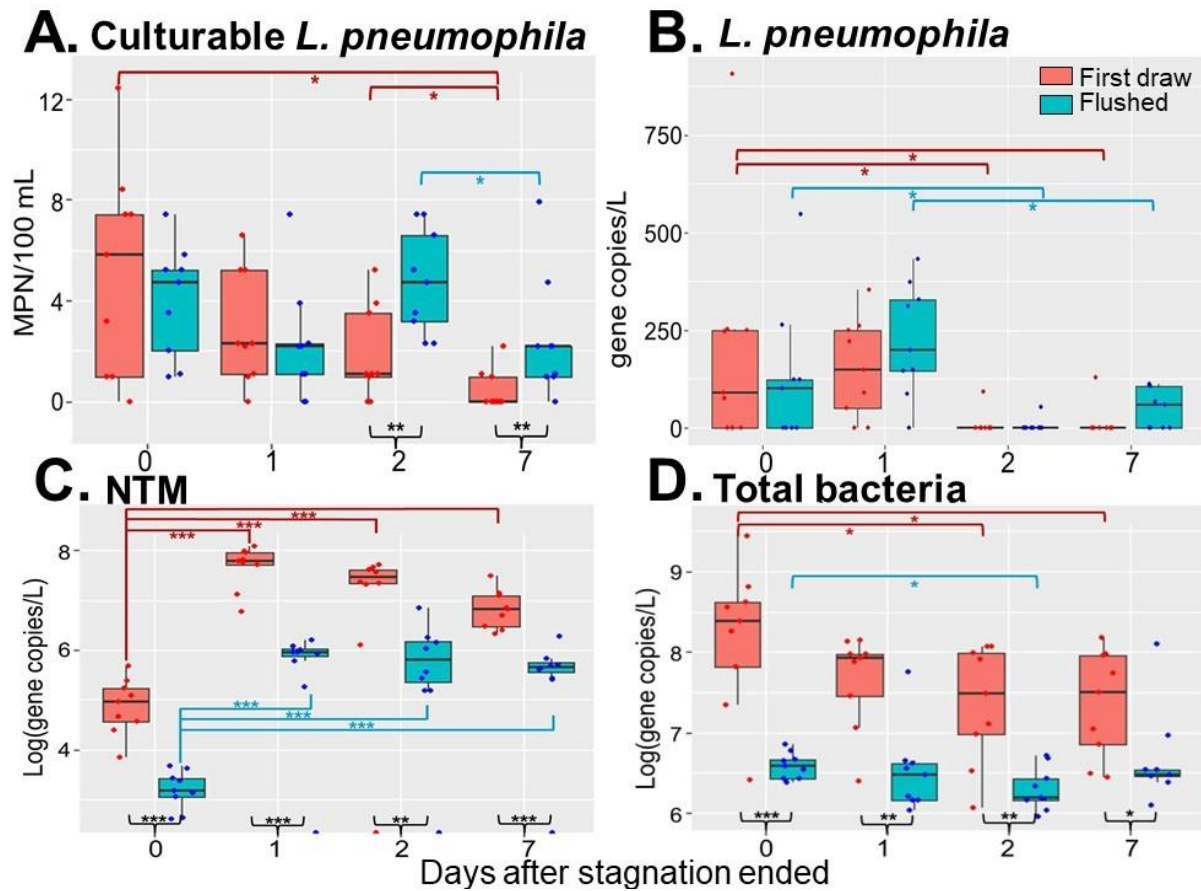


Figure 19: Microbial abundances in shower water (n=9) over time before (red) and after (blue) 5 minutes of flushing after 95 days of stagnation (day 0). *Legionella pneumophila* quantified with Legiolert A., and ddPCR analysis B., Nontuberculous mycobacteria quantified with ddPCR C., and total bacteria quantified with ddPCR D. Significant differences as determined with paired Wilcoxon tests are denoted by brackets, with black brackets indicating differences between the paired first draw and flush samples, red brackets denoting differences between first draw samples, and blue brackets denoting differences between flushed samples. Significance was indicated by asterisks, with \*, \*\*, and \*\*\* denote p-values of  $\leq 0.05$ ,  $\leq 0.01$ , and  $\leq 0.001$ , respectively.

Linear models generated for each quantified microorganism in the first draw and flushed samples highlighted different physiochemical parameters that help explain the dynamics observed (Table 4). In the models generated from the first draw samples, day sampled was the dominant parameter for explaining observations seen in both cultured and molecularly quantified *L.*

*pneumophila*, whereas characteristics of the water itself (e.g., chlorine and pH) and other quantified microorganisms were parameters that explained the variance in NTM and total bacteria concentrations. With the exception of NTM, the flushed models generated were not significant and explained less of the variance than the first draw models (Table 4). In other studies conducted in response to the extended DW stagnation events caused by the Covid-19 shutdowns, pH was found to be a critical component of decreased water quality due to the influences on metal corrosion, and from a microbial perspective, pH was linked to elevated levels of microbial gene markers<sup>185</sup>, heterotrophic plate counts<sup>201</sup>, and molecularly identified NTM<sup>201</sup>. Microorganisms are sensitive to pH ranges in order to achieve optimal proliferation, so it being a major indicator of both NTM and overall bacterial densities is not unexpected<sup>32</sup>.

**Table 4: Summary of generated linear models in the first draw and flush samples. In the model components column, the percent of the variance explained by each variable is superscripted. All response variables were transformed to achieve normality as described in parentheses in the model column.**

Model (Transformation)	Model Components	Overall Model	
		Explained (%)	<i>p</i> -value
<b>First draw</b>			
<i>L. pneumophila</i> ([gene copies/L] <sup>0.6</sup> )	Day sampled <sup>20.3%</sup> + Temperature <sup>6.5%</sup> + pH <sup>3.2%</sup> + Cultured <i>L. pneumophila</i> <sup>7.3%</sup>	37.3	0.005
Cultured <i>L. pneumophila</i> (MPN/100 mL <sup>0.38</sup> )	Day sampled <sup>32.9%</sup> + Stall <sup>19.2%</sup> + pH <sup>3.7%</sup>	55.8	7.4x10 <sup>-6</sup>
Nontuberculous mycobacteria ([gene copies/L] <sup>0.1</sup> )	Stall <sup>2.1%</sup> + pH <sup>23.4%</sup> + Total chlorine <sup>11.9%</sup> + <i>L.</i> <i>pneumophila</i> <sup>3.5%</sup>	41	0.002
Total bacteria ([gene copies/L] <sup>-0.2</sup> )	Stall <sup>2.4%</sup> + Free chlorine <sup>18.7%</sup> + Total chlorine <sup>9.6%</sup> + NTM <sup>5.4%</sup>	36.2	0.006
<b>Flushed</b>			
<i>L. pneumophila</i> ([gene copies/L] <sup>0.02</sup> )	Cultured <i>L. pneumophila</i> <sup>12.7%</sup> + Stall <sup>1.8%</sup>	14.6	0.07
Cultured <i>L. pneumophila</i> (MPN/100 mL <sup>0.54</sup> )	Day sampled <sup>3.4%</sup> + Stall <sup>11.2%</sup> + <i>L. pneumophila</i> <sup>22.6%</sup> + Total bacteria <sup>3.4%</sup>	40.6	0.002
Nontuberculous mycobacteria ([gene copies/L] <sup>0.18</sup> )	Temperature <sup>3.9%</sup> + pH <sup>22.5%</sup>	26.4	0.006
Total bacteria ([gene copies/L] <sup>-0.5</sup> )	Day sampled <sup>0.7%</sup> + pH <sup>13.6%</sup>	14.3	0.08

Flushing was a commonly suggested method of water management for buildings with reduced occupancy during the COVID-19 shutdowns<sup>187</sup>, and there have been many studies looking at the efficacy of flushing as a crisis response strategy to maintain water quality<sup>185,186,191,192</sup>. Much of the material published during this time did not give clear guidelines on how to effectively flush: only a few of these documents included details about the number of outlets to flush, which outlets to flush, frequency of flushing, duration of flushing, or any health and safety considerations to the essential workers performing the task<sup>187</sup>. The results from this study suggest that flushing is not an over-arching solution, but instead a tool to use when responding to changes in water quality. Flushing was effective at reducing overall microbial loads in shower water directly after the flush, but there was minimal impact after short term overnight stagnation until 7 consecutive days of flushing occurred. For the microorganisms of public health significance that were quantified here, flushing either increased the abundances (NTM) or decreased the abundance only after 3-7 days of daily flushing (*L. pneumophila*); with the latter being outside the weekly to monthly suggested guidelines.

#### **4.3.2 Water-Conserving Showerheads Decreased Microbial Concentrations In Shower**

##### **Water, But Increased The Concentrations Of Aerosols Containing Gram-Negative Bacteria**

Unlike the microbial levels seen as a direct result from the extended water stagnation caused by the COVID-19 shutdown, showerheads that decreased flow rate only significantly impacted absolute abundances of microorganisms in shower water (Figure 20 and Appendix C Figure 1). In particular low flow showerheads with flow rates of 1.8 gpm had the largest total bacteria and NTM abundances (Figure 20A). However, for DWPI abundance, few differences were found between

the different showerhead flow rates, with NTM abundance only found to be statistically different between the 1.5 gpm head and 1.8 gpm head. No significant differences in *L. pneumophila* abundances were observed between any flow rate likely due to its infrequent detection (Figure 20A).

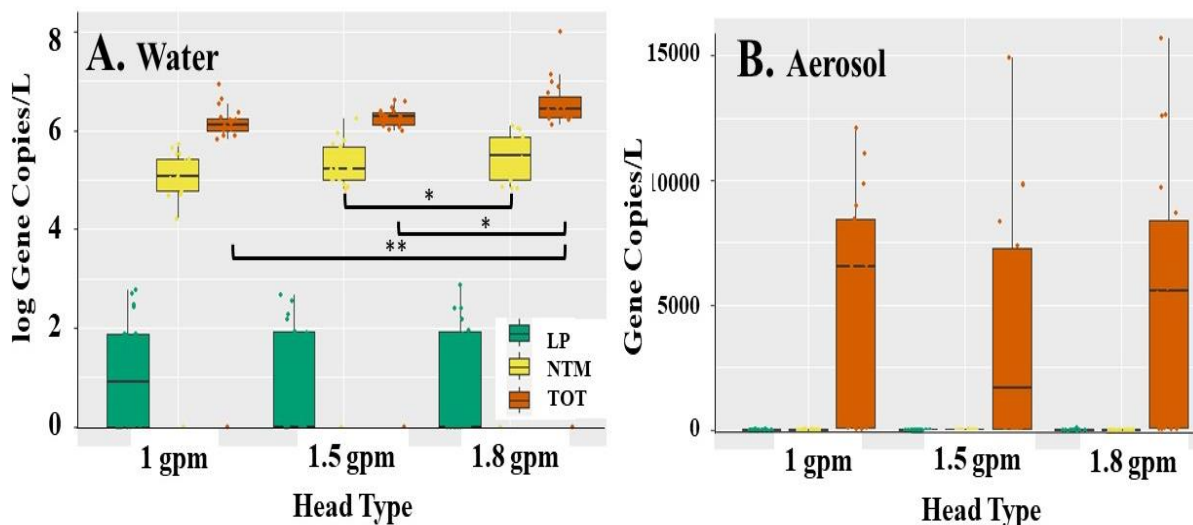


**Figure 20:** Box and whisker plots showing the absolute densities of *L. pneumophila* (LP, green), Nontuberculous mycobacteria (NTM, yellow), and total bacteria (TOT, orange) by showerhead flow rate in A. shower water and B. shower water associated aerosols (<10 $\mu$ m). Data is aggregated across the whole 8-week experimental timeframe (n=18). Significant differences are denoted by brackets, with \* and \*\* denoting p-values of < 0.05 and < 0.01, respectively.

Both total inhalable aerosol counts (0.3-5  $\mu$ m) and bio-respirable aerosol counts that may contain bacteria (2-5  $\mu$ m) did not significantly differ by showerhead flow rate during the sampling period (Figure 21). These results are not consistent with the results of other studies<sup>38,41,197</sup> who have reported conflicted correlations on the relationship between flow rate and particle distribution. These discrepancies are likely explained by the differing sampling strategies, methodologies used to quantify aerosols and fundamental differences in the showerhead design used despite the same flow rates. On average  $1 \times 10^9$  inhalable and  $3.7 \times 10^7$  bio-respirable aerosols

were produced during the 30 min of collection equating to approximately  $2.7 \times 10^8$  particles and  $9.8 \times 10^6$  particles in the average 8-minute shower, respectively.

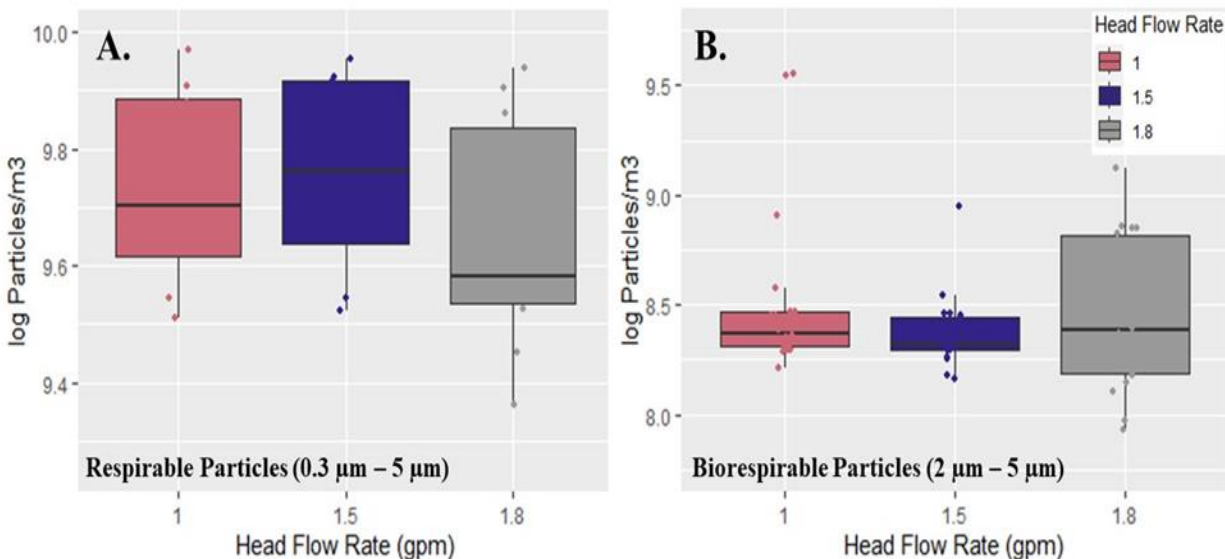


**Figure 21: Box and whisker plots showing the absolute numbers of aerosolized particles by showerhead flow rate between the diameters of A.  $0.3 \mu\text{m} - 5 \mu\text{m}$  and B.  $2 \mu\text{m} - 5 \mu\text{m}$ . Data is aggregated across the whole 8 - week experimental timeframe (n=18).**

While inhalation of biorespirable aerosols has been repeatedly cited as the main route of exposure for both NTM and *L. pneumophila*<sup>6,68,202–204</sup>, rarely is the microbial quality of DW-associated aerosols assessed, likely because of methodological difficulties. However, this study found differences in the partitioning behavior of NTM from the water to the water-associated aerosols phase. Specifically, NTM was found to partition twice as much from the water to biorespirable aerosol phase in the lowest flow showerheads (Table 5) compared to the highest flow head (i.e., 0.005% compared to 0.0024% partition, respectively). Furthermore, the lowest flowrate heads transferred total bacteria from the water to the aerosol phase more frequently than the higher flow heads (Table 5). *L. pneumophila* defies the trends of total bacteria and NTM with higher densities transferred at higher flow rates. These emission ratios suggest that even though the

absolute densities of DWPIs are not significantly affected by flow rate in the aerosol samples, the likelihood of a respirable aerosol containing NTM being generated is higher in low-flow showerheads and the opposite for *L. pneumophila*: respirable bioaerosol generation was highest in the highest flow showerhead. Overall, showerheads with a flow rate of 1.5 gal/min seemed to have less DWPI partitioning while still reducing water use, which may be due to the optimization of lower flow rate and reduced shear stress on the biofilm forming within the fixture.

**Table 5: Average aerosolization partitioning percentages for DWPIs and total bacteria.**

	Average aerosolization partitioning percentage $\pm$ standard deviation (%)			<i>p</i> -value from ANOVA
	1 gpm	1.5 gpm	1.8 gpm	
<b>Total bacteria</b>	0.39 $\pm$ 0.42	0.22 $\pm$ 0.34	0.12 $\pm$ 0.17	0.01
<b><i>L. pneumophila</i></b>	2.93 $\pm$ 2.06	1.01 $\pm$ 1.62	9.1 $\pm$ 9.9	0.05
<b>Nontuberculous mycobacteria</b>	0.005 $\pm$ 0.008	0.002 $\pm$ 0.002	0.002 $\pm$ 0.002	0.04

Comparing aerosolization partitioning between the ABS showerheads used in [Chapter 2](#) with the same flow rate to the 1.8 gpm showerheads used here, different partitioning behaviors are observed with the exception of *L. pneumophila* (Appendix A Table 4). More specifically, aerosolization partitioning for NTM were three orders of magnitude less in the previous study than seen here despite utilizing the same methodologies. Therefore, the most likely explanation for these differences in aerosolization is that the system, and possibly the biofilm itself, has changed over time: samples described in Chapter 2 were collected in 2020, and samples in this chapter were taken in 2022. In between these two sampling campaigns, there were varying levels of use that would have aged the plumbing system between the two sampling campaigns, which may have influenced the biofilm to behave more like an established plumbing system. There may also be more NTM-specific reasons based on their growth dynamics and behavior. Despite NTM showing

a strong preference for surface adhesion in pure culture within 6 hours, many NTM species have long generation times, which could cause the increase in abundance seen between these two sampling endeavors<sup>84</sup>. Additionally, NTM is known to survive intracellularly in certain species of amoeba, so it is possible that the lower NTM partitioning in earlier sampling endeavors were caused by greater numbers of the overall NTM community proliferating in amoeba, where aerosolization would be less likely<sup>205</sup>.

#### **4.3.3 Microbial Community Membership Varied With Flow Rate**

The overall microbial community (alpha and beta diversity) was significantly different in air and water samples (Appendix C Figures 2 and 3), with distinct differences further occurring between the different flow rates. In particular, OTU diversity was greater in aerosol than water samples, and diversity in water samples decreased as a function of flow rate (Appendix C Figure 4A and 4B). Pairing this information with the increased overall total bacteria densities of the water samples from the highest flow rate (Figure 20), this information suggests that showerheads with a higher flow rate may select for rapid growing and more stress-tolerant organisms which outcompete other microbiota, resulting in less diversity. This hypothesis is substantiated by the fact that higher flow rate showerheads will increase nutrient availability, free chlorine concentrations and hydraulic stress – all factors known to influence the DW microbiome and select for more specialized organisms<sup>1,24,77</sup>. Conversely, lower flow showerheads produce aerosols with similar total microbials loads to higher flow rates but have a much more diverse microbiome, likely due to more nutrient and disinfectant gradients occurring in the system.

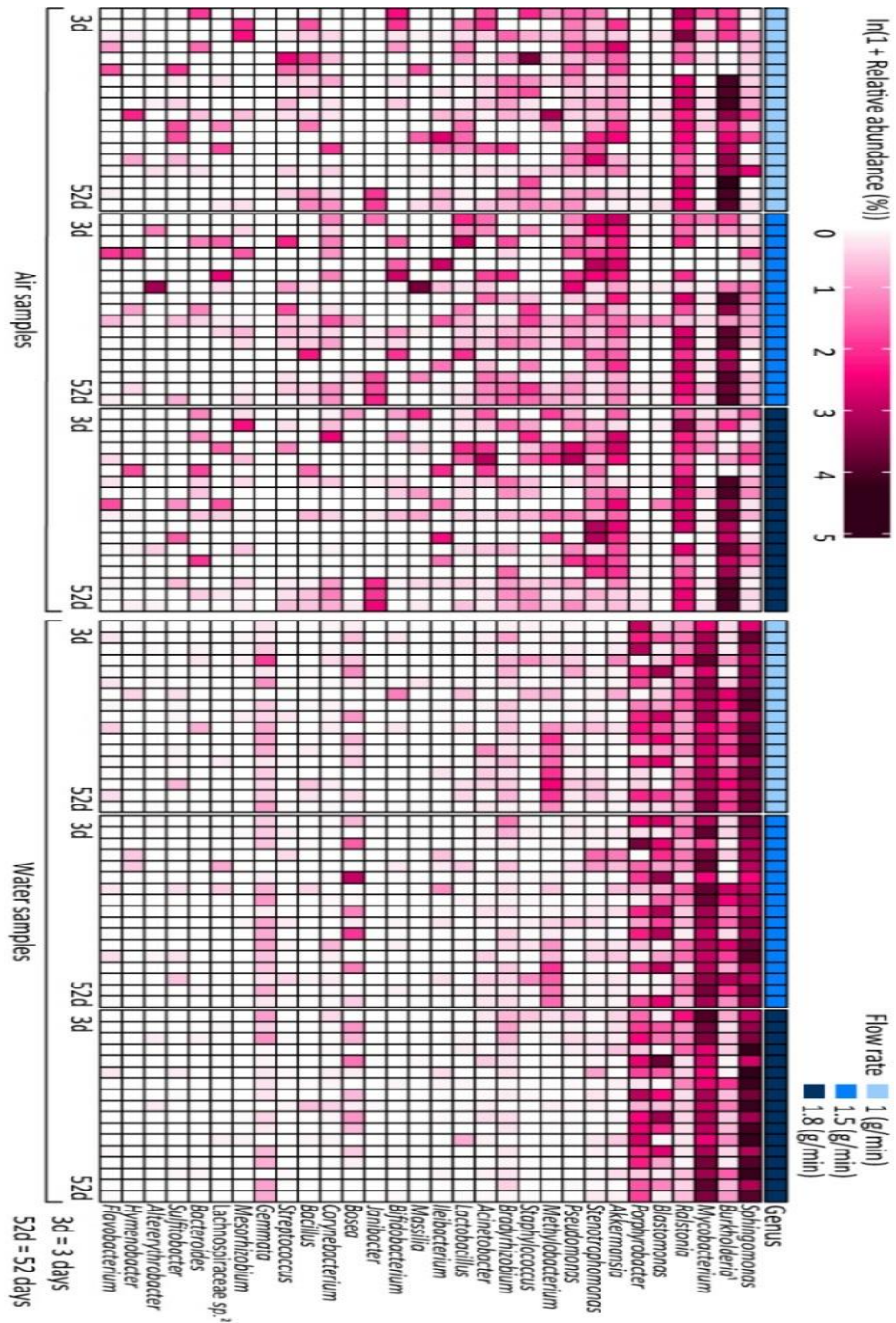


Figure 22: Relative abundance of the 30 most abundant bacterial genera in all samples. In the figure, Burkholderial1 and Lachnospiraceae sp.2 refer to Burkholderia-Caballeronia-Paraburkholderia and Lachnospiraceae NK4A136 group, respectively. Every heatmap box is correlated to a sample, and is organized by day sampled as well as flow rate.

Comparing the dominant microbiome in water and aerosol samples (Figure 22) revealed that the majority of the relative abundance of water samples were composed of a few genera (e.g., *Sphingomonas*, *Burkholderia sp.*, *Mycobacterium*, and *Prophyrbacter*) whereas aerosols samples showed more taxonomic diversity in its core microbiome. Common core microbiome members of both water and aerosols samples were *Sphingomonas*, *Burkholderia-Caballeronia-Paraburkholderia*, and *Ralstonia* which are microorganisms commonly associated with DW<sup>153</sup>, and known to contain DWPIs linked to nosocomial infections<sup>206–208</sup>. In the water samples, the relative abundances of *Sphingomonas* and *Ralstonia* appear to be flow dependent, with *Ralstonia* being more consistently detected in higher abundances in the 1 gal/min showerhead samples and *Sphingomonas* being more enriched in the 1.8 gal/min showerhead samples. Both of these genera are known DW biofilm formers and are often found in water systems with significant physical and nutrient stress<sup>89,207,208</sup>, however there has not been extensive investigation into the impacts of flow rate or other types on hydraulic pressures specifically for these microorganisms.

Metabolic functionality analysis between the 1 gal/min and 1.8 gal/min showerhead water samples showed statistically significant differences in 9 microbial metabolic profiles (Appendix C Figure 5). Specifically, the lipopolysaccharide biosynthesis traits in 1 gal/min showerheads were present at almost twice the relative abundance found in 1.8 gal/min showerhead (0.236% vs. 0.134%, respectively) (Appendix C Figure 5). Lipopolysaccharides are an integral part of Gram-negative bacterial cell membranes, and are often a trigger for the human immune system<sup>32</sup>. Additionally, work conducted on lipopolysaccharides suggest that they reduce biofilm-forming capabilities of microorganisms<sup>133</sup>, so their increased synthesis in the 1 gal/min showerheads may indicate less biofilm formation, however, lipopolysaccharide formation indicate higher levels of Gram-negative microorganisms and as a consequence, potential pathogenicity<sup>134</sup>. Because

showerhead flow rate was observed to affect the greater microbiome of the samples and the presence of potential pathogens due to cell membrane functionality, water-conserving showerheads may have unintended consequences on microbial water quality.

#### **4.3.4 Showerhead Age Is The Key Factor That Influenced Microbial Dynamics**

Microbial dynamics for both the absolute quantification data and microbial community data were impacted by showerhead age, which has been echoed in the previous chapters. Absolute densities of *L. pneumophila*, NTM, and total bacteria in both phases followed trends seen in Chapter 2, which attests to the reproducibility of results using this analysis pipeline from this system and may indicate more universal trends about how consistent use patterns over time impact microbiological dynamics (Appendix A Figures 2 and 3, Appendix C Figure 6). *L. pneumophila* was not consistently quantified in either the water or aerosol samples over time, but detection was most consistent across the system at the first incident of sampling. NTM concentrations were generally uniform throughout the sampling campaign, however there were decreases in NTM levels after day 38 before abundances recovering to initial concentrations by day 52. There were similar dynamics in the total bacteria quantified in the water samples, but bacteria in the aerosols greatly increased at day 38. This dip before and after the 30-day mark of continuous use for NTM and total bacteria was also captured in samples described in Chapter 2: this may be caused by stochastic variation in microbial densities, however these changes may also be an indicator of other systemic processes happening during startup with a brand new showerhead. There has been little work previously conducted that has studied the temporal dynamics of the native microbiota in full-scale DW systems, however, previous work has identified that biofilm formation from the native DW community has two distinct formation phases before and after 30 days of continuous use<sup>47</sup>,

and the work conducted in Chapter 2 found significant linkages between the absolute abundances of certain microorganisms and the greater microbial community based on these biofilm age phases<sup>153</sup>.

The influence of showerhead age and potential biofilm effects are also mirrored in the greater microbial communities of both sample types (Figure 22), with *Burkholderia-Caballeronia-Paraburkholderia* being the best example of these trends in both aerosol and water samples. In the aerosol samples, *Burkholderia sp.* made up a large amount of the total relative abundance regardless of time and flow rate of the showerhead. However, its establishment dynamics in both water and aerosol samples were complex with a decrease in relative abundance between the first incidence of sampling and early biofilm formation (before 30 days), followed by it increasing dramatically and becoming the dominant taxa after 30 days. Much of the non-clinical literature has focused on the detection of *Burkholderia* in DW and associated biofilms<sup>1,209</sup>, but some work studying the biofilm-forming mechanisms of *Burkholderia cepacia* suggests that these microorganisms often co-colonize biofilms with *Pseudomonas sp.*<sup>210</sup>, which is a known member of the DW microbiome<sup>1,13</sup> and has been recovered consistently in the INHALE shower laboratory as discussed in Chapters 2 and 3. It is possible that since *Burkholderia* has been reported to proliferate in pre-established biofilms, it was unenriched in the sample until after initial biofilm attachment occurred<sup>211,212</sup>. Similar dynamics were observed with the relative abundance of *Methylobacterium* from the samples taken from lower flow rate showerheads. *Methylobacterium* is commonly found in building plumbing and participate in biofilm formation<sup>6,46</sup>, so it is possible that the hydraulic environments created in the low-flow showerheads contribute to the abundances recovered in the samples. There are many other instances of known synergistic effects of complex microbial communities in environmental<sup>21,90,213–215</sup> and clinical<sup>172,173</sup> contexts, so exploring the

effects of polymicrobial biofilm dynamics as a function of time and how this consequently impacts the microbiome of the shower water and associated aerosols is a necessary avenue for more research.

#### **4.4 Conclusions**

Both sampling endeavors highlighted in this chapter investigated the impacts of shower system water use patterns, either by dramatically changing use patterns in response to decreased building occupancy or the reduction of overall water consumption by using low-flow showerheads. The work done directly after the COVID-19 shutdown revealed that prolonged stagnation increased microbial loads in the shower water of both DWPIs and total bacteria, and that differing flushing regimes (one weekly short flushing event is the primary water management strategy suggested to building operators to maintain water quality) resulted in improvements in water quality for some DWPIs and negative outcomes for others. Linear models revealed that pH was a major parameter in explaining absolute abundance of DWPIs, but more detailed mechanistic work must be done in order to fully understand this connection. In the samples taken from water-conserving showerheads, overall microbial densities in water increased as a function of flow rate, but abundances in aerosols were unaffected. Showerhead flow rate significantly altered the microbial communities exiting in the water and aerosol phases, with aerosols produced from the lowest flow rate showerheads (1 gal/min) containing more potentially pathogenic gram-negative bacteria and higher DWPI partitioning behavior than faster flow rate showerheads. Future work should focus on assessing the pathogenicity of these aerosols to help inform microbial risk assessment tools.

There are many additional avenues of investigation that need to be considered in order to better understand how novel water use patterns affect the microbiome. Both studies highlighted that isolated grab sampling events are not comprehensive in evaluating microbial dynamics, and that longer sampling campaigns are necessary when characterizing systems. Additionally, some of the observations in these studies could be attributed to the virgin nature of the INHALE shower laboratory itself: dynamics may be different in more established plumbing systems. The results of the low flow study in particular showcase the need to sample respirable aerosols in addition to water in order to most accurately ascertain risk of altering water use patterns.

## **5.0 Concluding Remarks And Recommendations To Stakeholders**

### **5.1 Overall Summary**

This thesis primarily investigated the influence of showerhead materials and shower use patterns on the microbial communities found in produced shower water, shower water-associated aerosols, and biofilms. While showerhead material, including antimicrobial showerheads, did not significantly alter water chemistry or DWPI abundance across environmental matrices, it did impact microbial community composition. Notably, across all studies, showerhead age consistently explained the most variation in microbial community structure and composition, with aerosolization behavior of DWPIs also varying based on showerhead age. Follow-up bench-scale studies further supported the antimicrobial shower results, concluding that silver is not an effective antimicrobial agent against DWPIs and in the cases where increased silver dose is used, result in increased biofilm formation. Finally, choices regarding water usage, either through prolonged stagnation or installation of water-conserving showerheads, altered microbial dynamics within the system, with showerhead flow rate being a significant factor in explaining community composition. Low-flow rate showerheads produced the smallest concentration of aerosolized total bacteria but contained a significantly high proportion of gram-negative organism which could contain pathogens and higher DWPI partitioning likelihood. Extended periods of stagnation in showers led to increased DWPI and total bacterial concentrations which were only reduced after extended flushing campaign well beyond the current guideline. Overall, these research findings can be translated into a set of recommendations for various stakeholders spanning the advancement of fundamental science to practical guidance on showerhead design and operation. The following

sections provide a set of recommendations based on this work that I think should be considered as we move forward to reduced DWPI exposure in buildings.

## **5.2 Considerations For Future Research**

The insight gained into shower dynamics observed in this dissertation provides valuable information for all stakeholders interested in reducing exposure to DWPIs. In particular, this work contributes to the DW engineering and public health fields, by identifying critical areas that need innovation, such as antimicrobial materials testing for POU fixtures and the addition of showerhead age to current quantitative microbial risk assessment models, to address the real-world dynamics of shower use. In order to test materials and the showerheads created from them effectively, showerhead properties should be tested in real-world conditions with real-world use patterns using a model shower system to determine its effectiveness when utilized by consumers. Moreover, this body of work underscores the necessity of moving away from water grab samples in studies evaluating DWPIs in shower systems. Instead, a comprehensive approach involving sampling for paired biofilm, water, and bioaerosol samples over extended periods is advocated to accurately characterize and develop predictive models for potential exposure. Furthermore, this dissertation has demonstrated the need to assess the respirable fraction of bioaerosols instead of total aerosols as results obtained with this fraction have provided results that can be contrary to the literature in the case of NTM aerosolization<sup>33</sup>. The native DW biofilm that grows in building plumbing and fixtures is a poorly understood component of the DW system, and further research must be conducted to better characterize the potential for the biofilm to enrich DWPIs<sup>1,24</sup>, provide a priming environment to improve virulence<sup>29</sup>, and determine when detachment will likely occur<sup>45</sup>,

possibly with the use of emerging non-destructive technologies (e.g., sensors) or novel techniques. Finally, the influence of silver on biofilm characteristics, specifically changing kinetics to favor staying in a biofilm after exposure to high levels of silver, should be further investigated to determine if these phenotypic differences are permanent and if they translate to increased virulence. Further studies should also characterize how different spray patterns and human interactions with the shower system, such as cleaning regimes and different fan usages, further impact DWPI abundance and the greater microbiome.

Perhaps the most important takeaway from the work contained in this dissertation is the need for interdisciplinary collaboration between researchers in order to fully understand the shower system: the expertise from plumbers, environmental engineers, microbiologists, chemists, material scientists, public health experts, and bioinformaticians are all leveraged to complete this dissertation, and it is the opinion of the author that the future of environmental engineering rests on the ability to incorporate the knowledge and techniques used in other fields to further the understanding of the complex systems that are studied. Further, the work conducted in the microbiome of the showering system and how it relates to public health could benefit from closer involvement of certain fields more immediately than others. Microbiologists who can perform rigorous genomic and proteomic assessment to generate insight on biological mechanisms in all microbial phases (e.g., biofilms, planktonically, and in aerosols) should be consulted for studies involving the elucidation of microorganism characteristics. Materials engineers and product innovators should also be involved in studies that test their products, and feedback between design and consequences of use must be established for effective antimicrobial POU devices to be created and effectively used. Experts in the fate and transport of aerosols (both researchers and experts in air exchange in buildings) that can help model bioaerosols from showerheads and determine

strategies to minimize their inhalation once formed should also become common collaborators in this type of work. Finally, there needs to be greater collaboration with public health practitioners and social workers to assess the human component of DWPI exposure and to help link potential use patterns and behaviors (e.g., showerhead cleaning, overhead fan use, etc.) in domestic settings to health outcomes. Environmental engineering has always been a melting pot of expertise, and encouraging this multidisciplinary approach is essential as the field evolves.

### **5.3 Considerations For Consumers And Building Managers**

The results from this study have direct implications outside of the laboratory for consumers and building managers alike. It is important to note that while DWPIs are an emerging public health concern, the majority of consumers are not at significant risk of developing an infection caused by a DWPI due to their immunocompetency, so these considerations may not be necessary for every person who showers. However, it should be noted that recent evidence has suggested that even otherwise healthy people can become infected with NTM after repeated exposure<sup>16</sup>. Based on this body of work, the author has identified considerations in three areas:

#### **5.3.1 Material Choice Does Not Impact DWPI Densities In Shower Water Or Aerosols**

The central takeaway reiterated throughout this dissertation is the limited impact of showerhead material choice (ABS, metal, various antimicrobials) on the absolute abundances of DWPIs emitted during showering. Specifically, this dissertation found that four different types of antimicrobial showerheads, intended to decrease bacterial concentrations in shower water, failed

to effectively reduce DWPI density in either the produced water or aerosols compared to their inexpensive ABS plastic showerhead competitors regardless of their possible antimicrobial performance in the laboratory. Therefore, from an economic and health perspective building managers and consumers should consider other DWPI reduction strategies instead of antimicrobial showerheads. Furthermore, and possibly more worrisome, building managers and healthcare infection control preventionists should be aware that many marketed antimicrobial showerheads are not tested under real-use scenarios and may not contain the marketed active material in detectable amounts (as observed in Chapter 3) which could jeopardize the safety of vulnerable groups.

### **5.3.2 Water-Conserving Showerheads Increase Aerosol Generation And Containment Of Potentially Pathogenic Microorganisms**

Flow-reducing showerheads tested in this work did not significantly impact DWPI density in produced shower water or aerosols but did create more respirable aerosols containing a higher proportion of gram-negative organisms and higher DWPI partitioning frequency than showerheads with higher flow rates. Based on these findings more research is needed to ascertain whether the Gram-negative organisms enriched in aerosols generated from low-flow showerheads pose an increased risk to consumers. It is the author's recommendation that consumers should consider using water-conserving showerheads with flow rates between 1.5 gal/min and 1.8 gal/min to maximize the tradeoffs of environmental and financial benefits of using a low flow showerhead and the potential for elevated DWPI partitioning. Additionally, it may be prudent for immunocompromised people to refrain from using low flow showerheads until more comprehensive risk assessment has been performed.

### 5.3.3 Shower Water Usage And Management Practices

Because shower use behavior (period of stagnation) was found to significantly impact DWPI abundances, consumers should be aware of the management and maintenance that is done in the buildings they shower in.

Single-family homes: potential DWPI exposure can be reduced from showering by using all the showers in the home on a consistent basis (i.e. not allowing extended stagnation to occur) in addition to setting the hot water heater of the building to be greater than 60 °C if there is scald protection at the tap to reduce microbial proliferation in the tank.

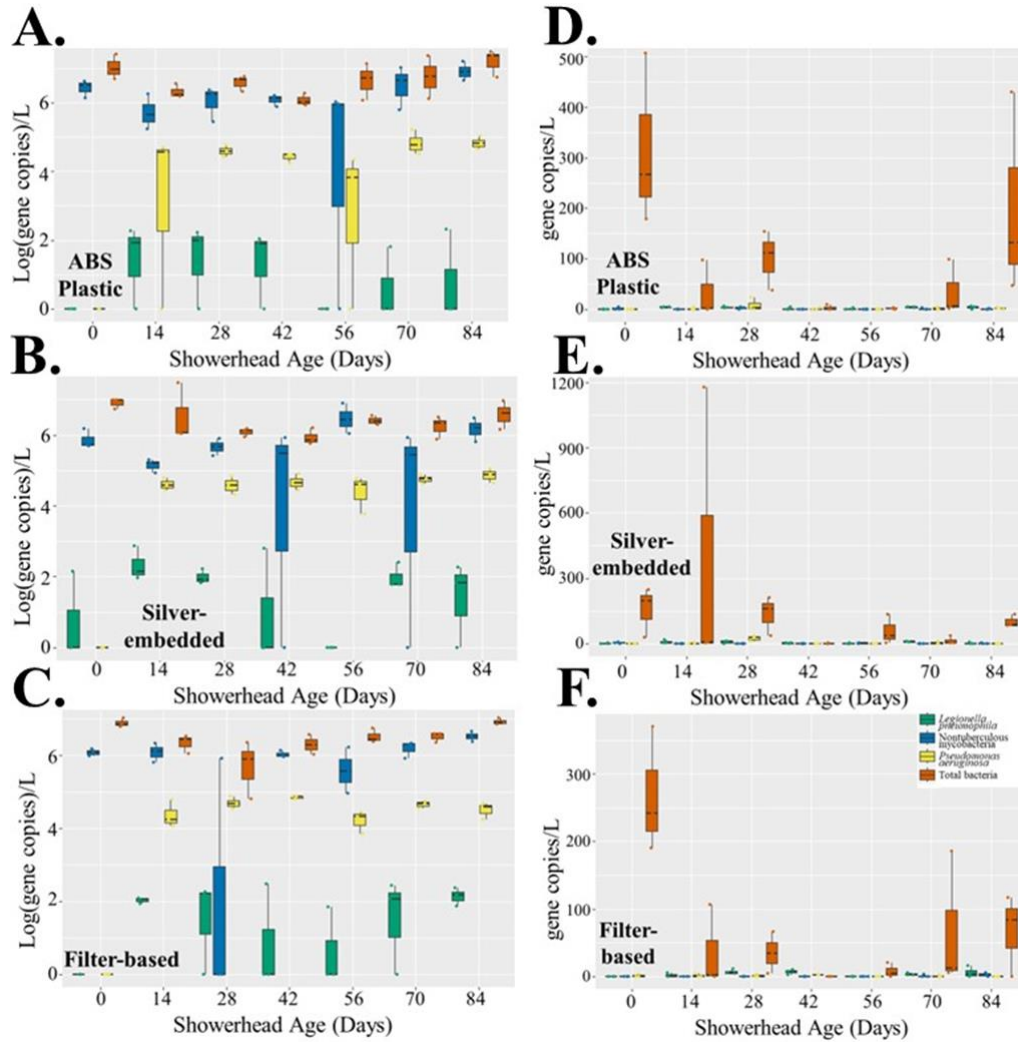
Multi-unit buildings or shared facilities: inquiring about details of water use and maintenance of building plumbing (e.g., if there are bathrooms that aren't used or the frequency of water heater cleaning) can help determine if there is added risk of elevated DWPI loads. When traveling, considering the water use patterns of the accommodations is another place the average person can partially mitigate their exposure to DWPIs: staying in a seasonal accommodation directly after reopening may still have elevated microbial loads in the DW over a hotel that is near capacity year-round.

For building operators who maintain building plumbing, it is essential to have a water management plan in place to preserve water quality. There are many guidance documents available that help with this process<sup>216</sup>, but there is no “one size fits all” solution: each building has different characteristics, and thus will have different needs to maintain microbial water quality. General guidance for managing DWPIs include setting hot water heaters at 60 °C, maintaining that temperature throughout hot water recirculating loops, cleaning and descaling water tanks annually,

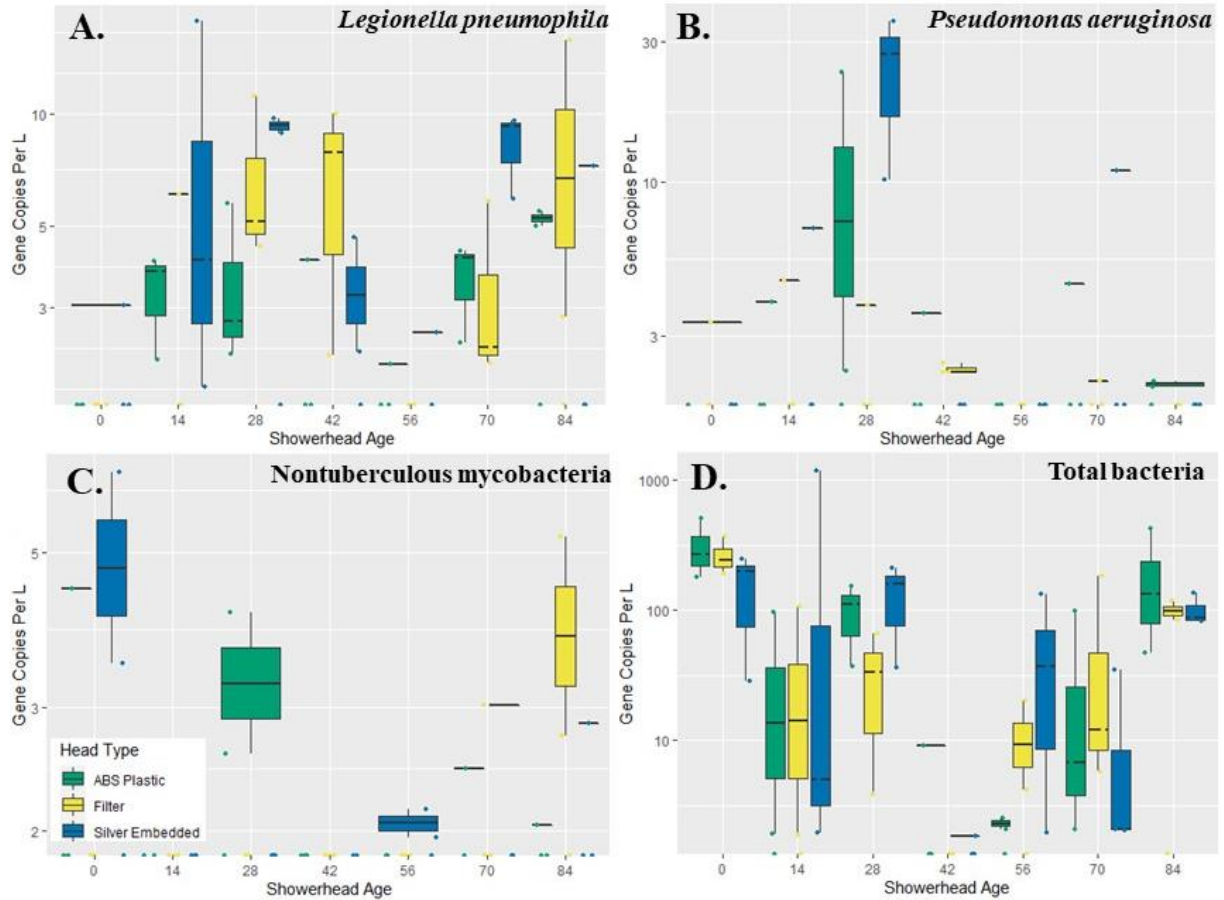
and general monitoring for issues that may arise<sup>216</sup>. These standard operations can help combat DWPI proliferation during normal operational use, but additional considerations for crisis situations must be included to maintain water quality through periods of altered use patterns. The results from the work in [Chapter 4](#) showed that isolated incidents of flushing, as advised by many organizations<sup>187</sup>, were not an effective strategy for reducing DWPIs in events where extended DW stagnation occurred. Therefore, water management plans for reduced occupancy must consider implementing more rigorous flushing protocols, the author would recommend daily flushing of distal outlets in the plumbing system with hot water for a minimum of 5 min over the course of 7 days prior to increasing building occupancy after reduced use. In addition to these larger flushing regimes, considerations into the management of produced aerosols during flushing (e.g., increased ventilation or implementation of air filtration) should also be considered to reduce worker airborne exposure to DWPIs during remediation.

Regardless of the showerhead choices or water management practices used, reducing the inhalation of DWPI-containing aerosols is the best method for reducing possible infection, so always showering with as much air exchange as possible by turning on the fan or having a door or window open can help disrupt the gradual deposition of the bioaerosols, and ultimately help minimize the overall risk of DWPI infection.

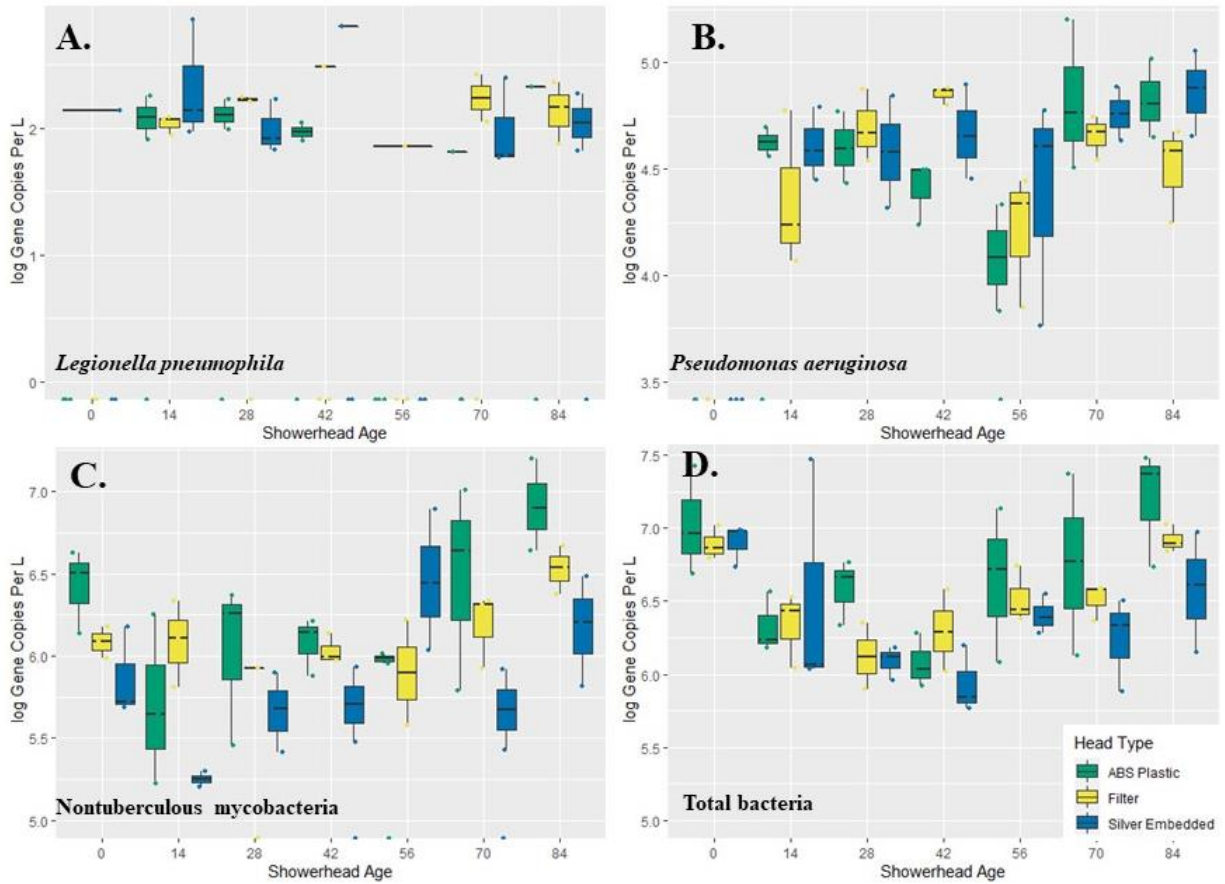
## Appendix A Chapter 2 Supplementary Information



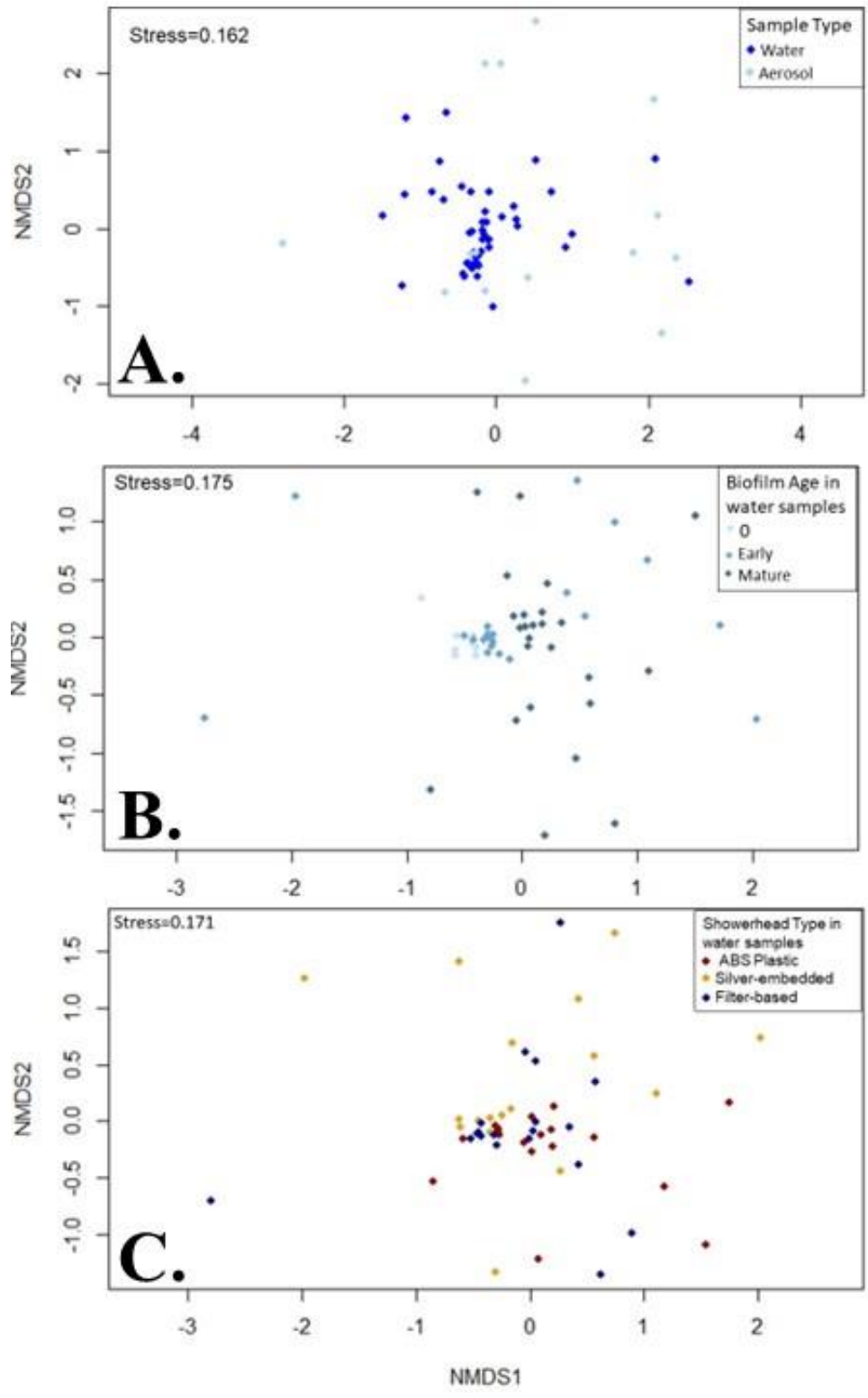
**Appendix A Figure 1: Absolute gene copy concentrations in shower water over time by showerhead type. A. *L. pneumophila*, B. *P. aeruginosa*, C. NTM, and D. total bacteria observed across 14 weeks of operation in ABS plastic (green), filter-based antimicrobial (yellow), and silver-embedded (blue) showerheads in shower water associated aerosols. Each showerhead type shows all the data collected from three experimental showerhead replicates for that specific time point.**



Appendix A Figure 2: Absolute gene copy concentrations in shower water associated aerosols over time. A. *L. pneumophila*, B. *P. aeruginosa*, C. NTM, and D. total bacteria observed across 14 weeks of operation in ABS plastic (green), filter-based antimicrobial (yellow), and silver-embedded (blue) showerheads in shower water associated aerosols. Each showerhead type shows all the data collected from three experimental showerhead replicates for that specific time point.



**Appendix A Figure 3: Absolute gene copy concentrations in shower water over time. A. *L. pneumophila*, B. *P. aeruginosa*, C. NTM, and D. total bacteria observed across 14 weeks of operation in ABS plastic (green), filter-based antimicrobial (yellow), and silver-embedded (blue) showerheads in shower water. Each showerhead type shows all the data collected from three experimental showerhead replicates for that specific time point.**



Appendix A Figure 4: Non-metric Multidimensional Scaling plot by A. sample type, B. biofilm age bin of water samples, and C. showerhead type of water samples.

**Appendix A Table 1: Different physical and chemical water quality parameters measured in this study and corresponding analytical method used.**

<b>Parameter</b>	<b>Units</b>	<b>Analytical Technique</b>	<b>LOD/LOQ</b>
<b>Temperature</b>	°C	Thermometer	
<b>pH</b>		pH electrode	
<b>Free Chlorine</b>	mg/L as Cl <sub>2</sub>	DPD method	0.01/0.02
<b>Total Chlorine</b>	mg/L as Cl <sub>2</sub>	DPD method	0.01/0.02
<b>Ammonia</b>	mg/L as NH <sub>3</sub> -N	Salicylate method	0.01/0.01
<b>Orthophosphate</b>	mg/L as PO <sub>4</sub> <sup>3-</sup>	Ascorbic acid method	0.01/0.02
<b>Total Organic Carbon</b>	mg/L	TOC analyzer	0.01/0.01
<b>Dissolved Organic Carbon</b>	mg/L	TOC analyzer (0.45 μm filtered)	0.01/0.01
<b>Total Iron</b>	mg/L	ICP-MS	0.01/0.01
<b>Total Copper</b>	mg/L	ICP-MS	0.01/0.01
<b>Total Silver</b>	mg/L	ICP-MS	0.01/0.01
<b>Total Lead</b>	mg/L	ICP-MS	0.01/0.01
<b>Total Calcium</b>	mg/L	ICP-MS	0.01/0.01
<b>Total Magnesium</b>	mg/L	ICP-MS	0.01/0.01
<b>Dissolved Iron</b>	mg/L	ICP-MS (0.45 μm filtered)	0.01/0.01
<b>Dissolved Copper</b>	mg/L	ICP-MS (0.45 μm filtered)	0.01/0.01
<b>Dissolved Silver</b>	mg/L	ICP-MS (0.45 μm filtered)	0.01/0.01
<b>Dissolved Lead</b>	mg/L	ICP-MS (0.45 μm filtered)	0.01/0.01
<b>Dissolved Calcium</b>	mg/L	ICP-MS (0.45 μm filtered)	0.01/0.01
<b>Dissolved Magnesium</b>	mg/L	ICP-MS (0.45 μm filtered)	0.01/0.01

**Appendix A Table 2: Molecular primers, thresholds, and assay sensitivity for ddPCR analysis.**

Target Species	Forward (5'-3')	Reverse (5'-3')	Approx. Amplicon Size (bp)	Ref	Limit of Detection (copies/20 µL)	Limit of Quantification (copies/20 µL)	Threshold for water samples	Threshold for aerosol samples
<i>Legionella pneumophila</i>	<i>LpneuF</i>	<i>LpneuR</i>						
<i>Lmip</i> gene	CCGAT GCCAC ATCAT AGC	CCAAT TGAG CGCC ACTCA TAG	150	1	6.08	6.08	8800	6500
<i>Pseudomonas aeruginosa</i>	Ps-F	Ps-R						
<i>Orpl</i> gene	CGAGT ACAAC ATGGC TCTGG	ACCG GACG CTCTT TACCA TA	117	2	7.3	7.3	4500	12530
<i>Nontuberculous mycobacteria</i>	FatpE	RatpE						
<i>atpE</i> gene	CGGYG CCGGT ATCGG YGA	CGAA GACG AACA RSGCC AT	164	3	5.6	5.6	10600	9650
<i>Total bacteria</i>	Eub338	Eub518						
<i>16s rRNA</i> gene	ACTCC TACGG GAGGC AG	ATTAC CGCG GCTGC TGG	200	4	5.3	53	12900	11100
<b>Thermocycling Conditions: 95 °C for 5 min, [95 °C for 0.5 min, 57 °C for 1 min, 72 °C for 1 min] x 45, 4 °C for 5 min, 90 °C for 5 min</b>								
<b>References: 1. Wullings, B. A. et al. 2011. Appl Environ Microbiol 77 (2), 634-641 2. Feizabadi MM et al. 2010. Infect Genet Evol 10: 1247-1251 3. Radomski, N., et al., 2013. BMC Microbiol, 13(1), 277 4. Fierer, N., et al., 2005. App, Env, Microbiol, 71(7), 4117-4120</b>								

Appendix A Table 3: Average values of water quality parameters.

	0						14						28						
	Age	ABS Plastic	Silver-embedded	Filter-based	ABS Plastic	Silver-embedd	Filter-based	ABS Plastic	Silver-embedd	Filter-based	ABS Plastic	Silver-embedded	Filter-based	ABS Plastic	Silver-embedded	Filter-based			
Dissolved	Ca	34.2±0.6	33.4±0.3	34.3±0.8	34.5±0.5	34.9±0.6	90.7±93.9	36.1±0.1	36.9±0.8	37.3±1.1									
	Mg	12.1±0.5	9.7±0.3	9.2±0.2	9.7±0.2	9.4±0.1	22.6±22.5	10.7±0.2	9.1±0.1	8.8±0.1									
	Pb	<LOD	<LOD	<LOD	<LOD	<LOD	<LOD	<LOD	<LOD	<LOD	<LOD								
	Ag	<LOD	<LOD	<LOD	<LOD	<LOD	<LOD	<LOD	<LOD	<LOD	<LOD								
	Cu	0.04±0.02	0.03±7.7x10 <sup>-3</sup>	0.05±3.3x10 <sup>-3</sup>	0.04±2.5x10 <sup>-3</sup>	0.09±0.09	0.1±0.09	0.03±4.4x10 <sup>-3</sup>	0.04±7.3x10 <sup>-3</sup>	0.05±4.5x10 <sup>-3</sup>									
	Fe	0.1±0.03	0.2±0.1	0.2±0.01	0.2±0.03	0.3±0.02	0.7±0.6	0.4±0.05	0.5±8.8x10 <sup>-3</sup>	0.5±0.02									
	Org C	1.4±0.1	0.9±0.03	1.1±0.1	0.2±0.2	0.5±0.8	1.6±0.4	2.0±0.2	0.5±0.2	0.8±0.1									
	Ca	33.9±0.06	32.5± 2.1	34.1±1.1	34.3±1.6	35.7±0.7	36.5±0.6	36.2±0.5	36.4±1.0	36.6±0.3									
	Mg	12.1±0.3	9.2±0.6	9.1±0.3	9.4±0.3	9.5±0.3	9.4±0.2	10.5±0.1	9.1±0.07	8.8±0.06									
	Pb	<LOD	<LOD	<LOD	<LOD	<LOD	<LOD	<LOD	<LOD	<LOD	<LOD								
	Ag	<LOD	<LOD	<LOD	<LOD	<LOD	<LOD	<LOD	<LOD	<LOD	<LOD								
	Cu	0.03±1x10 <sup>-3</sup>	0.04±4x10 <sup>-3</sup>	0.07±0.02	0.04±1x10 <sup>-3</sup>	0.04±0.02	0.04±4.5x10 <sup>-3</sup>	0.03±3.4x10 <sup>-3</sup>	0.05±4.9x10 <sup>-3</sup>	0.05±7.3x10 <sup>-3</sup>									
	Fe	0.1±0.02	0.1±0.03	0.2±0.03	0.3±0.07	0.2±0.1	0.3±0.01	0.4±0.03	0.5±0.02	0.5±0									
	Org C	1.5±0.05	1.5±0.3	1.4±0.2	1.2±0.2	1.3±0.06	1.3±0.2	0.9±0.2	1.0±0.1	1.1±0.2									
	Total	Ortho-PO <sub>3</sub> -	1.3±0.2	1.7±0.04	1.5±0.2	1.2±0.1	1.1±0.2	1.1±0.5	1.2±0.2	1.2±0.2	1.2±0.1								
		Ammonia	0.1±0.06	0.04±0.02	0.02±0	0.03±0.01	0.02±0.02	0.04±0.01	0.01±0.01	0±0	0.02±0.01								
Total Cl		0.01±0	0.0±0	0.02±0.02	0.09±0.02	0.1±0.1	0.09±0.03	0.07±0.02	0.08±0.01	0.1±0.02									
Free Cl		0.01±0	0.01±0	0.05±0.1	0.2±0.06	0.2±0.07	0.04±0.04	0.02±0.03	0.12±0.08	0.1±0.08									
Temp (°C)		36.2±0.4	37.2±0.7	36.9±0.8	36.8± 1.1	37.8±0.3	36.8±1.5	36.9±0.8	38.4± 1.4	37.6±1.5									
pH		8.6±0.07	8.1±0.7	8.1±0.05	8.1±0.05	8.0± 5x10 <sup>-3</sup>	8.0±0.02	8.5±0.02	8.1±0.04	8.0±0.05									
Type		ABS Plastic	Silver-embedded	Filter-based	ABS Plastic	Silver-embedd	Filter-based	ABS Plastic	Silver-embedded	Filter-based									
Age		0						14						28					

43.6±5.8	43±2.0	47.5±5.3	52.8±1.7	56.2±1.2	61.0±8.8	51.9±1.4	\$0.4±0.4	51.6±0.6	0.6±1.2
7.4±0.3	7.5±0.2	7.9±0.8	8.0±0.2	8.1±0.09	9.0±1.3	7.5±0.2	7.0±0.05	6.9±0.09	0.6±0.02
<LOD									
<LOD									
0.03±5.9x10 <sup>-3</sup>	0.05±0.01	0.05±5.4x10 <sup>-3</sup>	0.04±5.5x10 <sup>-3</sup>	0.04±5.5x10 <sup>-3</sup>	0.05±0.01	0.04±2.0x10 <sup>-3</sup>	0.05±7.2x10 <sup>-3</sup>	0.06±5.5x10 <sup>-3</sup>	0.03±4.1x10 <sup>-3</sup>
0.2±0.06	0.2±0.02	0.2±0.03	0.2±0.02	0.2±0.02	0.2±0.03	0.2±0.02	0.2±0.03	0.2±0.06	0.1±0.03
0.2±0.3	0.5±0.7	0.4±0.5	2.7±0.02	2.5±0.2	3.0±0.4	1.4±0.1	2.0±0.3	2.1±0.3	0.4±0.7
41.3±0.6	42.7±1.6	45.1±0.6	54.5±1.2	54.5±0.8	\$6.6±1.0	50.4±0.3	51.1±0.7	50.0±0.5	43.5±0.6
7.5±0.09	7.6±0.05	7.6±0.2	8.3±0.1	8.2±0.07	8.3±0.2	7.5±0.09	7.1±0.06	7.0±0.2	6.0±0.1
<LOD									
<LOD									
0.1±0.2	0.04±1.1x10 <sup>-3</sup>	0.05±4.8x10 <sup>-3</sup>	0.05±4.7x10 <sup>-3</sup>	0.05±4.7x10 <sup>-3</sup>	0.05±2.6x10 <sup>-3</sup>	0.05±4.8x10 <sup>-3</sup>	0.06±9.8x10 <sup>-3</sup>	0.06±4.5x10 <sup>-3</sup>	0.04±0.01
0.2±0.01	0.2±0.03	0.2±0.01	0.2±0.03	0.2±0.02	0.2±0.02	0.2±0.02	0.2±0.02	0.2±0.02	0.1±0.03
0.4±0.2	0.4±0.2	0.4±0.05	2.6±0.2	2.4±0.1	2.6±0.2	1.5±0.3	1.2±0.1	1.1±0.05	0.4±0.7
0.8±0.6	0.6±0.6	1.2±0.07	1.2±0.06	1.1±0.03	1.1±0.3	1.2±0.04	0.9±0.8	0.7±0.6	1.2±0.3
0.01±0.01	0.01±0.01	0.02±0.02	0.1±0.05	0.02±0.01	0.03±0.02	0.01±0.01	0±0	0.02±0.03	0.07±0.06
0.1±0.05	0.2±0.08	0.04±0.01	0.1±0.04	0.06±0.03	0.04±0.02	0.06±0.03	0.07±0.01	0.05±0.03	0.05±0.01
0.1±0.05	0.1±0.02	0.1±0.05	0.06±0.03	0.05±0.03	0.02±0.03	0.07±0.09	0.05±0.01	7x10 <sup>-3</sup> ±0.01	0.05±0.04
37.8±0.7	37.8±1.2	37.1±1.1	36.8±0.6	38.3±1.1	37.2±1.4	37.0±1.6	38.0±1.0	37.5±1.2	37.1±1.1
7.9±0.06	7.9±0.04	7.9±0.04	7.9±0.03	7.8±0.02	7.8±0.03	7.9±0.05	7.8±0.03	7.5±0.03	7.8±0.04
<b>42</b>			<b>56</b>			<b>70</b>			<b>84</b>
<b>ABS Plastic</b>	<b>Silver-embedded</b>	<b>Filter-based</b>	<b>ABS Plastic</b>	<b>Silver-embedded</b>	<b>Filter-based</b>	<b>ABS Plastic</b>	<b>Silver-embedded</b>	<b>Filter-based</b>	<b>ABS Plastic</b>

44.7±0.2	44.9±1.4
0.6±0.07	0.6±0.02
0.01±1.3×10 <sup>3</sup>	0.01±3.9×10 <sup>-3</sup>
<LOD	<LOD
0.2±0.1	0.08±0.02
0.2±0.02	0.1±0.04
1.4±0.1	0.8±0.7
45.7±1.4	46.2±1.8
6.6±0.7	6.2±0.3
1.2×10 <sup>2</sup> ±3×10 <sup>3</sup>	<LOD
<LOD	<LOD
0.7±0.8	0.2±1.2
0.2±0.1	0.2±0.08
0.5±0.8	0.7±0.7
1.2±0.5	1.1±0.5
0.04±0.03	0.04±0.02
0.03±0.03	0.04±0.02
0.02±0.01	0.01±0
38.0±1.1	37.5±0.7
7.8±0.08	7.7±0.03
<b>Silver- embedded</b>	<b>Filter- based</b>

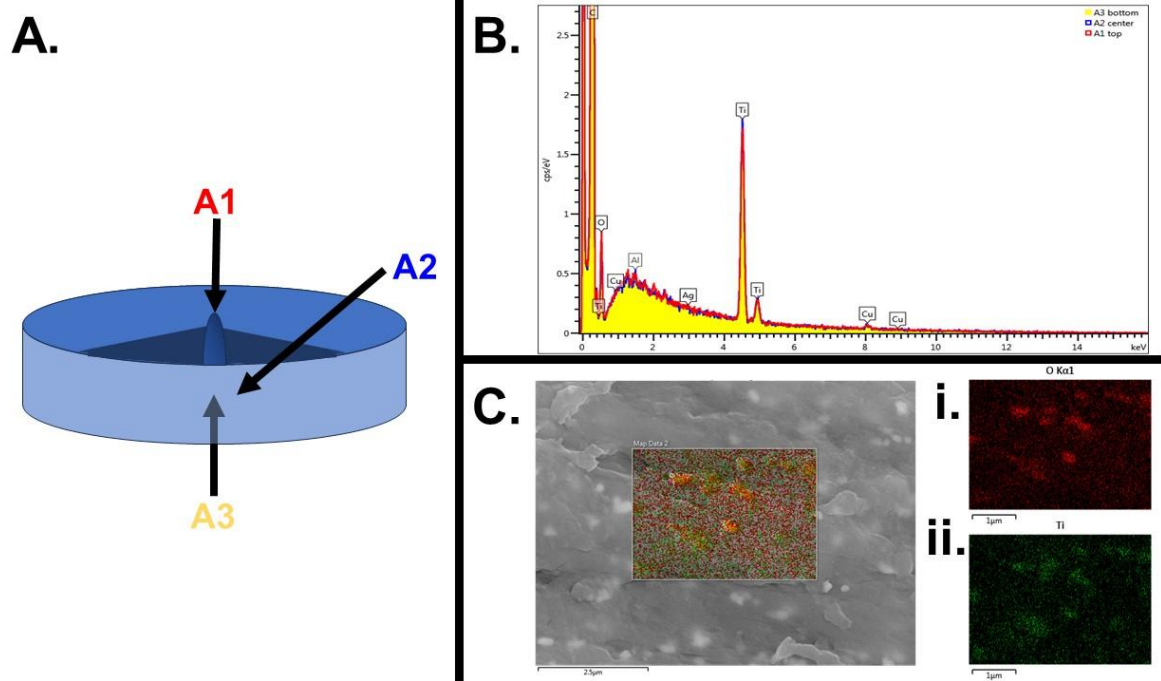
**Appendix A Table 4: Average aerosol partitioning values of DWPIs and total bacteria by head type**

Target	Average aerosolization partitioning percentage (%) $\pm$ standard deviation			Significance of showerhead type (ANOVA <i>p</i> -value)
	ABS Plastic	Silver-embedded	Filter-based	
<i>L. pneumophila</i>	1.06 $\pm$ 2.1	3.27 $\pm$ 5.8	1.71 $\pm$ 3.0	0.3
<i>P. aeruginosa</i>	5.33x10 <sup>-5</sup> $\pm$ 1.34x10 <sup>-4</sup>	1.07x10 <sup>-4</sup> $\pm$ 2.35x10 <sup>-4</sup>	2.16x10 <sup>-5</sup> $\pm$ 5.85x10 <sup>-5</sup>	0.2
Nontuberculous mycobacteria	1.02x10 <sup>-6</sup> $\pm$ 3.22x10 <sup>-6</sup>	1.14x10 <sup>-6</sup> $\pm$ 3.17x10 <sup>-6</sup>	2.8x10 <sup>-7</sup> $\pm$ 8.34x10 <sup>-7</sup>	0.2
Total bacteria	1.74x10 <sup>-5</sup> $\pm$ 2.67x10 <sup>-5</sup>	3.28x10 <sup>-5</sup> $\pm$ 4.90x10 <sup>-5</sup>	1.76x10 <sup>-5</sup> $\pm$ 2.13x10 <sup>-5</sup>	0.5

### **Appendix A Procedure 1: Threshold determination for ddPCR quantification**

Thresholding was achieved by taking a sample that had already been run on the instrument, and spiking a known amount of gblock into the matrix for each primer type used in this study. Spiked samples were run using the same method described in the manuscript, and the amplitude plots for the spiked and unspiked sample were compared. Thresholds were tried between the positive and negative bands: each concentration output for potential threshold was back calculated, and the concentration of the unspiked sample was subtracted from the spiked sample concentration. This process was iterated until a threshold was chosen that yielded a spiked sample concentration that matched the initial gblock concentration initially put into the sample after the subtraction of the concentration of the unspiked sample.

Appendix B : Chapter 3 Supplementary Information



Appendix B Figure 1: Summary of SEM-EDS analysis conducted on silver-containing inserts of the silver-embedded head A. Annotated diagram of the sampling sites of the shower insert, with A1 being the ‘top’ of the insert, A2 being taken from the side wall, and A3 being the ‘bottom’ of the insert. B. Representative EDS scan from an insert with red corresponding to sampling site A1, blue corresponding to sampling site A2, and yellow corresponding to sampling site A3. C. Representative SEM image taken from the showerhead insert, with maps of i. oxygen and ii. titanium.

**A.**

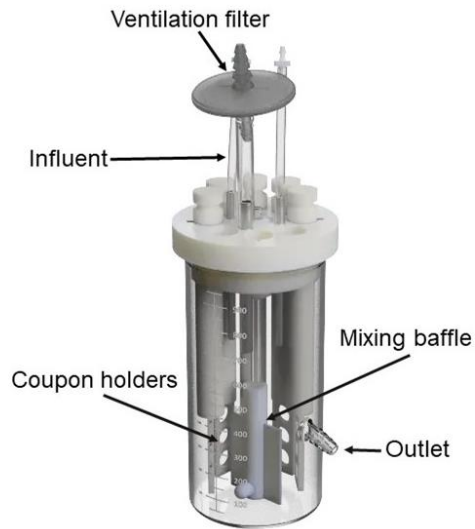
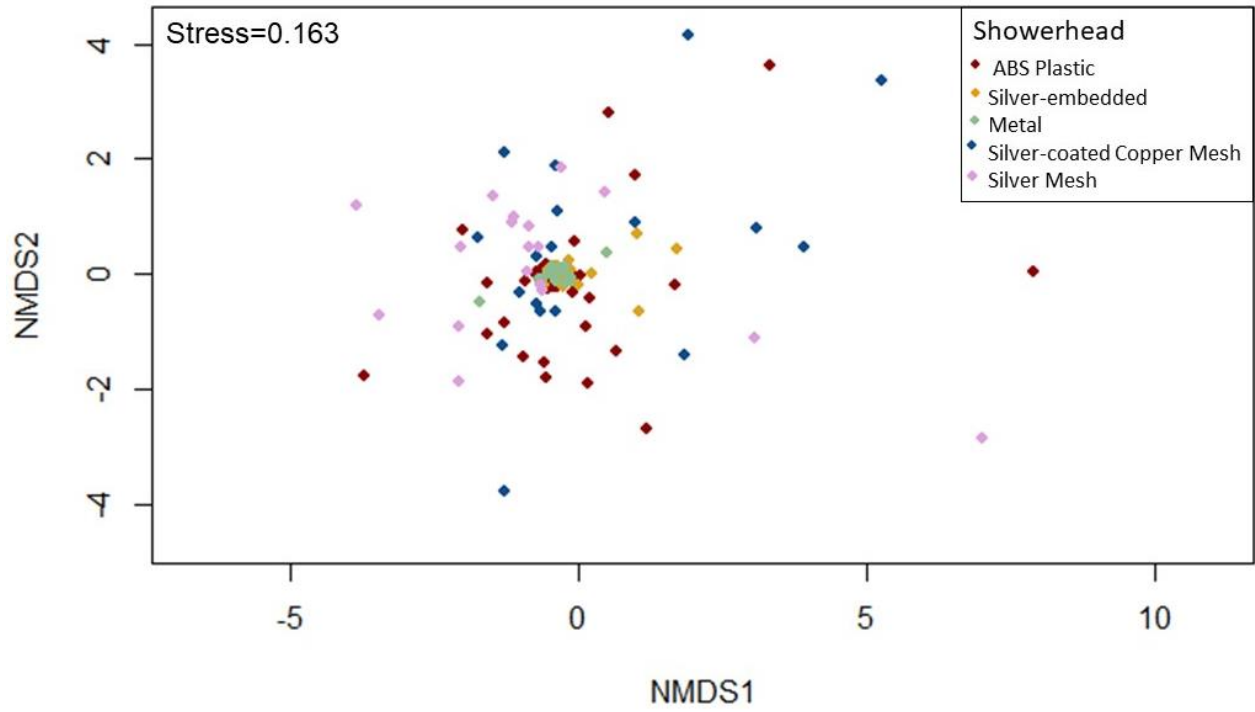


Image source: BioSurfaces Technology Corporation

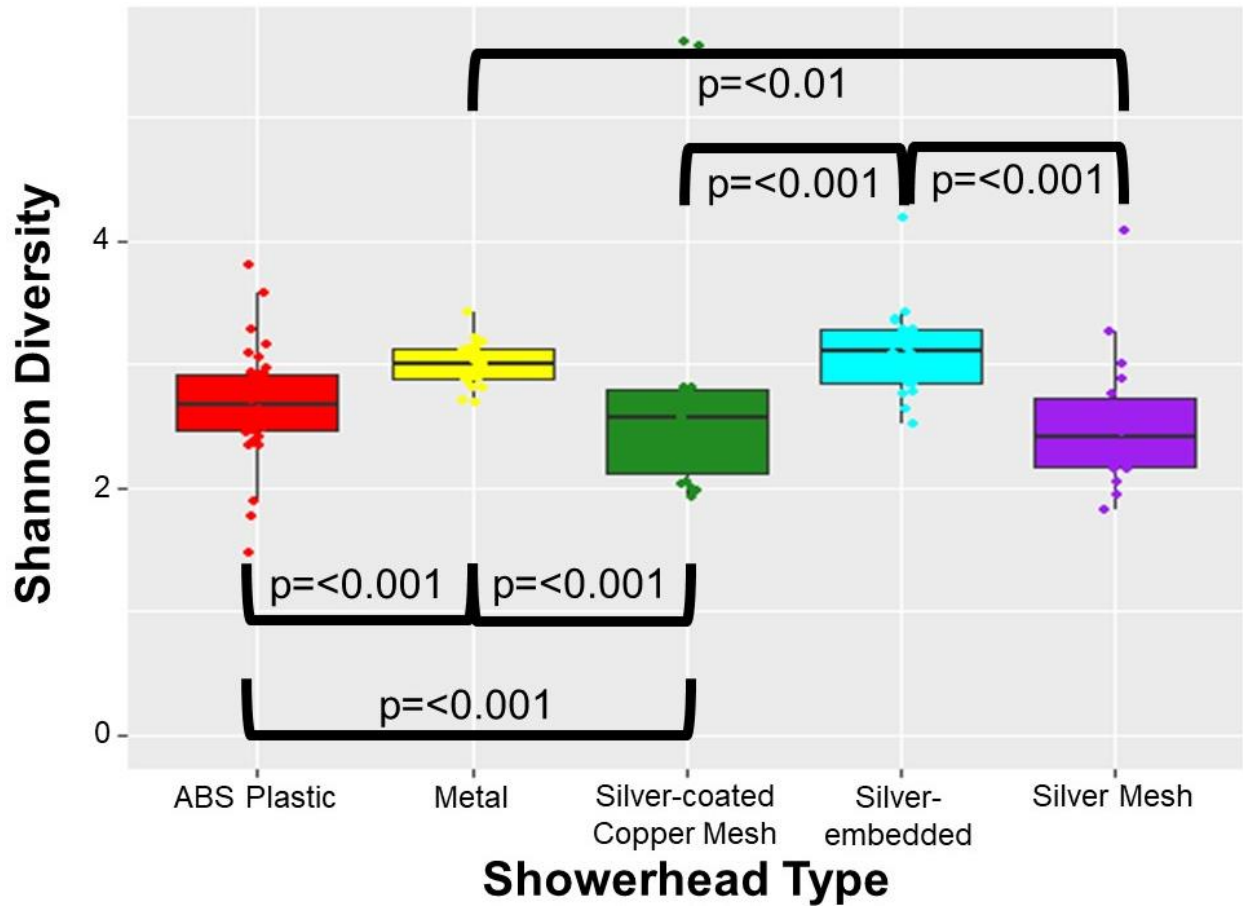
**B.**



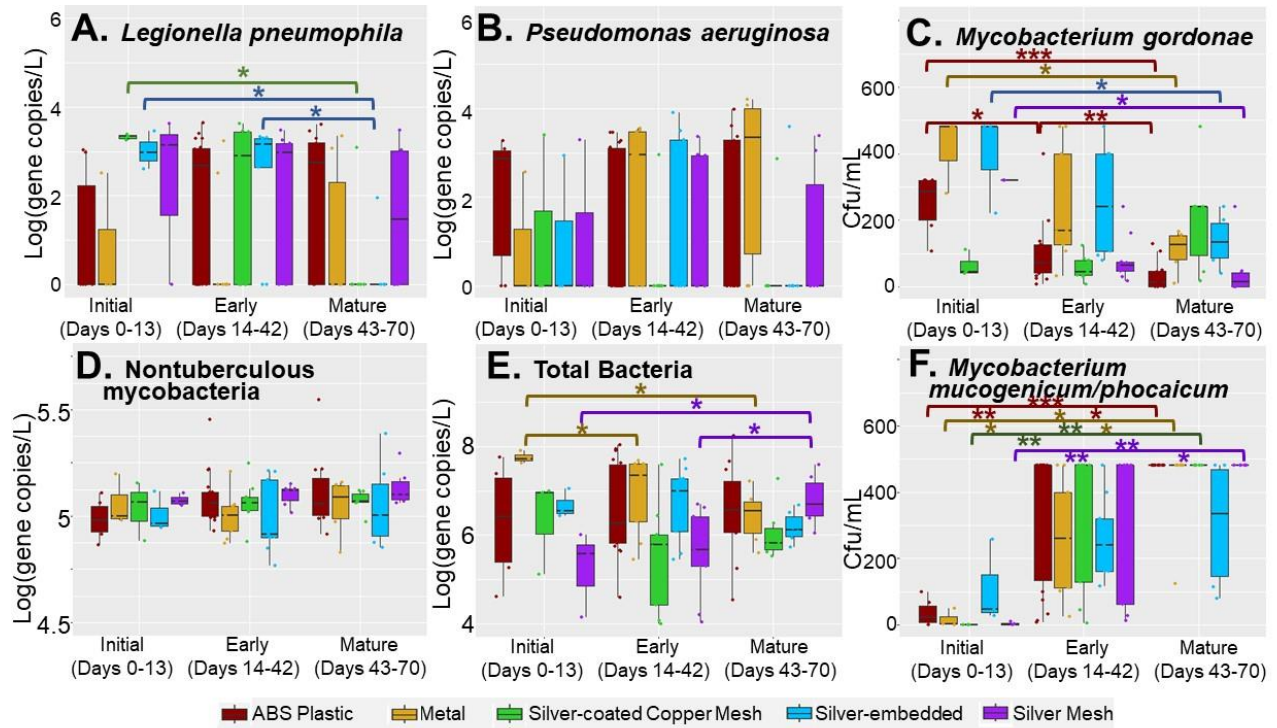
**Appendix B Figure 2: CDC Biofilm Reactor Schematic. A. Annotated diagram of a CDC Biofilm Reactor, and B. A representative experimental reactor set up. The red star indicates the location of the influent, the yellow star indicates the location of the reactor itself, and the blue star indicates the location of the pump.**



Appendix B Figure 3: Non-metric Multidimensional Scaling plot of water samples by showerhead type



Appendix B Figure 4: Shannon diversity calculated from water samples by showerhead type

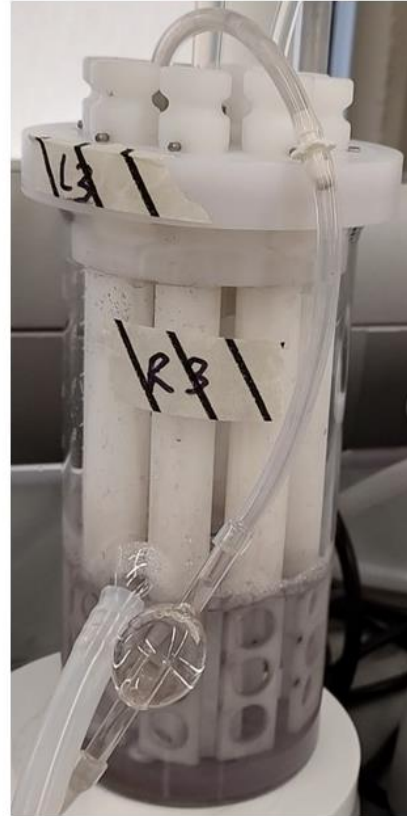


**Appendix B Figure 5: Viable concentrations of A. *L. pneumophila*, B. *P. aeruginosa*, C. *M. gordonae*, D. NTM, E. total bacteria, and F. *M. mucogenicum/phocaicum* for ABS plastic (red), metal (yellow), silver-coated copper mesh (green), silver-embedded (blue), and silver mesh (purple) showerheads by biofilm formation stage. Significant differences are marked with a colored bracket and star corresponding to the showerhead type and p-value (\* =  $p \leq 0.05$ , \*\* =  $p \leq 0.01$ , \*\*\* =  $p \leq 0.001$ )**

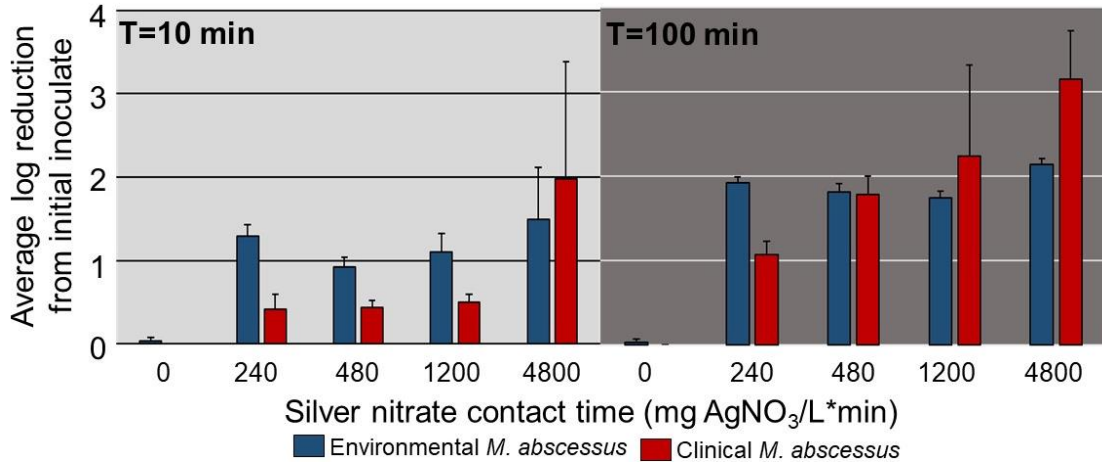
**A.**



**B.**



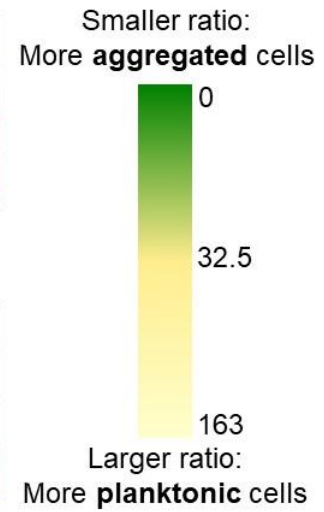
**Appendix B Figure 6: Visual discoloration cause by silver nitrate of the reactors with 480 mg Ag<sup>+</sup>/L\*min (A.) and 4800 mg Ag<sup>+</sup>/L\*min (B.) after 7 days of reactor operation.**



**Appendix B Figure 7: Average log reduction  $\pm$  standard deviation of environmental (dark blue) and clinical (dark red) *M. abscessus* exposed to various silver nitrate concentrations for 10 minutes (light grey) or 100 minutes (dark grey). Each bar represents n=3 samples. The initial inoculate concentration for environmental and clinical isolates were  $2.8 \times 10^6$  cfu/mL and  $3.4 \times 10^6$  cfu/mL, respectively.**

### Clinical *M. abscessus*

Time (hr)	35	14.3	17	18.3	37.5	13.2	21.7	21	31.5	25
	33	45	69.5	61.5	35	72	34.7	37	47	51
	24	12.3	163	0	42.9	153	37.3	152	156	0
	0	0	0	0	0	0	0	0	0	0



### Environmental *M. abscessus*

Time (hr)	35	8.4	4.9	10.9	12.1	6.9	5.7	6.4	14.6	10.6
	33	20.3	30.3	15.7	13.1	23.5	5.9	20	13.7	18.4
	24	26.2	36	31.2	17.6	39	16	41	24.4	20.7
	0	0	0	0	0	0	0	0	0	0

Appendix B Figure 8: Planktonic vs. aggregate *M. abscessus* ratios (ranges in parentheses) for clinical (0–163) and B. environmental (0–41) isolates for the initial inoculates (each tile is one technical replicate, for a total of  $n = 9$  per isolate  $\times$  time). Green cells represent a smaller ratio, signifying a larger proportion of aggregated *M. abscessus* cells, while yellow cells represent a higher ratio, signifying a larger proportion of planktonic *M. abscessus* cells. The dark yellow cells represent the 50th percentile. The ratios were obtained by dividing the planktonic OD600 measurements by the aggregate OD600 measurements.

**Appendix B Table 1: Different physical and chemical water quality parameters measured in this study and corresponding analytical method used**

<b>Parameter</b>	<b>Units</b>	<b>Analytical Technique</b>	<b>LOD/LOQ</b>
<b>Temperature</b>	°C	Thermometer	
<b>pH</b>		pH electrode	
<b>Free Chlorine</b>	mg/L as Cl <sub>2</sub>	DPD method	0.01/0.02
<b>Total Chlorine</b>	mg/L as Cl <sub>2</sub>	DPD method	0.01/0.02
<b>Ammonia</b>	mg/L as NH <sub>3</sub> -N	Salicylate method	0.01/0.01
<b>Orthophosphate</b>	mg/L as PO <sub>4</sub> <sup>3-</sup>	Ascorbic acid method	0.01/0.02
<b>Total Organic Carbon</b>	mg/L	TOC analyzer	0.01/0.01
<b>Dissolved Organic Carbon</b>	mg/L	TOC analyzer (0.45 µm filtered)	0.01/0.01
<b>Total Iron</b>	mg/L	ICP-MS	0.01/0.01
<b>Total Copper</b>	mg/L	ICP-MS	0.01/0.01
<b>Total Silver</b>	mg/L	ICP-MS	0.01/0.01
<b>Total Lead</b>	mg/L	ICP-MS	0.01/0.01
<b>Total Calcium</b>	mg/L	ICP-MS	0.01/0.01
<b>Total Magnesium</b>	mg/L	ICP-MS	0.01/0.01
<b>Dissolved Iron</b>	mg/L	ICP-MS (0.45 µm filtered)	0.01/0.01
<b>Dissolved Copper</b>	mg/L	ICP-MS (0.45 µm filtered)	0.01/0.01
<b>Dissolved Silver</b>	mg/L	ICP-MS (0.45 µm filtered)	0.01/0.01
<b>Dissolved Lead</b>	mg/L	ICP-MS (0.45 µm filtered)	0.01/0.01
<b>Dissolved Calcium</b>	mg/L	ICP-MS (0.45 µm filtered)	0.01/0.01
<b>Dissolved Magnesium</b>	mg/L	ICP-MS (0.45 µm filtered)	0.01/0.01

**Appendix B Table 2: Molecular primers, thresholds, and assay sensitivity for ddPCR analysis**

Target Species	Forward (5'-3')	Reverse (5'-3')	Approx. Amplicon Size (bp)	Ref	Limit of Detection and Quantification (copies/20 µL)	Threshold for water samples
<i>Legionella pneumophila</i>	<i>LpneuF</i>	<i>LpneuR</i>				
<i>Lmip</i> gene	CCGAT GCCAC ATCAT AGC	CCAAT TGAG CGCC ACTCA TAG	150	1	6.08	7793
<i>Pseudomonas aeruginosa</i>	Ps-F	Ps-R				
<i>Orpl</i> gene	CGAGT ACAAC ATGGC TCTGG	ACCG GACG CTCTT TACCA TA	117	2	7.3	5560
<i>Nontuberculous mycobacteria</i>	FatpE	RatpE				
<i>atpE</i> gene	CGGYG CCGGT ATCGG YGA	CGAA GACG ACA RSGCC AT	164	3	5.6	9800
<i>Total bacteria</i>	Eub338	Eub518				
<i>16s rRNA</i> gene	ACTCC TACGG GAGGC AG	ATTAC CGCG GCTGC TGG	200	4	5.3	9500
<b>Thermocycling Conditions</b>						
<i>L. pneumophila</i> and <i>P. aeruginosa</i>	95 °C for 5 min, [95 °C for 1 min, 56 °C for 1 min, 72 °C for 2 min] x 45, 4 °C for 5 min, 90 °C for 5 min					
NTM	95 °C for 5 min, [95 °C for 1 min, 59 °C for 1 min, 72 °C for 2 min] x 45, 4 °C for 5 min, 90 °C for 5 min					
<i>Total bacteria</i>	95 °C for 5 min, [95 °C for 1 min, 60 °C for 1 min, 72 °C for 2 min] x 45, 4 °C for 5 min, 90 °C for 5 min					
<p><b>References: 1. Wullings, B. A. et al. 2011. Appl Environ Microbiol 77 (2), 634-641 2. Feizabadi MM et al. 2010. Infect Genet Evol 10: 1247-1251 3. Radomski, N., et al., 2013. BMC Microbiol, 13(1), 277 4. Fierer, N., et al., 2005. App, Env, Microbiol, 71(7), 4117-4120</b></p>						

**Appendix B Table 3: Average values of water quality parameters**

Showerhead type	ABS Plastic	Metal	Silver Mesh	Silver-coated Copper Mesh	Silver-embedded
Temperature	24.7 ± 2.6	24.6 ± 3.6	24.8 ± 2.5	23.7 ± 2.3	25.3 ± 2.8
pH	7.3 ± 0.6	7.3 ± 0.7	7.4 ± 0.4	7.4 ± 0.5	7.3 ± 0.5
ORP	222.4 ± 99.0	179.6 ± 44.6	269.7 ± 106.5	235.2 ± 89.4	181.2 ± 35.1
Free Chlorine	0.01 ± 0.01	0.01 ± 0.02	0.02 ± 0.02	0.02 ± 0.02	0.01 ± 0.01
Total Chlorine	0.02 ± 0.03	0.01 ± 0.01	0.04 ± 0.03	0.03 ± 0.04	0.01 ± 0.01
Orthophosphate	1.1 ± 0.2	1.1 ± 0.2	1.1 ± 0.2	1.1 ± 0.1	1.0 ± 0.1
Total Carbon	10.3 ± 2.1	11.0 ± 0.8	10.4 ± 1.4	10.5 ± 1.7	11.0 ± 0.9
Inorganic Carbon	9.0 ± 1.9	9.6 ± 0.8	9.2 ± 1.3	9.2 ± 1.3	9.5 ± 0.8
Total Organic Carbon	1.2 ± 0.5	1.4 ± 0.3	1.3 ± 0.5	1.3 ± 0.6	1.5 ± 0.4
Total Dissolved Carbon	10.5 ± 1.2	10.8 ± 0.9	10.3 ± 1.2	10.4 ± 1.5	10.8 ± 0.9
Dissolved Inorganic Carbon	9.4 ± 1.1	9.6 ± 0.8	9.2 ± 1.3	9.2 ± 1.4	9.5 ± 0.8
Dissolved Organic Carbon	1.1 ± 0.4	1.2 ± 0.4	1.1 ± 0.4	1.2 ± 0.5	1.3 ± 0.3
Total Silver	3.3 x 10 <sup>-3</sup> ± 0.01	5.6 x 10 <sup>-4</sup> ± 2.4 x 10 <sup>-3</sup>	8.9 x 10 <sup>-3</sup> ± 0.02	0.1 ± 0.2	0.01 ± 0.02
Total Magnesium	3.9 x 10 <sup>3</sup> ± 625.6	4.0 x 10 <sup>3</sup> ± 664.0	3.9 x 10 <sup>3</sup> ± 791.3	3.9 x 10 <sup>3</sup> ± 802.2	3.9 x 10 <sup>3</sup> ± 636.5
Total Copper	59.1 ± 36.3	86.5 ± 36.1	45.7 ± 22.3	101.3 ± 78.6	88.7 ± 21.8
Total Iron	248.8 ± 463.2	440.1 ± 674.7	51.4 ± 14.2	52.7 ± 12.1	417.0 ± 599.5
Total Lead	0.2 ± 0.3	1.4 ± 1.0	0.3 ± 0.5	0.2 ± 0.2	0.4 ± 0.4
Total Zinc	77.9 ± 47.8	121.5 ± 27.4	55.8 ± 58.2	45.2 ± 38.8	118.6 ± 43.8
Total Manganese	5.0 ± 13.8	11.4 ± 24.0	0.7 ± 0.8	0.7 ± 0.8	5.7 ± 10.6
Total Cadmium	0.02 ± 0.1	9.0 x 10 <sup>-3</sup> ± 7.4 x 10 <sup>-3</sup>	3.3 x 10 <sup>-3</sup> ± 0.02	5.0 x 10 <sup>-3</sup> ± 0.02	4.5 x 10 <sup>-3</sup> ± 7.9 x 10 <sup>-3</sup>
Dissolved Silver	0 ± 0.01	0 ± 0	0.02 ± 0.07	0.1 ± 0.1	0.1 ± 0.4
Dissolved Magnesium	3.8 x 10 <sup>3</sup> ± 608.5	3.9 x 10 <sup>3</sup> ± 609.5	3.9 x 10 <sup>3</sup> ± 700.6	3.9 x 10 <sup>3</sup> ± 740.0	3.8 x 10 <sup>3</sup> ± 583.5
Dissolved Copper	41.9 ± 31.7	63.2 ± 34.8	28.0 ± 14.0	56.5 ± 28.0	67.8 ± 27.0
Dissolved Iron	186.0 ± 385.6	320.8 ± 516.5	61.5 ± 50.0	86.7 ± 136.2	307.9 ± 513.2
Dissolved Lead	0.02 ± 0.06	0.6 ± 0.5	0.2 ± 0.7	0 ± 0.06	0.1 ± 0.1
Dissolved Zinc	55.2 ± 41.6	99.0 ± 29.7	30.7 ± 30.0	25.4 ± 19.6	91.3 ± 31.9
Dissolved Manganese	5.3 ± 22.8	1.7 ± 3.0	0.6 ± 2.0	1.8 ± 5.3	0.6 ± 0.6
Dissolved Cadmium	0 ± 0.01	0.09 ± 0.3	5.6 x 10 <sup>-3</sup> ± 0.02	0.01 ± 0.05	2.8 x 10 <sup>-3</sup> ± 4.6 x 10 <sup>-3</sup>

**Appendix B Table 4: Summary of generated linear models in water samples. In the model components column, ± indicates positive or negative association and the percent of the variance explained by each variable is superscripted.**

Model (Transformation)	Model Components	Overall Model	
		Explained (%)	p-value
<i>L. pneumophila</i> (logarithmic)	-Biofilm Age <sup>1.8%</sup> , - Stall <sup>5.5%</sup> , -pH <sup>2.5%</sup> , -Orthophosphate <sup>1.9%</sup>	11.9	0.01
<i>P. aeruginosa</i> (logarithmic)	-Biofilm Age <sup>3.1%</sup> , -Campaign <sup>5.1%</sup> , -Viable <i>L. pneumophila</i> <sup>2.3%</sup> , - Cultured <i>M. mucogenicum/phocaicum</i> <sup>2%</sup>	12.5	0.008
Nontuberculous mycobacteria (logarithmic)	-Campaign <sup>2.8%</sup> , -Viable <i>P. aeruginosa</i> <sup>2.7%</sup> , -Viable total bacteria <sup>13.2%</sup> , - Orthophosphate <sup>6%</sup>	24.7	6.2x10 <sup>-6</sup>
Total bacteria (logarithmic)	-Temperature <sup>0.7%</sup> , -Dissolved Magnesium <sup>4.4%</sup> , -Dissolved Copper <sup>8%</sup> , - Viable nontuberculous mycobacteria <sup>12.2%</sup> , -Campaign <sup>5.4%</sup>	30.7	3.8x10 <sup>-7</sup>
Microbial community (Hellinger)	-Total Copper <sup>1.5%</sup> , -Stall <sup>1.9%</sup> , -Total Zinc <sup>2.5%</sup> , -Showerhead Type <sup>10.2%</sup> , - Biofilm Age <sup>5%</sup>	21.1	

**Appendix B Table 5: Average diversity values of water samples  $\pm$  standard deviation. Sample size is denoted in parentheses under value.**

<b>Diversity Metric</b>	<b>Biofilm Age</b>		<b>Showerhead Type</b>		
<b>Richness</b>	29.2 $\pm$ 47 (n=54)	Initial (Days 0-13)	28.1 $\pm$ 20.9 (n=9)	ABS Plastic	21 $\pm$ 10.4 (n=36)
				Metal	29 $\pm$ 4.6 (n=18)
		Early (Days 14-42)	26 $\pm$ 54.2 (n=18)	Silver-embedded	33.4 $\pm$ 16.4 (n=18)
				Silver-coated Copper Mesh	52.3 $\pm$ 109.3 (n=18)
		Mature (Days 43-70)	34.6 $\pm$ 44.4 (n=18)	Silver Mesh	19.2 $\pm$ 21.2 (n=18)
		<b>Evenness</b>	0.92 $\pm$ 0.05 (n=54)	Initial (Days 0-13)	0.92 $\pm$ 0.05 (n=9)
Metal	0.9 $\pm$ 0.04 (n=18)				
Early (Days 14-42)	0.93 $\pm$ 0.04 (n=18)			Silver-embedded	0.9 $\pm$ 0.03 (n=18)
				Silver-coated Copper Mesh	0.93 $\pm$ 0.06 (n=18)
Mature (Days 43-70)	0.89 $\pm$ 0.07 (n=18)			Silver Mesh	0.93 $\pm$ 0.06 (n=18)
<b>Diversity</b>	2.8 $\pm$ 0.7 (n=54)			Initial (Days 0-13)	2.9 $\pm$ 0.5 (n=9)
		Metal	3.0 $\pm$ 0.2 (n=18)		
		Early (Days 14-42)	2.7 $\pm$ 0.6 (n=18)	Silver-embedded	3.1 $\pm$ 0.4 (n=18)
				Silver-coated Copper Mesh	2.8 $\pm$ 1.1 (n=18)
		Mature (Days 43-70)	2.9 $\pm$ 0.6 (n=18)	Silver Mesh	2.5 $\pm$ 0.5 (n=18)

**Appendix B Table 6: Average diversity values of biofilm samples  $\pm$  standard deviation for A. hose samples and B. swab samples**

**A.**

Diversity Metric		Showerhead Type	
<b>Richness</b>	$50.0 \pm 60.4$	ABS Plastic	$38.0 \pm 39.7$
		Metal	$127 \pm 159.8$
		Silver-embedded	$53.5 \pm 39.7$
		Silver-coated Copper Mesh	$24.3 \pm 6.8$
		Silver Mesh	$127 \pm 30$
<b>Evenness</b>	$0.86 \pm 0.08$	ABS Plastic	$0.89 \pm 0.07$
		Metal	$0.9 \pm 0.04$
		Silver-embedded	$0.9 \pm 0.007$
		Silver-coated Copper Mesh	$0.84 \pm 0.07$
		Silver Mesh	$0.79 \pm 0.1$
<b>Diversity</b>	$2.9 \pm 1.1$	ABS Plastic	$2.8 \pm 1.2$
		Metal	$3.7 \pm 2$
		Silver-embedded	$2.8 \pm 1.9$
		Silver-coated Copper Mesh	$2.7 \pm 0.3$
		Silver Mesh	$2.9 \pm 0.8$

**B.**

Diversity Metric		Time Taken	
<b>Richness</b>	$27.8 \pm 28.1$	Before sampling	$33.1 \pm 37.4$
		After sampling	$22.6 \pm 12.7$
<b>Evenness</b>	$0.96 \pm 0.04$	Before sampling	$0.97 \pm 0.02$
		After sampling	$0.96 \pm 0.05$
<b>Diversity</b>	$3.0 \pm 0.6$	Before sampling	$3.1 \pm 0.6$
		After sampling	$2.8 \pm 0.6$

## Appendix B Procedure 1: CDC Biofilm Reactor Method Development

The reactors were operated so that the hydraulic retention time within the reactors were roughly 10 minutes to ensure a reasonable contact time during silver exposure as well as contextualizing silver treatment close to the average showering duration. All reactors were covered in foil during experimental operation to minimize light exposure inside the reactor.

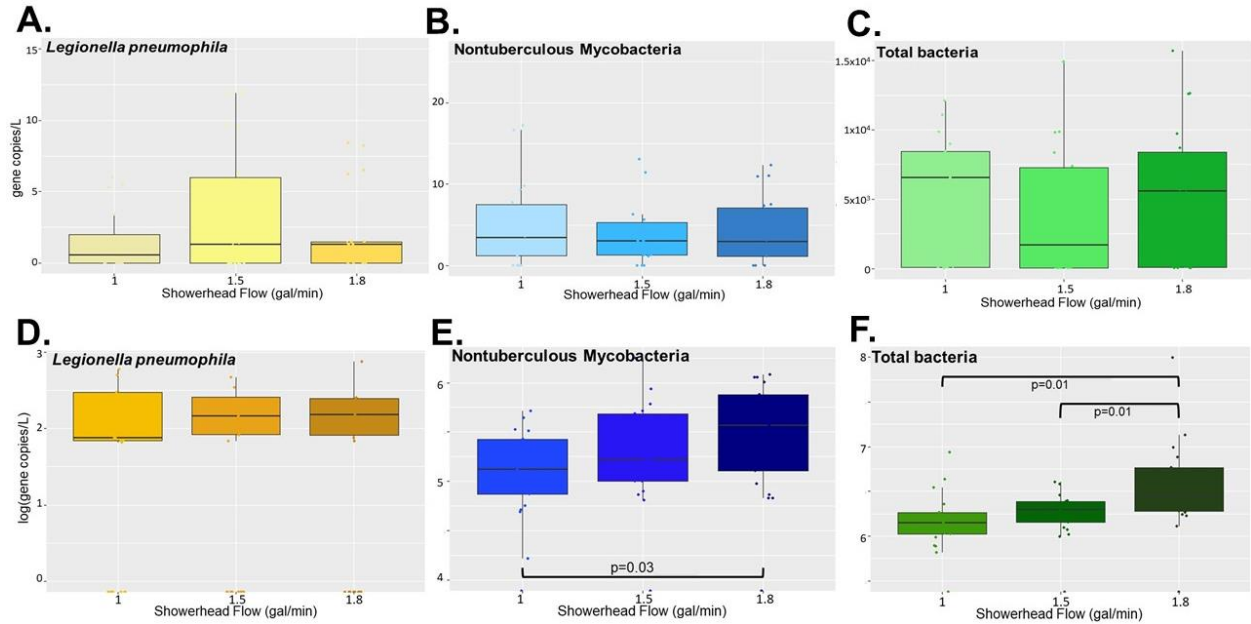
### *Initial characterization of reactors, Mycobacterium abscessus strains, and silver nitrate fate and transport*

A variety of initial experiments were conducted to characterize the reactor system components. *M. abscessus* isolates were assessed for their ability to form a biofilm on ABS coupons that were designed to fit inside the reactor coupon holders. Coupons were sterilized by washing with 1% laboratory soap and sterile deionized water ten times. Then were allowed to dry within a sterile fume hood. These coupons were then added to a tissue culture plate well filled with either environmental or clinical *M. abscessus* planktonic culture in R2A media at different cell densities, which were assessed by culturing on solid R2A media at the time of coupon inoculation. Coupons in culture were incubated for 72 hours at 37 °C with gentle shaking. Biofilm recovery was conducted in accordance with previous work by Williams et al.<sup>154</sup>. Briefly, coupons with biofilm attached were dunked into diluted R2A liquid media three times, then placed into a 1% Tween80 - dilute R2A solution and processed for three rounds of sonication at 42 kHz for 1 min and vortexed at maximum speed for 30 sec. The resulting biofilm suspension was plated at various dilutions onto R2A agar to assess biofilm density. The initial inoculate concentration for both isolates was chosen so that the initial biofilm density on the coupons was approximately the same as the NTM biofilm density measured in the INHALE shower laboratory during the experiments outlined in [Chapter 3.2.5](#).

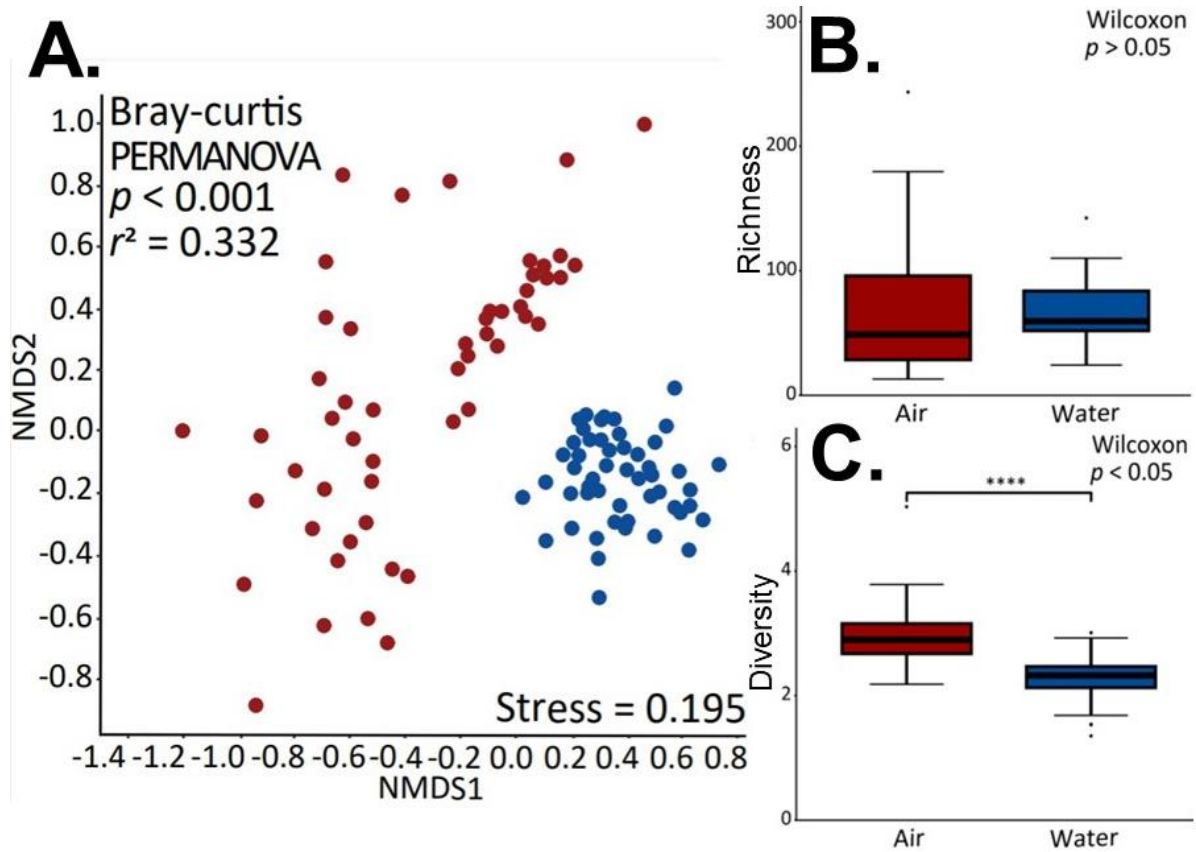
Isolate sensitivity to silver nitrate was conducted in a series of microplate experiments. Both *M. abscessus* isolates were grown in liquid R2A media to  $1.25 \times 10^5$  cfu/mL as denoted in plate counts on R2A agar (the average NTM biofilm concentration recovered from [Chapter 3.2.5](#)), then transferred to a 96 well plate. Silver nitrate solutions at a range of 0-480 mg/L Ag<sup>+</sup> were added to the wells and incubated at 37 °C with gentle agitation for 10 minutes to produce CTs of 0-4800 mg/L min. After incubation, the plate was centrifuged at 5000 rpm for 2 minutes to pellet the cells, the supernatant was carefully removed, and the pellet was resuspended in fresh R2A media. The reduction in *M. abscessus* was determined via plate counts from the resuspended pellet. This methodology was repeated using silver nitrate concentrations between 0 mg/L and 48 mg/L and an incubation period of 100 minutes (achieving the same CT as the shorter, more concentrated trial) to determine if concentration or exposure time is the driving parameter leading disinfection.

Loss of silver in the reactor system due to adhesion to reactor components was assessed prior to conducting the final set of experiments as well due to anecdotal evidence so that the dose of silver nitrate that was administered in the influent is the dose that the biofilm is exposed to for the appropriate contact time. To assess this, a feed solution consisting of deionized water and a known concentration of silver nitrate was flowed through a reactor for 10 minutes (the time that the biofilm would be exposed to silver nitrate). After 10 minutes of operation, the pump was turned off, the reactor was drained, and the system was refilled with deionized water and allowed to sit for 24 hours. Samples were taken of the feed solution, every minute from the reactor effluent, and over the course of the 24 hours for ICP-MS analysis to assess the adsorption and desorption of silver ions in the reactor.

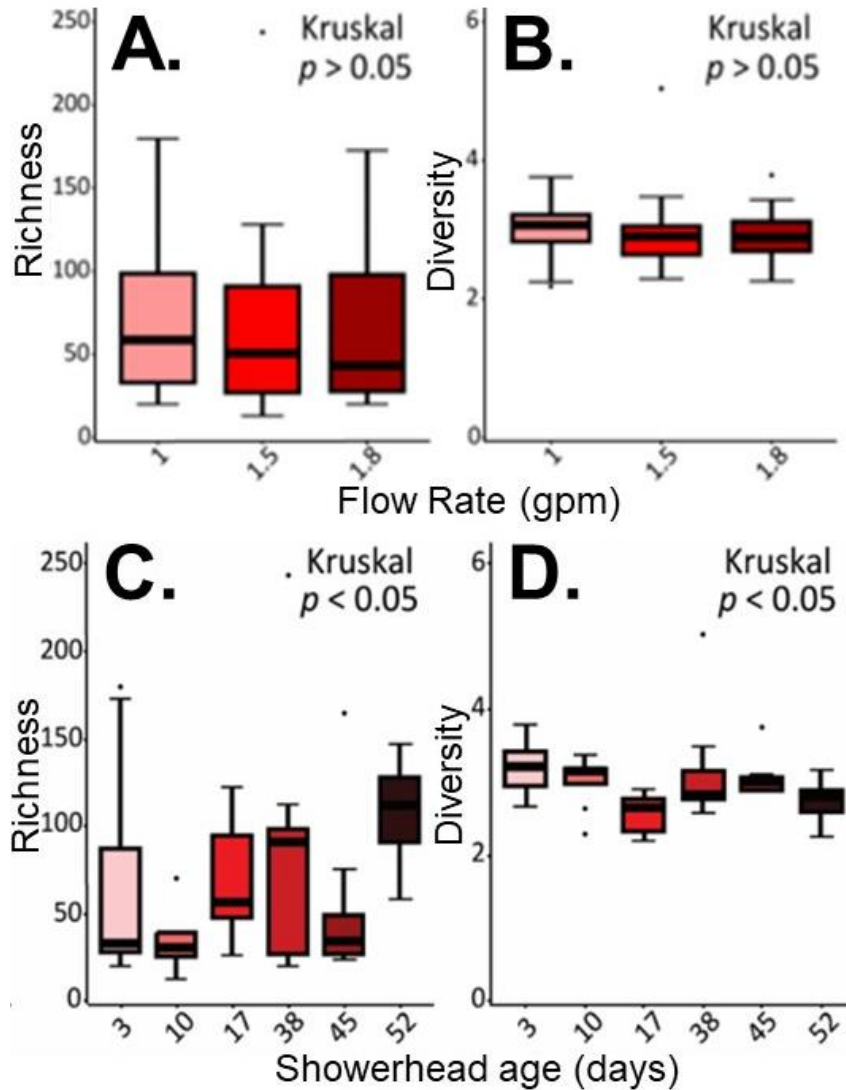
## Appendix C : Chapter 4 Supplementary Information



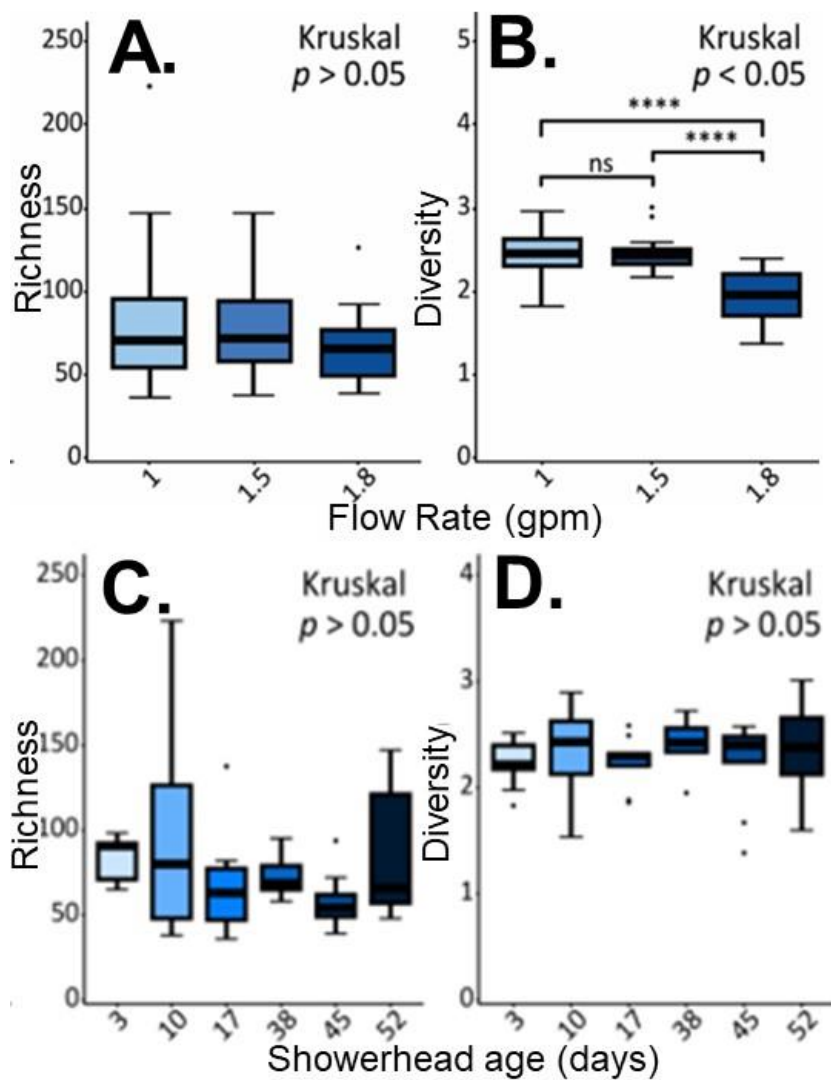
**Appendix C Figure 1: Absolute gene copy concentrations in shower water and associated aerosols by showerhead flow rate. A. *L. pneumophila* in shower aerosols, B. NTM in shower aerosols, C. total bacteria in shower aerosols, D. *L. pneumophila* in shower water, E. NTM in shower water, and F. total bacteria in shower water observed for all three showerheads. Each showerhead type shows all the data collected from all replicates for that specific showerhead.**



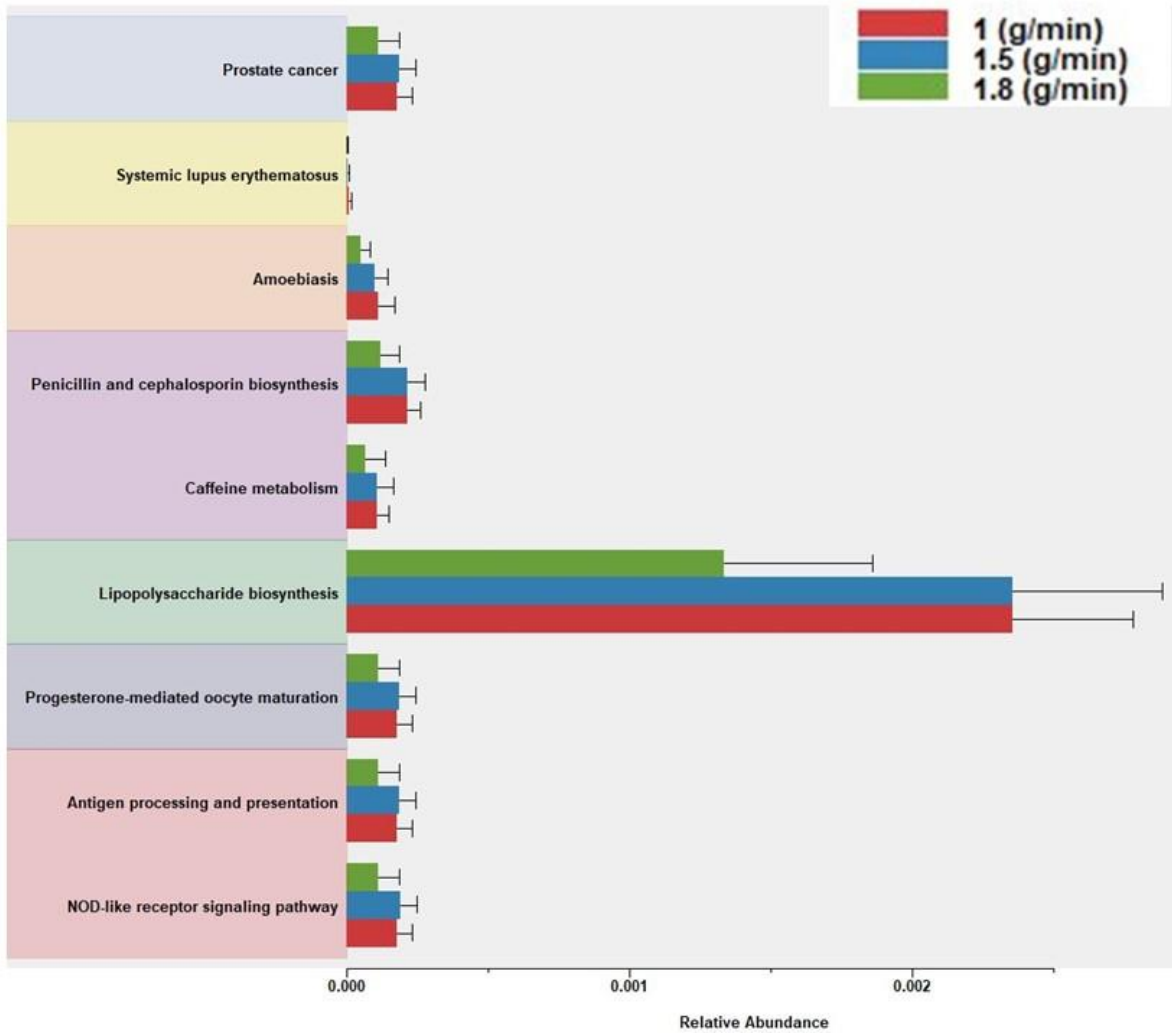
**Appendix C Figure 2: Diversity of water and aerosol samples. A.** Non-metric multidimensional scaling (NMDS) plots of bacterial OTUs represented by the Bray–Curtis dissimilarity index. Comparison of **B.** richness and **C.** diversity of bacterial OTUs in air and water samples estimated by the Chao1 estimator and Shannon index, respectively. Significant differences are marked with a colored bracket and star corresponding to the showerhead type and p-value (\* =  $p \leq 0.05$ , \*\* =  $p \leq 0.01$ , \*\*\* =  $p \leq 0.001$ ).



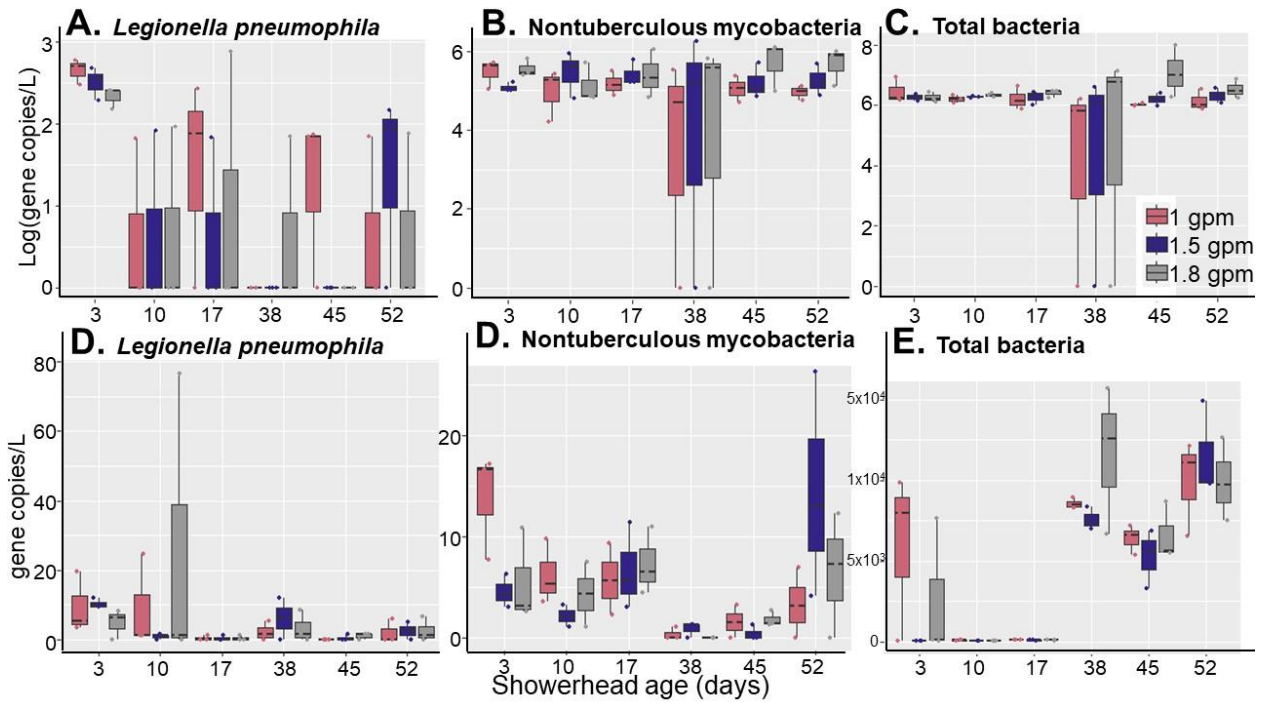
Appendix C Figure 3: Alpha diversity of aerosol samples. The effects of flow rate on A. Chao1 estimator of richness and B. Shannon index diversity. The effects of showerhead age on C. Chao1 estimator of richness and C. Shannon index diversity. Significance and the statistical analysis used are contained in the upper right hand corner of each plot.



Appendix C Figure 4: Alpha diversity of water samples. The effects of flow rate on A. Chao1 estimator of richness and B. Shannon index diversity. The effects of showerhead age on C. Chao1 estimator of richness and C. Shannon index diversity. Significance and the statistical analysis used are contained in the upper right hand corner of each plot.



Appendix C Figure 5: Significant functional traits in water samples by flow rate obtained from PICRUST analysis.



Appendix C Figure 6: Absolute gene copy concentrations in shower water and associated aerosols over time.

A. *L. pneumophila* in shower water, B. NTM in shower water, C. total bacteria in shower water, D. *L. pneumophila* in shower aerosols, E. NTM in shower aerosols, and F. total bacteria in shower aerosols observed for all three showerheads. Each showerhead type shows all the data collected from all replicates for that specific showerhead.

## Bibliography

- (1) Proctor, C.; Garner, E.; Hamilton, K. A.; Ashbolt, N. J.; Caverly, L. J.; Falkinham, J. O.; Haas, C. N.; Prevost, M.; Prevots, D. R.; Pruden, A.; Raskin, L.; Stout, J.; Haig, S.-J. Tenets of a Holistic Approach to Drinking Water-Associated Pathogen Research, Management, and Communication. *Water Res.* **2022**, *211*, 117997. <https://doi.org/10.1016/j.watres.2021.117997>.
- (2) Collier, S. A.; Deng, L.; Adam, E. A.; Benedict, K. M.; Beshearse, E. M.; Blackstock, A. J.; Bruce, B. B.; Derado, G.; Edens, C.; Fullerton, K. E.; Gargano, J. W.; Geissler, A. L.; Hall, A. J.; Havelaar, A. H.; Hill, V. R.; Hoekstra, R. M.; Reddy, S. C.; Scallan, E.; Stokes, E. K.; Yoder, J. S.; Beach, M. J. Estimate of Burden and Direct Healthcare Cost of Infectious Waterborne Disease in the United States - Volume 27, Number 1—January 2021 - *Emerging Infectious Diseases Journal - CDC*. <https://doi.org/10.3201/eid2701.190676>.
- (3) Adjemian, J.; Olivier, K. N.; Seitz, A. E.; Falkinham, J. O.; Holland, S. M.; Prevots, D. R. Spatial Clusters of Nontuberculous Mycobacterial Lung Disease in the United States. *Am. J. Respir. Crit. Care Med.* **2012**, *186* (6), 553–558. <https://doi.org/10.1164/rccm.201205-0913OC>.
- (4) *Surveillance for Waterborne Disease Outbreaks Associated with Drinking Water — United States, 2013–2014 - PMC*. <https://www.ncbi.nlm.nih.gov/pmc/articles/PMC5679581/> (accessed 2023-10-26).
- (5) Cunha, B. A.; Burillo, A.; Bouza, E. Legionnaires' Disease. *The Lancet* **2016**, *387* (10016), 376–385. [https://doi.org/10.1016/S0140-6736\(15\)60078-2](https://doi.org/10.1016/S0140-6736(15)60078-2).
- (6) Feazel, L. M.; Baumgartner, L. K.; Peterson, K. L.; Frank, D. N.; Harris, J. K.; Pace, N. R. Opportunistic Pathogens Enriched in Showerhead Biofilms. *Proc. Natl. Acad. Sci.* **2009**, *106* (38), 16393–16399. <https://doi.org/10.1073/pnas.0908446106>.
- (7) *Legionnaires Disease History and Patterns | Legionella | CDC*. <https://www.cdc.gov/legionella/about/history.html> (accessed 2020-06-05).
- (8) Ratnatunga, C. N.; Lutzky, V. P.; Kupz, A.; Doolan, D. L.; Reid, D. W.; Field, M.; Bell, S. C.; Thomson, R. M.; Miles, J. J. The Rise of Non-Tuberculosis Mycobacterial Lung Disease. *Front. Immunol.* **2020**, *11*.
- (9) Kunz, J. M. Surveillance of Waterborne Disease Outbreaks Associated with Drinking Water — United States, 2015–2020. *MMWR Surveill. Summ.* **2024**, *73*. <https://doi.org/10.15585/mmwr.ss7301a1>.
- (10) Fraser, D. W.; Tsai, T. R.; Orenstein, W.; Parkin, W. E.; Beecham, H. J.; Sharrar, R. G.; Harris, J.; Mallison, G. F.; Martin, S. M.; McDade, J. E.; Shepard, C. C.; Brachman, P. S.;

- the Field Investigation Team\*. Legionnaires' Disease: Description of an Epidemic of Pneumonia. *N. Engl. J. Med.* **1977**, 297 (22), 1189–1197. <https://doi.org/10.1056/NEJM197712012972201>.
- (11) Faverio, P.; De Giacomi, F.; Bodini, B. D.; Stainer, A.; Fumagalli, A.; Bini, F.; Luppi, F.; Aliberti, S. Nontuberculous Mycobacterial Pulmonary Disease: An Integrated Approach beyond Antibiotics. *ERJ Open Res.* **2021**, 7 (2), 00574–02020. <https://doi.org/10.1183/23120541.00574-2020>.
- (12) Sood Akshay; Sreedhar Rajgopal; Kulkarni Pradeep; Nawoor Abdur Ray. Hypersensitivity Pneumonitis-like Granulomatous Lung Disease with Nontuberculous Mycobacteria from Exposure to Hot Water Aerosols. *Environ. Health Perspect.* **2007**, 115 (2), 262–266. <https://doi.org/10.1289/ehp.9542>.
- (13) Bentzmann, S. de; Plésiat, P. The Pseudomonas Aeruginosa Opportunistic Pathogen and Human Infections. *Environ. Microbiol.* **2011**, 13 (7), 1655–1665. <https://doi.org/10.1111/j.1462-2920.2011.02469.x>.
- (14) Chan, E. D.; Iseman, M. D. Slender, Older Women Appear to Be More Susceptible to Nontuberculous Mycobacterial Lung Disease. *Gen. Med.* **2010**, 7 (1), 5–18. <https://doi.org/10.1016/j.genm.2010.01.005>.
- (15) Cystic Fibrosis Foundation, Community Voice. *2018 Survey*; Bethesda, MD, 2018.
- (16) Falkinham, J. O. Nontuberculous Mycobacteria from Household Plumbing of Patients with Nontuberculous Mycobacteria Disease. *Emerg. Infect. Dis.* **2011**, 17 (3), 419–424. <https://doi.org/10.3201/eid1703.101510>.
- (17) Falkinham, J. o., Iii. Surrounded by Mycobacteria: Nontuberculous Mycobacteria in the Human Environment. *J. Appl. Microbiol.* **2009**, 107 (2), 356–367. <https://doi.org/10.1111/j.1365-2672.2009.04161.x>.
- (18) Berry, D.; Xi, C.; Raskin, L. Microbial Ecology of Drinking Water Distribution Systems. *Curr. Opin. Biotechnol.* **2006**, 17 (3), 297–302. <https://doi.org/10.1016/j.copbio.2006.05.007>.
- (19) Angenent, L. T.; Kelley, S. T.; Amand, A. St.; Pace, N. R.; Hernandez, M. T. Molecular Identification of Potential Pathogens in Water and Air of a Hospital Therapy Pool. *Proc. Natl. Acad. Sci.* **2005**, 102 (13), 4860–4865. <https://doi.org/10.1073/pnas.0501235102>.
- (20) Craun, G. F.; Brunkard, J. M.; Yoder, J. S.; Roberts, V. A.; Carpenter, J.; Wade, T.; Calderon, R. L.; Roberts, J. M.; Beach, M. J.; Roy, S. L. Causes of Outbreaks Associated with Drinking Water in the United States from 1971 to 2006. *Clin. Microbiol. Rev.* **2010**, 23 (3), 507–528. <https://doi.org/10.1128/CMR.00077-09>.
- (21) Moritz, M. M.; Flemming, H.-C.; Wingender, J. Integration of Pseudomonas Aeruginosa and Legionella Pneumophila in Drinking Water Biofilms Grown on Domestic Plumbing

- Materials. *Int. J. Hyg. Environ. Health* **2010**, *213* (3), 190–197. <https://doi.org/10.1016/j.ijheh.2010.05.003>.
- (22) Haig, S.-J.; Kotlarz, N.; M. Kalikin, L.; Chen, T.; Guikema, S.; J. LiPuma, J.; Raskin, L. Emerging Investigator Series: Bacterial Opportunistic Pathogen Gene Markers in Municipal Drinking Water Are Associated with Distribution System and Household Plumbing Characteristics. *Environ. Sci. Water Res. Technol.* **2020**, *6* (11), 3032–3043. <https://doi.org/10.1039/D0EW00723D>.
- (23) Bornstein, N.; Vieilly, C.; Nowicki, M.; Paucod, J. C.; Fleurette, J. Epidemiological Evidence of Legionellosis Transmission through Domestic Hot Water Supply Systems and Possibilities of Control. *Isr. J. Med. Sci.* **1986**, *22* (9), 655–661.
- (24) Falkinham, J.; Pruden, A.; Edwards, M. Opportunistic Premise Plumbing Pathogens: Increasingly Important Pathogens in Drinking Water. *Pathogens* **2015**, *4* (2), 373–386. <https://doi.org/10.3390/pathogens4020373>.
- (25) Alleron, L.; Khemiri, A.; Koubar, M.; Lacombe, C.; Coquet, L.; Cosette, P.; Jouenne, T.; Frere, J. VBNC Legionella Pneumophila Cells Are Still Able to Produce Virulence Proteins. *Water Res.* **2013**, *47* (17), 6606–6617. <https://doi.org/10.1016/j.watres.2013.08.032>.
- (26) Ramamurthy, T.; Ghosh, A.; Pazhani, G. P.; Shinoda, S. Current Perspectives on Viable but Non-Culturable (VBNC) Pathogenic Bacteria. *Front. Public Health* **2014**, *2*.
- (27) Bollin, G. E. Aerosols Containing Legionella Pneumophila Generated by Shower Heads and Hot-Water Faucets. **1985**, *50*, 4.
- (28) Al-Quadani, T.; Price, C. T.; Abu Kwaik, Y. Exploitation of Evolutionarily Conserved Amoeba and Mammalian Processes by Legionella. *Trends Microbiol.* **2012**, *20* (6), 299–306. <https://doi.org/10.1016/j.tim.2012.03.005>.
- (29) Escoll, P.; Rolando, M.; Gomez-Valero, L.; Buchrieser, C. From Amoeba to Macrophages: Exploring the Molecular Mechanisms of Legionella Pneumophila Infection in Both Hosts. In *Molecular Mechanisms in Legionella Pathogenesis*; Hilbi, H., Ed.; Current Topics in Microbiology and Immunology; Springer Berlin Heidelberg: Berlin, Heidelberg, 2014; pp 1–34. [https://doi.org/10.1007/82\\_2013\\_351](https://doi.org/10.1007/82_2013_351).
- (30) *Legionella Pneumophila Pathogenesis: A Fateful Journey from Amoebae to Macrophages / Annual Review of Microbiology.* [https://www.annualreviews.org/doi/full/10.1146/annurev.micro.54.1.567?url\\_ver=Z39.88-2003&rfr\\_id=ori%3Arid%3Acrossref.org&rfr\\_dat=cr\\_pub%3Dpubmed](https://www.annualreviews.org/doi/full/10.1146/annurev.micro.54.1.567?url_ver=Z39.88-2003&rfr_id=ori%3Arid%3Acrossref.org&rfr_dat=cr_pub%3Dpubmed) (accessed 2019-08-29).
- (31) Berk, S. G.; Ting, R. S.; Turner, G. W.; Ashburn, R. J. Production of Respirable Vesicles Containing Live Legionella Pneumophila Cells by Two Acanthamoeba Spp. *APPL Env. MICROBIOL* **1998**, *64*, 8.

- (32) Michael Madigan; Kelly Bender; Daniel Buckley; W. Matthew Sattley; David Stahl. *Brock Biology of Microorganisms*, 15th ed.; Pearson, 2019.
- (33) Shen, Y.; Haig, S.-J.; Prussin, A. J., II; LiPuma, J. J.; Marr, L. C.; Raskin, L. Shower Water Contributes Viable Nontuberculous Mycobacteria to Indoor Air. *PNAS Nexus* **2022**, pgac145. <https://doi.org/10.1093/pnasnexus/pgac145>.
- (34) Falkinham, J. O.; Iseman, M. D.; de Haas, P.; van Soolingen, D. Mycobacterium Avium in a Shower Linked to Pulmonary Disease. *J. Water Health* **2008**, 6 (2), 209–213. <https://doi.org/10.2166/wh.2008.232>.
- (35) US EPA, O. *How We Use Water*. <https://www.epa.gov/watersense/how-we-use-water> (accessed 2023-12-20).
- (36) Wilkes, C. R.; Mason, A. D.; Hern, S. C. Probability Distributions for Showering and Bathing Water-Use Behavior for Various U.S. Subpopulations. *Risk Anal.* **2005**, 25 (2), 317–337. <https://doi.org/10.1111/j.1539-6924.2005.00592.x>.
- (37) Zhou, Y.; Mui, K. W.; Wong, L. T.; Tsui, P. H.; Chan, W. K. Aerosol Generation Rates for Showerheads. *Build. Serv. Eng. Res. Technol.* **2019**, 40 (5), 595–610. <https://doi.org/10.1177/0143624418824839>.
- (38) Zhou, Y.; Benson, J. M.; Irvin, C.; Irshad, H.; Cheng, Y.-S. Particle Size Distribution and Inhalation Dose of Shower Water Under Selected Operating Conditions. *Inhal. Toxicol.* **2007**, 19 (4), 333–342. <https://doi.org/10.1080/08958370601144241>.
- (39) Collins, S.; Stevenson, D.; Bennett, A.; Walker, J. Occurrence of Legionella in UK Household Showers. *Int. J. Hyg. Environ. Health* **2017**, 220 (2, Part B), 401–406. <https://doi.org/10.1016/j.ijheh.2016.12.001>.
- (40) Thomson, R.; Tolson, C.; Carter, R.; Coulter, C.; Huygens, F.; Hargreaves, M. Isolation of Nontuberculous Mycobacteria (NTM) from Household Water and Shower Aerosols in Patients with Pulmonary Disease Caused by NTM. *J. Clin. Microbiol.* **2013**, 51 (9), 3006–3011. <https://doi.org/10.1128/JCM.00899-13>.
- (41) Estrada-Perez, C. E.; Kinney, K. A.; Maestre, J. P.; Hassan, Y. A.; King, M. D. Droplet Distribution and Airborne Bacteria in an Experimental Shower Unit. *Water Res.* **2018**, 130, 47–57. <https://doi.org/10.1016/j.watres.2017.11.039>.
- (42) Proctor, C. R.; Reimann, M.; Vriens, B.; Hammes, F. Biofilms in Shower Hoses. *Water Res.* **2018**, 131, 274–286. <https://doi.org/10.1016/j.watres.2017.12.027>.
- (43) R. Proctor, C.; Gächter, M.; Kötzsch, S.; Rölli, F.; Sigrüst, R.; Walser, J.-C.; Hammes, F. Biofilms in Shower Hoses – Choice of Pipe Material Influences Bacterial Growth and Communities. *Environ. Sci. Water Res. Technol.* **2016**, 2 (4), 670–682. <https://doi.org/10.1039/C6EW00016A>.

- (44) Abraham C. Cullom; Rebekah L. Martin; Krista Williams; Amanda Williams; Amy Pruden; Yang Song; Marc A. Edwards. Critical Review: Propensity of Premise Plumbing Pipe Materials to Enhance or Diminish Growth of Legionella and Other Opportunistic Pathogens. *Pathogens* **2020**, *9* (957), 1–34. <https://doi.org/doi:10.3390/pathogens9110957>.
- (45) Costerton, J. W.; Lewandowski, Z.; Caldwell, D. E.; Korber, D. R.; Lappin-Scott, H. M. Microbial Biofilms. *Annu. Rev. Microbiol.* **1995**, *49* (1), 711–745. <https://doi.org/10.1146/annurev.mi.49.100195.003431>.
- (46) Gebert, M. J.; Delgado-Baquerizo, M.; Oliverio, A. M.; Webster, T. M.; Nichols, L. M.; Honda, J. R.; Chan, E. D.; Adjemian, J.; Dunn, R. R.; Fierer, N. Ecological Analyses of Mycobacteria in Showerhead Biofilms and Their Relevance to Human Health. *mBio* **2018**, *9* (5), e01614-18. <https://doi.org/10.1128/mBio.01614-18>.
- (47) A. A. Morvay; M. Decun; M. Scurtu; C. Sala; A. Morar; M. Sarandan. Biofilm Formation on Materials Commonly Used in Household Drinking Water Systems. *Water Sci. Technol. Water Supply* **2011**, *11* (2), 252–257. <https://doi.org/10.2166/ws.2011.053>.
- (48) Haig, S.-J.; Kotlarz, N.; LiPuma, J. J.; Raskin, L. A High-Throughput Approach for Identification of Nontuberculous Mycobacteria in Drinking Water Reveals Relationship between Water Age and Mycobacterium Avium. *mBio* **2018**, *9* (1). <https://doi.org/10.1128/mBio.02354-17>.
- (49) Blanc, D. S.; Carrara, Ph.; Zanetti, G.; Francioli, P. Water Disinfection with Ozone, Copper and Silver Ions, and Temperature Increase to Control Legionella: Seven Years of Experience in a University Teaching Hospital. *J. Hosp. Infect.* **2005**, *60* (1), 69–72. <https://doi.org/10.1016/j.jhin.2004.10.016>.
- (50) Stout, J. E.; Yu, V. L. Experiences of the First 16 Hospitals Using Copper-Silver Ionization for Legionella Control: Implications for the Evaluation of Other Disinfection Modalities. *Infect. Control Hosp. Epidemiol.* **2003**, *24* (8), 563–568. <https://doi.org/10.1086/502251>.
- (51) Rohr, U.; Senger, M.; Selenka, F.; Turley, R.; Wilhelm, M. Four Years of Experience with Silver-Copper Ionization for Control of Legionella in a German University Hospital Hot Water Plumbing System. *Clin. Infect. Dis.* **1999**, *29* (6), 1507–1511. <https://doi.org/10.1086/313512>.
- (52) Stout, J. E.; Lin, Y.-S. E.; Goetz, A. M.; Muder, R. R. Controlling Legionella in Hospital Water Systems: Experience with the Superheat-and-Flush Method and Copper-Silver Ionization. *Infect. Control Hosp. Epidemiol.* **1998**, *19* (12), 911–914. <https://doi.org/10.2307/30142016>.
- (53) Wu, J.; Cao, M.; Tong, D.; Finkelstein, Z.; Hoek, E. M. V. A Critical Review of Point-of-Use Drinking Water Treatment in the United States. *Npj Clean Water* **2021**, *4* (1), 1–25. <https://doi.org/10.1038/s41545-021-00128-z>.

- (54) *Point Of Use Water Treatment Systems Market Report, 2030*. <https://www.grandviewresearch.com/industry-analysis/point-of-use-water-treatment-systems-market> (accessed 2022-12-09).
- (55) ReportLinker. *Global Shower Heads and Shower Panels Market to Reach \$3.8 Billion by 2026*. GlobeNewswire News Room. <https://www.globenewswire.com/news-release/2022/05/30/2452539/0/en/Global-Shower-Heads-and-Shower-Panels-Market-to-Reach-3-8-Billion-by-2026.html> (accessed 2022-12-09).
- (56) In2itive. *ISO 22196:2011*. Viroxy. <https://www.viroxylabs.com/microbiological-testing-services/disinfectant-efficacy-testing/iso-221962011/> (accessed 2022-08-16).
- (57) Mather, M.; Jacobsen, L. A.; Ard, K. M. P. *Www.Prb.Org Population Bulletin. Popul. Bull.* **2015**.
- (58) Gleick, P. H. Climate Change, Hydrology, and Water Resources. *Rev. Geophys.* **1989**, *27* (3), 329–344. <https://doi.org/10.1029/RG027i003p00329>.
- (59) US EPA, O. *WaterSense*. <https://www.epa.gov/watersense> (accessed 2022-11-17).
- (60) Li, T. *Oasense Shower | Highest allowed shower head flow rate per states and cities 2022*. OASENSE. <https://www.oasense.com/post/showerhead-gpm-us> (accessed 2023-12-21).
- (61) Bédard, E.; Boppe, I.; Kouamé, S.; Martin, P.; Pinsonneault, L.; Valiquette, L.; Racine, J.; Prévost, M. Combination of Heat Shock and Enhanced Thermal Regime to Control the Growth of a Persistent Legionella Pneumophila Strain. *Pathogens* **2016**, *5* (2), 35. <https://doi.org/10.3390/pathogens5020035>.
- (62) Orsi, G. B.; Vitali, M.; Marinelli, L.; Ciorba, V.; Tufi, D.; Del Cimmuto, A.; Ursillo, P.; Fabiani, M.; De Santis, S.; Protano, C.; Marzuillo, C.; De Giusti, M. Legionella Control in the Water System of Antiquated Hospital Buildings by Shock and Continuous Hyperchlorination: 5 Years Experience. *BMC Infect. Dis.* **2014**, *14* (1), 394. <https://doi.org/10.1186/1471-2334-14-394>.
- (63) Velten, S.; Boller, M.; Köster, O.; Helbing, J.; Weilenmann, H.-U.; Hammes, F. Development of Biomass in a Drinking Water Granular Active Carbon (GAC) Filter. *Water Res.* **2011**, *45* (19), 6347–6354. <https://doi.org/10.1016/j.watres.2011.09.017>.
- (64) Ramírez-Castillo, F. Y.; Loera-Muro, A.; Jacques, M.; Garneau, P.; Avelar-González, F. J.; Harel, J.; Guerrero-Barrera, A. L. Waterborne Pathogens: Detection Methods and Challenges. *Pathog. Basel Switz.* **2015**, *4* (2), 307–334. <https://doi.org/10.3390/pathogens4020307>.
- (65) *The Efficacy of the Medi-Shower Silver Impregnated Showerhead*. Medi-shower. <https://medi-shower.co.uk/studies/the-efficacy-of-the-medishower-silver-impregnated-showerhead> (accessed 2021-04-06).

- (66) Yetiş, Ö.; Ali, S.; Karia, K.; Bassett, P.; Wilson, P. *Persistent Colonisation of Antimicrobial Silver-Impregnated Shower Heads and Hoses Presents A Risk for Acquisition of Pseudomonas Aeruginosa in Healthcare Settings*; preprint; In Review, 2022. <https://doi.org/10.21203/rs.3.rs-1403389/v1>.
- (67) Yetiş, Ö.; Ali, S.; Karia, K.; Wilson, P. Failure of a Hollow-Fibre Shower Filter Device to Prevent Exposure of Patients to Pseudomonas Aeruginosa. *J. Hosp. Infect.* **2022**, *130*, 1–6. <https://doi.org/10.1016/j.jhin.2022.08.007>.
- (68) Bollin, G. E.; Plouffe, J. F.; Para, M. F.; Hackman, B. Aerosols Containing Legionella Pneumophila Generated by Shower Heads and Hot-Water Faucets. *Appl. Environ. Microbiol.* **1985**, *50* (5), 1128–1131.
- (69) McDowell, M. A.; Fryar, C. D.; Ogden, C. L.; Flegal, K. M. Anthropometric Reference Data for Children and Adults: United States, 2003-2006: (623932009-001), 2008. <https://doi.org/10.1037/e623932009-001>.
- (70) Nieto-Caballero, M.; Savage, N.; Keady, P.; Hernandez, M. High Fidelity Recovery of Airborne Microbial Genetic Materials by Direct Condensation Capture into Genomic Preservatives. *J. Microbiol. Methods* **2019**, *157*, 1–3. <https://doi.org/10.1016/j.mimet.2018.12.010>.
- (71) Hach USA. Nitrogen, Ammonia Salicylate Method, 2022. <file:///C:/Users/sarah/Downloads/DOC316.53.01077.pdf>.
- (72) Hach USA. Phosphorus, Reactive (Orthophosphate) USEPA PhosVer 3 (Ascorbic Acid) Method, 2022. <file:///C:/Users/sarah/Downloads/DOC316.53.01119.pdf>.
- (73) Hach USA. Chlorine, Free and Total, Low Range USEPA DPD Method, 2022. [file:///C:/Users/sarah/Downloads/DOC316.53.01450\\_5ed.pdf](file:///C:/Users/sarah/Downloads/DOC316.53.01450_5ed.pdf).
- (74) Lievens, A.; Jacchia, S.; Kagkli, D.; Savini, C.; Querci, M. Measuring Digital PCR Quality: Performance Parameters and Their Optimization. *PLOS ONE* **2016**, *11* (5), e0153317. <https://doi.org/10.1371/journal.pone.0153317>.
- (75) Caporaso, J. G.; Lauber, C. L.; Walters, W. A.; Berg-Lyons, D.; Huntley, J.; Fierer, N.; Owens, S. M.; Betley, J.; Fraser, L.; Bauer, M.; Gormley, N.; Gilbert, J. A.; Smith, G.; Knight, R. Ultra-High-Throughput Microbial Community Analysis on the Illumina HiSeq and MiSeq Platforms. *ISME J.* **2012**, *6* (8), 1621–1624. <https://doi.org/10.1038/ismej.2012.8>.
- (76) Bolyen, E.; Rideout, J. R.; Dillon, M. R.; Bokulich, N. A.; Abnet, C. C.; Al-Ghalith, G. A.; Alexander, H.; Alm, E. J.; Arumugam, M.; Asnicar, F.; Bai, Y.; Bisanz, J. E.; Bittinger, K.; Brejnrod, A.; Brislawn, C. J.; Brown, C. T.; Callahan, B. J.; Caraballo-Rodríguez, A. M.; Chase, J.; Cope, E. K.; Da Silva, R.; Diener, C.; Dorrestein, P. C.; Douglas, G. M.; Durall, D. M.; Duvallet, C.; Edwardson, C. F.; Ernst, M.; Estaki, M.; Fouquier, J.; Gauglitz, J. M.; Gibbons, S. M.; Gibson, D. L.; Gonzalez, A.; Gorlick, K.; Guo, J.; Hillmann, B.; Holmes, S.; Holste, H.; Huttenhower, C.; Huttley, G. A.; Janssen, S.; Jarmusch, A. K.; Jiang, L.; Kaehler, B. D.; Kang, K. B.; Keefe, C. R.; Keim, P.; Kelley, S. T.; Knights, D.; Koester, I.; Kosciolk,

- T.; Kreps, J.; Langille, M. G. I.; Lee, J.; Ley, R.; Liu, Y.-X.; Loftfield, E.; Lozupone, C.; Maher, M.; Marotz, C.; Martin, B. D.; McDonald, D.; McIver, L. J.; Melnik, A. V.; Metcalf, J. L.; Morgan, S. C.; Morton, J. T.; Naimey, A. T.; Navas-Molina, J. A.; Nothias, L. F.; Orchanian, S. B.; Pearson, T.; Peoples, S. L.; Petras, D.; Preuss, M. L.; Pruesse, E.; Rasmussen, L. B.; Rivers, A.; Robeson, M. S.; Rosenthal, P.; Segata, N.; Shaffer, M.; Shiffer, A.; Sinha, R.; Song, S. J.; Spear, J. R.; Swafford, A. D.; Thompson, L. R.; Torres, P. J.; Trinh, P.; Tripathi, A.; Turnbaugh, P. J.; Ul-Hasan, S.; van der Hooft, J. J. J.; Vargas, F.; Vázquez-Baeza, Y.; Vogtmann, E.; von Hippel, M.; Walters, W.; Wan, Y.; Wang, M.; Warren, J.; Weber, K. C.; Williamson, C. H. D.; Willis, A. D.; Xu, Z. Z.; Zaneveld, J. R.; Zhang, Y.; Zhu, Q.; Knight, R.; Caporaso, J. G. Reproducible, Interactive, Scalable and Extensible Microbiome Data Science Using QIIME 2. *Nat. Biotechnol.* **2019**, *37* (8), 852–857. <https://doi.org/10.1038/s41587-019-0209-9>.
- (77) Haig, S.-J.; Kotlarz, N.; Kalikin, L. M.; Chen, T.; Guikema, S.; LiPuma, J. J.; Raskin, L. Emerging Investigator Series: Bacterial Opportunistic Pathogen Gene Markers in Municipal Drinking Water Are Associated with Distribution System and Household Plumbing Characteristics. *Environ. Sci. Water Res. Technol.* **2020**, *6* (11), 3032–3043. <https://doi.org/10.1039/D0EW00723D>.
- (78) Legendre, P.; Gallagher, E. D. Ecologically Meaningful Transformations for Ordination of Species Data. *Oecologia* **2001**, *129* (2), 271–280. <https://doi.org/10.1007/s004420100716>.
- (79) Oksanen, J.; Simpson, G. L.; Blanchet, F. G.; Kindt, R.; Legendre, P.; Minchin, P. R.; O'Hara, R. B.; Solymos, P.; Stevens, M. H. H.; Szoecs, E.; Wagner, H.; Barbour, M.; Bedward, M.; Bolker, B.; Borcard, D.; Carvalho, G.; Chirico, M.; Caceres, M. D.; Durand, S.; Evangelista, H. B. A.; FitzJohn, R.; Friendly, M.; Furneaux, B.; Hannigan, G.; Hill, M. O.; Lahti, L.; McGlinn, D.; Ouellette, M.-H.; Cunha, E. R.; Smith, T.; Stier, A.; Braak, C. J. F. T.; Weedon, J. *Vegan: Community Ecology Package*, 2022. <https://CRAN.R-project.org/package=vegan> (accessed 2023-03-21).
- (80) *2020 US Code :: Title 15 - Commerce and Trade :: Chapter 22 - Trademarks :: Subchapter III - General Provisions :: Sec. 1125 - False designations of origin, false descriptions, and dilution forbidden.* Justia Law. <https://law.justia.com/codes/us/2020/title-15/chapter-22/subchapter-iii/sec-1125/> (accessed 2022-10-07).
- (81) *NSF Standards for Water Treatment Systems.* NSF. <https://www.nsf.org/consumer-resources/articles/standards-water-treatment-systems> (accessed 2022-10-17).
- (82) Tart, A. H.; Wozniak, D. J. Shifting Paradigms in *Pseudomonas Aeruginosa* Biofilm Research. In *Bacterial Biofilms*; Romeo, T., Ed.; Compans, R. W., Cooper, M. D., Honjo, T., Koprowski, H., Melchers, F., Oldstone, M. B. A., Olsnes, S., Vogt, P. K., Series Eds.; Current Topics in Microbiology and Immunology; Springer Berlin Heidelberg: Berlin, Heidelberg, 2008; Vol. 322, pp 193–206. [https://doi.org/10.1007/978-3-540-75418-3\\_9](https://doi.org/10.1007/978-3-540-75418-3_9).
- (83) Dowdell, K.; Haig, S.-J.; Caverly, L. J.; Shen, Y.; LiPuma, J. J.; Raskin, L. Nontuberculous Mycobacteria in Drinking Water Systems – The Challenges of Characterization and Risk

- Mitigation. *Curr. Opin. Biotechnol.* **2019**, *57*, 127–136. <https://doi.org/10.1016/j.copbio.2019.03.010>.
- (84) Falkinham, J. O. Mycobacterium Avium Complex: Adherence as a Way of Life. *AIMS Microbiol.* **2018**, *4* (3), 428–438. <https://doi.org/10.3934/microbiol.2018.3.428>.
- (85) Mullis, S. N.; Falkinham, J. O., III. Adherence and Biofilm Formation of Mycobacterium Avium, Mycobacterium Intracellulare and Mycobacterium Abscessus to Household Plumbing Materials. *J. Appl. Microbiol.* **2013**, *115* (3), 908–914. <https://doi.org/10.1111/jam.12272>.
- (86) Chattopadhyay, S.; Perkins, S. D.; Shaw, M.; Nichols, T. L. Evaluation of Exposure to Brevundimonas Diminuta and Pseudomonas Aeruginosa during Showering. *J. Aerosol Sci.* **2017**, *114*, 77–93. <https://doi.org/10.1016/j.jaerosci.2017.08.008>.
- (87) Falkinham, J. O. Epidemiology of Infection by Nontuberculous Mycobacteria. *Clin. Microbiol. Rev.* **1996**, *9* (2), 177–215.
- (88) Jia, S.; Shi, P.; Hu, Q.; Li, B.; Zhang, T.; Zhang, X.-X. Bacterial Community Shift Drives Antibiotic Resistance Promotion during Drinking Water Chlorination. *Environ. Sci. Technol.* **2015**, *49* (20), 12271–12279. <https://doi.org/10.1021/acs.est.5b03521>.
- (89) Gulati, P.; Ghosh, M. Biofilm Forming Ability of Sphingomonas Paucimobilis Isolated from Community Drinking Water Systems on Plumbing Materials Used in Water Distribution. *J. Water Health* **2017**, *15* (6), 942–954. <https://doi.org/10.2166/wh.2017.294>.
- (90) Delafont, V.; Bouchon, D.; Héchard, Y.; Moulin, L. Environmental Factors Shaping Cultured Free-Living Amoebae and Their Associated Bacterial Community within Drinking Water Network. *Water Res.* **2016**, *100*, 382–392. <https://doi.org/10.1016/j.watres.2016.05.044>.
- (91) LaPara, T. M.; Hope Wilkinson, K.; Strait, J. M.; Hozalski, R. M.; Sadowksy, M. J.; Hamilton, M. J. The Bacterial Communities of Full-Scale Biologically Active, Granular Activated Carbon Filters Are Stable and Diverse and Potentially Contain Novel Ammonia-Oxidizing Microorganisms. *Appl. Environ. Microbiol.* **2015**, *81* (19), 6864–6872. <https://doi.org/10.1128/AEM.01692-15>.
- (92) Shaw, J. L. A.; Monis, P.; Fabris, R.; Ho, L.; Braun, K.; Drikas, M.; Cooper, A. Assessing the Impact of Water Treatment on Bacterial Biofilms in Drinking Water Distribution Systems Using High-Throughput DNA Sequencing. *Chemosphere* **2014**, *117*, 185–192. <https://doi.org/10.1016/j.chemosphere.2014.06.077>.
- (93) Marchesi, I.; Marchegiano, P.; Bargellini, A.; Cencetti, S.; Frezza, G.; Miselli, M.; Borella, P. Effectiveness of Different Methods to Control Legionella in the Water Supply: Ten-Year Experience in an Italian University Hospital. *J. Hosp. Infect.* **2011**, *77* (1), 47–51. <https://doi.org/10.1016/j.jhin.2010.09.012>.
- (94) Parkinson, J.; Baron, J. L.; Hall, B.; Bos, H.; Racine, P.; Wagener, M. M.; Stout, J. E. Point-of-Use Filters for Prevention of Health Care–Acquired Legionnaires’ Disease: Field

- Evaluation of a New Filter Product and Literature Review. *Am. J. Infect. Control* **2020**, *48* (2), 132–138. <https://doi.org/10.1016/j.ajic.2019.09.006>.
- (95) Reasoner, D. J.; Blannon, J. C.; Geldreich, E. E. Microbiological Characteristics of Third-Faucet Point-of-Use Devices. *J. AWWA* **1987**, *79* (10), 60–66. <https://doi.org/10.1002/j.1551-8833.1987.tb02925.x>.
- (96) Barillo, D. J.; Marx, D. E. Silver in Medicine: A Brief History BC 335 to Present. *Burns* **2014**, *40*, S3–S8. <https://doi.org/10.1016/j.burns.2014.09.009>.
- (97) Liu, Z.; Stout, J. E.; Tedesco, L.; Boldin, M.; Hwang, C.; Diven, W. F.; Yu, V. L. Controlled Evaluation of Copper-Silver Ionization in Eradicating Legionella Pneumophila from a Hospital Water Distribution System. *J. Infect. Dis.* **1994**, *169* (4), 919–922.
- (98) Graves, J. L.; Tajkarimi, M.; Cunningham, Q.; Campbell, A.; Nonga, H.; Harrison, S. H.; Barrick, J. E. Rapid Evolution of Silver Nanoparticle Resistance in Escherichia Coli. *Front. Genet.* **2015**, *6*, 42. <https://doi.org/10.3389/fgene.2015.00042>.
- (99) M. Stabryla, L.; A. Johnston, K.; E. Millstone, J.; M. Gilbertson, L. Emerging Investigator Series: It's Not All about the Ion: Support for Particle-Specific Contributions to Silver Nanoparticle Antimicrobial Activity. *Environ. Sci. Nano* **2018**, *5* (9), 2047–2068. <https://doi.org/10.1039/C8EN00429C>.
- (100) Zhang, Y.; Pan, X.; Liao, S.; Jiang, C.; Wang, L.; Tang, Y.; Wu, G.; Dai, G.; Chen, L. Quantitative Proteomics Reveals the Mechanism of Silver Nanoparticles against Multidrug-Resistant *Pseudomonas Aeruginosa* Biofilms. *J. Proteome Res.* **2020**, *19* (8), 3109–3122. <https://doi.org/10.1021/acs.jproteome.0c00114>.
- (101) Li, L.; Mendis, N.; Trigui, H.; Oliver, J. D.; Faucher, S. P. The Importance of the Viable but Non-Culturable State in Human Bacterial Pathogens. *Front. Microbiol.* **2014**, *5*.
- (102) June, S. G.; Dziewulski, D. M. Copper and Silver Biocidal Mechanisms, Resistance Strategies, and Efficacy for Legionella Control. *J. AWWA* **2018**, *110* (12), E13–E35. <https://doi.org/10.1002/awwa.1144>.
- (103) Rodgers, M. R.; Blackstone, B. J.; Reyes, A. L.; Covert, T. C. Colonisation of Point of Use Water Filters by Silver Resistant Non-Tuberculous Mycobacteria. *J. Clin. Pathol.* **1999**, *52* (8), 629–629. <https://doi.org/10.1136/jcp.52.8.629a>.
- (104) 14:00-17:00. *ISO 11731:2017*. ISO. <https://www.iso.org/standard/61782.html> (accessed 2023-05-10).
- (105) *Standard Test Method for Isolation and Enumeration of Pseudomonas aeruginosa from Water*. <https://www.astm.org/d5246-19.html> (accessed 2023-05-10).
- (106) Douglas, G. M.; Maffei, V. J.; Zaneveld, J. R.; Yurgel, S. N.; Brown, J. R.; Taylor, C. M.; Huttenhower, C.; Langille, M. G. I. PICRUSt2 for Prediction of Metagenome Functions. *Nat. Biotechnol.* **2020**, *38* (6), 685–688. <https://doi.org/10.1038/s41587-020-0548-6>.

- (107) *Assembling CDC Reactor*; 2021. <https://www.youtube.com/watch?v=UvN8J2Qx-18> (accessed 2023-09-01).
- (108) Azeredo, J.; Azevedo, N. F.; Briandet, R.; Cerca, N.; Coenye, T.; Costa, A. R.; Desvaux, M.; Di Bonaventura, G.; Hébraud, M.; Jaglic, Z.; Kačániová, M.; Knøchel, S.; Lourenço, A.; Mergulhão, F.; Meyer, R. L.; Nychas, G.; Simões, M.; Tresse, O.; Sternberg, C. Critical Review on Biofilm Methods. *Crit. Rev. Microbiol.* **2017**, *43* (3), 313–351. <https://doi.org/10.1080/1040841X.2016.1208146>.
- (109) Sharma, S. K.; Upadhyay, V. Epidemiology, Diagnosis & Treatment of Non-Tuberculous Mycobacterial Diseases. *Indian J. Med. Res.* **2020**, *152* (3), 185–226. [https://doi.org/10.4103/ijmr.IJMR\\_902\\_20](https://doi.org/10.4103/ijmr.IJMR_902_20).
- (110) Lin, Y. E.; Vidic, R. D.; Stout, J. E.; McCartney, C. A.; Yu, V. L. Inactivation of Mycobacterium Avium by Copper and Silver Ions. *Water Res.* **1998**, *32* (7), 1997–2000. [https://doi.org/10.1016/S0043-1354\(97\)00460-0](https://doi.org/10.1016/S0043-1354(97)00460-0).
- (111) Silvestry-Rodriguez, N.; Sicairos-Ruelas, E. E.; Gerba, C. P.; Bright, K. R. Silver as a Disinfectant. In *Reviews of Environmental Contamination and Toxicology*; Reviews of Environmental Contamination and Toxicology; Springer: New York, NY, 2007; pp 23–45. [https://doi.org/10.1007/978-0-387-69163-3\\_2](https://doi.org/10.1007/978-0-387-69163-3_2).
- (112) Lin, Y. -s. E.; Vidic, R. D.; Stout, J. E.; Yu, V. L. BIndividual-Combined-Effects-Copper-Silver-Ions.Pdf. *Water Res.* **1996**, *30* (8), 1905–1913.
- (113) Spencer-Williams, I.; Meyer, M.; DePas, W.; Elliott, E.; Haig, S.-J. Assessing the Impacts of Lead Corrosion Control on the Microbial Ecology and Abundance of Drinking-Water-Associated Pathogens in a Full-Scale Drinking Water Distribution System. *Environ. Sci. Technol.* **2023**, *57* (48), 20360–20369. <https://doi.org/10.1021/acs.est.3c05272>.
- (114) DePas, W. H.; Bergkessel, M.; Newman, D. K. Aggregation of Nontuberculous Mycobacteria Is Regulated by Carbon-Nitrogen Balance. *mBio* **2019**, *10* (4), 10.1128/mbio.01715-19. <https://doi.org/10.1128/mbio.01715-19>.
- (115) Yang, C.; Mai, J.; Cao, X.; Burberry, A.; Cominelli, F.; Zhang, L. Ggpicrust2: An R Package for PICRUST2 Predicted Functional Profile Analysis and Visualization. *Bioinformatics*, 2023, *39*. <https://doi.org/10.1093/bioinformatics/btad470>.
- (116) Zhou, H.; He, K.; Chen, J.; Zhang, X. LinDA: Linear Models for Differential Abundance Analysis of Microbiome Compositional Data. *Genome Biol.* **2022**, *23* (1), 95. <https://doi.org/10.1186/s13059-022-02655-5>.
- (117) US EPA, O. *National Primary Drinking Water Regulations*. <https://www.epa.gov/ground-water-and-drinking-water/national-primary-drinking-water-regulations> (accessed 2024-03-24).

- (118) US EPA, O. *Secondary Drinking Water Standards: Guidance for Nuisance Chemicals*. <https://www.epa.gov/sdwa/secondary-drinking-water-standards-guidance-nuisance-chemicals> (accessed 2024-03-24).
- (119) Clark, B. N.; Masters, S. V.; Edwards, M. A. Lead Release to Drinking Water from Galvanized Steel Pipe Coatings. *Environ. Eng. Sci.* **2015**, *32* (8), 713–721. <https://doi.org/10.1089/ees.2015.0073>.
- (120) Declerck, P.; Behets, J.; Margineanu, A.; van Hoef, V.; De Keersmaecker, B.; Ollevier, F. Replication of *Legionella Pneumophila* in Biofilms of Water Distribution Pipes. *Microbiol. Res.* **2009**, *164* (6), 593–603. <https://doi.org/10.1016/j.micres.2007.06.001>.
- (121) *Standard Test Method for Determining the Antimicrobial Activity of Antimicrobial Agents Under Dynamic Contact Conditions*. <https://www.astm.org/e2149-20.html> (accessed 2023-07-05).
- (122) Schwartz, T.; Kohnen, W.; Jansen, B.; Obst, U. Detection of Antibiotic-Resistant Bacteria and Their Resistance Genes in Wastewater, Surface Water, and Drinking Water Biofilms. *FEMS Microbiol. Ecol.* **2003**, *43* (3), 325–335. <https://doi.org/10.1111/j.1574-6941.2003.tb01073.x>.
- (123) Proctor, C. R.; Dai, D.; Edwards, M. A.; Pruden, A. Interactive Effects of Temperature, Organic Carbon, and Pipe Material on Microbiota Composition and *Legionella Pneumophila* in Hot Water Plumbing Systems. *Microbiome* **2017**, *5* (1), 130. <https://doi.org/10.1186/s40168-017-0348-5>.
- (124) Neu, L.; Hammes, F. Feeding the Building Plumbing Microbiome: The Importance of Synthetic Polymeric Materials for Biofilm Formation and Management. *Water* **2020**, *12* (6), 1774. <https://doi.org/10.3390/w12061774>.
- (125) Yonathan, K.; Mann, R.; Mahbub, K. R.; Gunawan, C. The Impact of Silver Nanoparticles on Microbial Communities and Antibiotic Resistance Determinants in the Environment. *Environ. Pollut.* **2022**, *293*, 118506. <https://doi.org/10.1016/j.envpol.2021.118506>.
- (126) Vaz-Moreira, I.; Nunes, O. C.; Manaia, C. M. Ubiquitous and Persistent Proteobacteria and Other Gram-Negative Bacteria in Drinking Water. *Sci. Total Environ.* **2017**, *586*, 1141–1149. <https://doi.org/10.1016/j.scitotenv.2017.02.104>.
- (127) Pinto, A. J.; Xi, C.; Raskin, L. Bacterial Community Structure in the Drinking Water Microbiome Is Governed by Filtration Processes. *Environ. Sci. Technol.* **2012**, *46* (16), 8851–8859. <https://doi.org/10.1021/es302042t>.
- (128) El-Chakhtoura, J.; Saikaly, P. E.; van Loosdrecht, M. C. M.; Vrouwenvelder, J. S. Impact of Distribution and Network Flushing on the Drinking Water Microbiome. *Front. Microbiol.* **2018**, *9*.

- (129) Mi, Z.; Dai, Y.; Xie, S.; Chen, C.; Zhang, X. Impact of Disinfection on Drinking Water Biofilm Bacterial Community. *J. Environ. Sci.* **2015**, *37*, 200–205. <https://doi.org/10.1016/j.jes.2015.04.008>.
- (130) Farhat, M.; Alkharsah, K. R.; Alkhamis, F. I.; Bukharie, H. A. Metagenomic Study on the Composition of Culturable and Non-Culturable Bacteria in Tap Water and Biofilms at Intensive Care Units. *J. Water Health* **2019**, *17* (1), 72–83. <https://doi.org/10.2166/wh.2018.213>.
- (131) Vaz-Moreira, I.; Nunes, O. C.; Manaia, C. M. Diversity and Antibiotic Resistance Patterns of Sphingomonadaceae Isolates from Drinking Water. *Appl. Environ. Microbiol.* **2011**, *77* (16), 5697–5706. <https://doi.org/10.1128/AEM.00579-11>.
- (132) Sun, S.; Zhou, Y.; Yu, H.; Li, W.; Zhou, W.; Luo, G.; Zhang, W. Effect of Pipe Materials on Bacterial Community, Redox Reaction, and Functional Genes. *Coatings* **2022**, *12* (11), 1747. <https://doi.org/10.3390/coatings12111747>.
- (133) Lau, P. C. Y.; Lindhout, T.; Beveridge, T. J.; Dutcher, J. R.; Lam, J. S. Differential Lipopolysaccharide Core Capping Leads to Quantitative and Correlated Modifications of Mechanical and Structural Properties in *Pseudomonas Aeruginosa* Biofilms. *J. Bacteriol.* **2009**, *191* (21), 6618–6631. <https://doi.org/10.1128/jb.00698-09>.
- (134) Maldonado, R. F.; Sá-Correia, I.; Valvano, M. A. Lipopolysaccharide Modification in Gram-Negative Bacteria during Chronic Infection. *FEMS Microbiol. Rev.* **2016**, *40* (4), 480–493. <https://doi.org/10.1093/femsre/fuw007>.
- (135) Formosa-Dague, C.; Castelain, M.; Martin-Yken, H.; Dunker, K.; Dague, E.; Sletmoen, M. The Role of Glycans in Bacterial Adhesion to Mucosal Surfaces: How Can Single-Molecule Techniques Advance Our Understanding? *Microorganisms* **2018**, *6* (2), 39. <https://doi.org/10.3390/microorganisms6020039>.
- (136) Landrygan-Bakri, J.; Wilson, M. J.; Williams, D. W.; Lewis, M. A. O.; Waddington, R. J. Real-Time Monitoring of the Adherence of *Streptococcus Anginosus* Group Bacteria to Extracellular Matrix Decorin and Biglycan Proteoglycans in Biofilm Formation. *Res. Microbiol.* **2012**, *163* (6), 436–447. <https://doi.org/10.1016/j.resmic.2012.07.006>.
- (137) Wong, E. H. J.; Ng, C. G.; Goh, K. L.; Vadivelu, J.; Ho, B.; Loke, M. F. Metabolomic Analysis of Low and High Biofilm-Forming *Helicobacter Pylori* Strains. *Sci. Rep.* **2018**, *8* (1), 1409. <https://doi.org/10.1038/s41598-018-19697-0>.
- (138) Chu, E. K.; Kilic, O.; Cho, H.; Groisman, A.; Levchenko, A. Self-Induced Mechanical Stress Can Trigger Biofilm Formation in Uropathogenic *Escherichia Coli*. *Nat. Commun.* **2018**, *9*, 4087. <https://doi.org/10.1038/s41467-018-06552-z>.
- (139) Fazeli-Nasab, B.; Sayyed, R. Z.; Mojahed, L. S.; Rahmani, A. F.; Ghafari, M.; Antonius, S.; Sukamto. Biofilm Production: A Strategic Mechanism for Survival of Microbes under Stress Conditions. *Biocatal. Agric. Biotechnol.* **2022**, *42*, 102337. <https://doi.org/10.1016/j.bcab.2022.102337>.

- (140) Stüken, A.; Haverkamp, T. H. A.; Dirven, H. A. A. M.; Gilfillan, G. D.; Leithaug, M.; Lund, V. Microbial Community Composition of Tap Water and Biofilms Treated with or without Copper–Silver Ionization. *Environ. Sci. Technol.* **2018**, *52* (6), 3354–3364. <https://doi.org/10.1021/acs.est.7b05963>.
- (141) Li, N.; Li, X.; Shi, Z.-Y.; Fan, X.-Y.; Zhou, Z.-W. Bacterial Communities, Potential Pathogens and Antibiotic Resistance Genes of Silver-Loaded Stainless Steel Pipe Wall Biofilm in Domestic Hot Water System. *J. Water Process Eng.* **2021**, *40*, 101935. <https://doi.org/10.1016/j.jwpe.2021.101935>.
- (142) Albalghiti, E.; Stabryla, L. M.; Gilbertson, L. M.; Zimmerman, J. B. Towards Resolution of Antibacterial Mechanisms in Metal and Metal Oxide Nanomaterials: A Meta-Analysis of the Influence of Study Design on Mechanistic Conclusions. *Environ. Sci. Nano* **2021**, *8* (1), 37–66. <https://doi.org/10.1039/D0EN00949K>.
- (143) Forstner, C.; Orton, T. G.; Wang, P.; Kopittke, P. M.; Dennis, P. G. Wastewater Treatment Processing of Silver Nanoparticles Strongly Influences Their Effects on Soil Microbial Diversity. *Environ. Sci. Technol.* **2020**, *54* (21), 13538–13547. <https://doi.org/10.1021/acs.est.0c01312>.
- (144) Wang, H.; Min, C.; Xia, F.; Xia, Y.; Tang, M.; Li, J.; Hu, Y.; Zou, M. Metagenomic Analysis Reveals the Short-Term Influences on Conjugation of bla<sub>NDM-1</sub> and Microbiome in Hospital Wastewater by Silver Nanoparticles at Environmental-Related Concentration. *Environ. Res.* **2023**, *228*, 115866. <https://doi.org/10.1016/j.envres.2023.115866>.
- (145) Przemieniecki, S. W.; Oćwieja, M.; Ciesielski, S.; Halecki, W.; Matras, E.; Gorczyca, A. Chemical Structure of Stabilizing Layers of Negatively Charged Silver Nanoparticles as an Effector of Shifts in Soil Bacterial Microbiome under Short-Term Exposure. *Int. J. Environ. Res. Public Health* **2022**, *19* (21), 14438. <https://doi.org/10.3390/ijerph192114438>.
- (146) Li, X.; Wang, H.; Hu, C.; Yang, M.; Hu, H.; Niu, J. Characteristics of Biofilms and Iron Corrosion Scales with Ground and Surface Waters in Drinking Water Distribution Systems. *Corros. Sci.* **2015**, *90*, 331–339. <https://doi.org/10.1016/j.corsci.2014.10.028>.
- (147) Kimbell, L. K.; Wang, Y.; McNamara, P. J. The Impact of Metal Pipe Materials, Corrosion Products, and Corrosion Inhibitors on Antibiotic Resistance in Drinking Water Distribution Systems. *Appl. Microbiol. Biotechnol.* **2020**, *104* (18), 7673–7688. <https://doi.org/10.1007/s00253-020-10777-8>.
- (148) Sun, H.; Shi, B.; Lytle, D. A.; Bai, Y.; Wang, D. Formation and Release Behavior of Iron Corrosion Products under the Influence of Bacterial Communities in a Simulated Water Distribution System. *Environ. Sci. Process. Impacts* **2014**, *16* (3), 576–585. <https://doi.org/10.1039/C3EM00544E>.
- (149) Boopathi, S.; Ramasamy, S.; Haridevamuthu, B.; Murugan, R.; Veerabadhran, M.; Jia, A.-Q.; Arockiaraj, J. Intercellular Communication and Social Behaviors in Mycobacteria. *Front. Microbiol.* **2022**, *13*, 943278. <https://doi.org/10.3389/fmicb.2022.943278>.

- (150) Brown-Elliott, B. A.; Philley, J. V. Rapidly Growing Mycobacteria. *Microbiol. Spectr.* **2017**, *5* (1), 10.1128/microbiolspec.tnmi7-0027-2016. <https://doi.org/10.1128/microbiolspec.tnmi7-0027-2016>.
- (151) Donohue, M. J. Epidemiological Risk Factors and the Geographical Distribution of Eight Mycobacterium Species. *BMC Infect. Dis.* **2021**, *21* (1), 258. <https://doi.org/10.1186/s12879-021-05925-y>.
- (152) Yang, J.; Hu, Y.; Zhang, Y.; Zhou, S.; Meng, D.; Xia, S.; Wang, H. Deciphering the Diversity and Assemblage Mechanisms of Nontuberculous Mycobacteria Community in Four Drinking Water Distribution Systems with Different Disinfectants. *Sci. Total Environ.* **2024**, *907*, 168176. <https://doi.org/10.1016/j.scitotenv.2023.168176>.
- (153) Pitell, S.; Haig, S.-J. Assessing the Impact of Anti-Microbial Showerheads on the Prevalence and Abundance of Opportunistic Pathogens in Shower Water and Shower Water-Associated Aerosols. *Front. Microbiomes* **2023**, *2*.
- (154) Williams, M. M.; Yakrus, M. A.; Arduino, M. J.; Cooksey, R. C.; Crane, C. B.; Banerjee, S. N.; Hilborn, E. D.; Donlan, R. M. Structural Analysis of Biofilm Formation by Rapidly and Slowly Growing Nontuberculous Mycobacteria. *Appl. Environ. Microbiol.* **2009**, *75* (7), 2091–2098. <https://doi.org/10.1128/AEM.00166-09>.
- (155) Neu, L.; Proctor, C. R.; Walser, J.-C.; Hammes, F. Small-Scale Heterogeneity in Drinking Water Biofilms. *Front. Microbiol.* **2019**, *10*.
- (156) Hou, J.; Wang, C.; Rozenbaum, R. T.; Gusnaniar, N.; De Jong, E. D.; Woudstra, W.; Geertsema-Doornbusch, G. I.; Atema-Smit, J.; Sjollem, J.; Ren, Y.; Busscher, H. J.; Van Der Mei, H. C. Bacterial Density and Biofilm Structure Determined by Optical Coherence Tomography. *Sci. Rep.* **2019**, *9* (1), 9794. <https://doi.org/10.1038/s41598-019-46196-7>.
- (157) Xi, C.; Marks, D. L.; Schlachter, S.; Luo, W.; M.d, S. A. B. High-Resolution Three-Dimensional Imaging of Biofilm Development Using Optical Coherence Tomography. *J. Biomed. Opt.* **2006**, *11* (3), 034001. <https://doi.org/10.1117/1.2209962>.
- (158) Wagner, M.; Horn, H. Optical Coherence Tomography in Biofilm Research: A Comprehensive Review: OCT in Biofilm Research. *Biotechnol. Bioeng.* **2017**, *114*. <https://doi.org/10.1002/bit.26283>.
- (159) Shen, Y.; Huang, C.; Monroy, G. L.; Janjaroen, D.; Derlon, N.; Lin, J.; Espinosa-Marzal, R.; Morgenroth, E.; Boppart, S. A.; Ashbolt, N. J.; Liu, W.-T.; Nguyen, T. H. Response of Simulated Drinking Water Biofilm Mechanical and Structural Properties to Long-Term Disinfectant Exposure. *Environ. Sci. Technol.* **2016**, *50* (4), 1779–1787. <https://doi.org/10.1021/acs.est.5b04653>.
- (160) Guo, L.; Ye, C.; Yu, X.; Horn, H. Induction of Bacteria in Biofilm into a VBNC State by Chlorine and Monitoring of Biofilm Structure Changes by Means of OCT. *Sci. Total Environ.* **2023**, *891*, 164294. <https://doi.org/10.1016/j.scitotenv.2023.164294>.

- (161) Lalley, J.; Dionysiou, D. D.; Varma, R. S.; Shankara, S.; Yang, D. J.; Nadagouda, M. N. Silver-Based Antibacterial Surfaces for Drinking Water Disinfection—an Overview. *Curr. Opin. Chem. Eng.* **2014**, *3*, 25–29. <https://doi.org/10.1016/j.coche.2013.09.004>.
- (162) Guo, J.; Qin, S.; Wei, Y.; Liu, S.; Peng, H.; Li, Q.; Luo, L.; Lv, M. Silver Nanoparticles Exert Concentration-Dependent Influences on Biofilm Development and Architecture. *Cell Prolif.* **2019**, *52* (4), e12616. <https://doi.org/10.1111/cpr.12616>.
- (163) Singh, N.; Paknikar, K. M.; Rajwade, J. RNA-Sequencing Reveals a Multitude of Effects of Silver Nanoparticles on *Pseudomonas Aeruginosa* Biofilms. *Environ. Sci. Nano* **2019**, *6* (6), 1812–1828. <https://doi.org/10.1039/C8EN01286E>.
- (164) Königs, A. M.; Flemming, H.-C.; Wingender, J. Nanosilver Induces a Non-Culturable but Metabolically Active State in *Pseudomonas Aeruginosa*. *Front. Microbiol.* **2015**, *6*.
- (165) Kusnetsov, J.; Iivanainen, E.; Elomaa, N.; Zacheus, O.; Martikainen, P. J. Copper and Silver Ions More Effective against Legionellae than against Mycobacteria in a Hospital Warm Water System. *Water Res.* **2001**, *35* (17), 4217–4225. [https://doi.org/10.1016/S0043-1354\(01\)00124-5](https://doi.org/10.1016/S0043-1354(01)00124-5).
- (166) Lin, Y.-s. E.; Vidic, R. D.; Stout, J. E.; Yu, V. L. Negative Effect of High pH on Biocidal Efficacy of Copper and Silver Ions in Controlling Legionella Pneumophila. *Appl. Environ. Microbiol.* **2002**, *68* (6), 2711–2715. <https://doi.org/10.1128/AEM.68.6.2711-2715.2002>.
- (167) Dziewulski, D. M.; Ingles, E.; Codru, N.; Strepelis, J.; Schoonmaker-Bopp, D. Use of Copper-Silver Ionization for the Control of Legionellae in Alkaline Environments at Health Care Facilities. *Am. J. Infect. Control* **2015**, *43* (9), 971–976. <https://doi.org/10.1016/j.ajic.2015.05.018>.
- (168) Song, Y.; Pruden, A.; Edwards, M. A.; Rhoads, W. J. Natural Organic Matter, Orthophosphate, pH, and Growth Phase Can Limit Copper Antimicrobial Efficacy for *Legionella* in Drinking Water. *Environ. Sci. Technol.* **2021**, *55* (3), 1759–1768. <https://doi.org/10.1021/acs.est.0c06804>.
- (169) Thuptimdang, P.; Limpiyakorn, T.; McEvoy, J.; Prüß, B. M.; Khan, E. Effect of Silver Nanoparticles on *Pseudomonas Putida* Biofilms at Different Stages of Maturity. *J. Hazard. Mater.* **2015**, *290*, 127–133. <https://doi.org/10.1016/j.jhazmat.2015.02.073>.
- (170) Lu, J.; Wang, Y.; Jin, M.; Yuan, Z.; Bond, P.; Guo, J. Both Silver Ions and Silver Nanoparticles Facilitate the Horizontal Transfer of Plasmid-Mediated Antibiotic Resistance Genes. *Water Res.* **2020**, *169*, 115229. <https://doi.org/10.1016/j.watres.2019.115229>.
- (171) Nessar, R.; Cambau, E.; Reyrat, J. M.; Murray, A.; Gicquel, B. Mycobacterium Abscessus: A New Antibiotic Nightmare. *J. Antimicrob. Chemother.* **2012**, *67* (4), 810–818. <https://doi.org/10.1093/jac/dkr578>.

- (172) Bisht, K.; Baishya, J.; Wakeman, C. A. Pseudomonas Aeruginosa Polymicrobial Interactions during Lung Infection. *Curr. Opin. Microbiol.* **2020**, *53*, 1–8. <https://doi.org/10.1016/j.mib.2020.01.014>.
- (173) Filkins, L. M.; O’Toole, G. A. Cystic Fibrosis Lung Infections: Polymicrobial, Complex, and Hard to Treat. *PLOS Pathog.* **2015**, *11* (12), e1005258. <https://doi.org/10.1371/journal.ppat.1005258>.
- (174) *How to Choose a Shower Head.* The Shower Head Store. <https://www.theshowerheadstore.com/blogs/news/how-to-choose-a-shower-head> (accessed 2024-01-18).
- (175) Liang, J.; Swanson, C. S.; Wang, L.; He, Q. Impact of Building Closures during the COVID-19 Pandemic on Legionella Infection Risks. *Am. J. Infect. Control* **2021**, *49* (12), 1564–1566. <https://doi.org/10.1016/j.ajic.2021.09.008>.
- (176) Dowdell, K. S.; Greenwald, H. D.; Joshi, S.; Grimard-Conea, M.; Pitell, S.; Song, Y.; Ley, C.; Kennedy, L. C.; Vosloo, S.; Huo, L.; Haig, S.-J.; Hamilton, K. A.; Nelson, K. L.; Pinto, A.; Prévost, M.; Proctor, C. R.; Raskin, L. M.; Whelton, A. J.; Garner, E.; Pieper, K. J.; Rhoads, W. J. Legionella Pneumophila Occurrence in Reduced-Occupancy Buildings in 11 Cities during the COVID-19 Pandemic; preprint; Public and Global Health, 2022. <https://doi.org/10.1101/2022.06.28.22277022>.
- (177) Dolan, F.; Lamontagne, J.; Link, R.; Hejazi, M.; Reed, P.; Edmonds, J. Evaluating the Economic Impact of Water Scarcity in a Changing World. *Nat. Commun.* **2021**, *12* (1), 1915. <https://doi.org/10.1038/s41467-021-22194-0>.
- (178) He, C.; Liu, Z.; Wu, J.; Pan, X.; Fang, Z.; Li, J.; Bryan, B. A. Future Global Urban Water Scarcity and Potential Solutions. *Nat. Commun.* **2021**, *12* (1), 4667. <https://doi.org/10.1038/s41467-021-25026-3>.
- (179) Al-Jasser, A. O. Chlorine Decay in Drinking-Water Transmission and Distribution Systems: Pipe Service Age Effect. *Water Res.* **2007**, *41* (2), 387–396. <https://doi.org/10.1016/j.watres.2006.08.032>.
- (180) Lautenschlager, K.; Boon, N.; Wang, Y.; Egli, T.; Hammes, F. Overnight Stagnation of Drinking Water in Household Taps Induces Microbial Growth and Changes in Community Composition. *Water Res.* **2010**, *44* (17), 4868–4877. <https://doi.org/10.1016/j.watres.2010.07.032>.
- (181) Nisar, M. A.; Ross, K. E.; Brown, M. H.; Bentham, R.; Whiley, H. Water Stagnation and Flow Obstruction Reduces the Quality of Potable Water and Increases the Risk of Legionellosis. *Front. Environ. Sci.* **2020**, *8*.
- (182) Zlatanović, Lj.; van der Hoek, J. P.; Vreeburg, J. H. G. An Experimental Study on the Influence of Water Stagnation and Temperature Change on Water Quality in a Full-Scale Domestic Drinking Water System. *Water Res.* **2017**, *123*, 761–772. <https://doi.org/10.1016/j.watres.2017.07.019>.

- (183) Moreland, A. Timing of State and Territorial COVID-19 Stay-at-Home Orders and Changes in Population Movement — United States, March 1–May 31, 2020. *MMWR Morb. Mortal. Wkly. Rep.* **2020**, *69*. <https://doi.org/10.15585/mmwr.mm6935a2>.
- (184) Delen, D.; Eryarsoy, E.; Davazdahemami, B. No Place Like Home: Cross-National Data Analysis of the Efficacy of Social Distancing During the COVID-19 Pandemic. *JMIR Public Health Surveill.* **2020**, *6* (2), e19862. <https://doi.org/10.2196/19862>.
- (185) Hozalski, R. M.; LaPara, T. M.; Zhao, X.; Kim, T.; Waak, M. B.; Burch, T.; McCarty, M. Flushing of Stagnant Premise Water Systems after the COVID-19 Shutdown Can Reduce Infection Risk by *Legionella* and *Mycobacterium* Spp. *Environ. Sci. Technol.* **2020**, *54* (24), 15914–15924. <https://doi.org/10.1021/acs.est.0c06357>.
- (186) S. Dowdell, K.; Greenwald Healy, H.; Joshi, S.; Grimard-Conea, M.; Pitell, S.; Song, Y.; Ley, C.; C. Kennedy, L.; Vosloo, S.; Huo, L.; Haig, S.-J.; A. Hamilton, K.; L. Nelson, K.; Pinto, A.; Prévost, M.; R. Proctor, C.; Raskin, L.; J. Whelton, A.; Garner, E.; J. Pieper, K.; J. Rhoads, W. Legionella Pneumophila Occurrence in Reduced-Occupancy Buildings in 11 Cities during the COVID-19 Pandemic. *Environ. Sci. Water Res. Technol.* **2023**. <https://doi.org/10.1039/D3EW00278K>.
- (187) Proctor, C. R.; Rhoads, W. J.; Keane, T.; Salehi, M.; Hamilton, K.; Pieper, K. J.; Cwiertny, D. M.; Prévost, M.; Whelton, A. J. Considerations for Large Building Water Quality after Extended Stagnation. *AWWA Water Sci.* **2020**, *2* (4), e1186. <https://doi.org/10.1002/aws2.1186>.
- (188) Kelechava, B. *ANSI/ASHRAE Standard 188-2021 for Legionnaires' Disease Risk Management*. The ANSI Blog. <https://blog.ansi.org/ansi-ashrae-standard-188-2021-legionnaires-risk/> (accessed 2024-01-19).
- (189) *Requirement to Reduce Legionella Risk in Healthcare Facility Water Systems to Prevent Cases and Outbreaks of Legionnaires Disease (LD) | CMS*. <https://www.cms.gov/medicare/provider-enrollment-and-certification/surveyscertificationgeninfo/policy-and-memos-to-states-and-regions-items/survey-and-cert-letter-17-30-> (accessed 2024-01-19).
- (190) Ensuring Water Quality in Building Premise Plumbing - Actions for Water Utilities During and After COVID-19.
- (191) M. Angert, D.; Ley, C.; Ra, K.; Noh, Y.; Zyaykina, N.; Montagnino, E.; Wei, R.; J. Whelton, A.; R. Proctor, C. Water Quality during Extended Stagnation and Flushing in a College Residential Hall. *Environ. Sci. Water Res. Technol.* **2023**, *9* (12), 3484–3496. <https://doi.org/10.1039/D3EW00038A>.
- (192) Ra, K.; Proctor, C.; Ley, C.; Angert, D.; Noh, Y.; Odimayomi, T.; Whelton, A. J. Four Buildings and a Flush: Lessons from Degraded Water Quality and Recommendations on Building Water Management. *Environ. Sci. Ecotechnology* **2024**, *18*, 100314. <https://doi.org/10.1016/j.ese.2023.100314>.

- (193) Hejazi, M.; Edmonds, J.; Clarke, L.; Kyle, P.; Davies, E.; Chaturvedi, V.; Wise, M.; Patel, P.; Eom, J.; Calvin, K.; Moss, R.; Kim, S. Long-Term Global Water Projections Using Six Socioeconomic Scenarios in an Integrated Assessment Modeling Framework. *Technol. Forecast. Soc. Change* **2014**, *81*, 205–226. <https://doi.org/10.1016/j.techfore.2013.05.006>.
- (194) Pérez-Blanco, C. D.; Hrast-Essenfelder, A.; Perry, C. Irrigation Technology and Water Conservation: A Review of the Theory and Evidence. *Rev. Environ. Econ. Policy* **2020**, *14* (2), 216–239. <https://doi.org/10.1093/reep/reaa004>.
- (195) US EPA, O. A *Water Conservation Guide for Commercial, Institutional and Industrial Users*. <https://www.epa.gov/sustainability/water-conservation-guide-commercial-institutional-and-industrial-users> (accessed 2024-01-19).
- (196) Abu-Bakar, H.; Williams, L.; Hallett, S. H. A Review of Household Water Demand Management and Consumption Measurement. *J. Clean. Prod.* **2021**, *292*, 125872. <https://doi.org/10.1016/j.jclepro.2021.125872>.
- (197) Niculita-Hirzel, H.; Goekce, S.; Jackson, C. E.; Suarez, G.; Amgwerd, L. Risk Exposure during Showering and Water-Saving Showers. *Water* **2021**, *13* (19), 2678. <https://doi.org/10.3390/w13192678>.
- (198) Binks, A. N.; Kenway, S. J.; Lant, P. A.; Head, B. W. Understanding Australian Household Water-Related Energy Use and Identifying Physical and Human Characteristics of Major End Uses. *J. Clean. Prod.* **2016**, *135*, 892–906. <https://doi.org/10.1016/j.jclepro.2016.06.091>.
- (199) Dieu-Hang, T.; Grafton, R. Q.; Martínez-Espiñeira, R.; Garcia-Valiñas, M. Household Adoption of Energy and Water-Efficient Appliances: An Analysis of Attitudes, Labelling and Complementary Green Behaviours in Selected OECD Countries. *J. Environ. Manage.* **2017**, *197*, 140–150. <https://doi.org/10.1016/j.jenvman.2017.03.070>.
- (200) Checa, J.; Carbonell, I.; Manero, N.; Martí, I. Comparative Study of Legiolert with ISO 11731-1998 Standard Method-Conclusions from a Public Health Laboratory. *J. Microbiol. Methods* **2021**, *186*, 106242. <https://doi.org/10.1016/j.mimet.2021.106242>.
- (201) J. Ley, C.; R. Proctor, C.; Singh, G.; Ra, K.; Noh, Y.; Odimayomi, T.; Salehi, M.; Julien, R.; Mitchell, J.; Pouyan Nejadhashemi, A.; J. Whelton, A.; Gim Aw, T. Drinking Water Microbiology in a Water-Efficient Building: Stagnation, Seasonality, and Physicochemical Effects on Opportunistic Pathogen and Total Bacteria Proliferation. *Environ. Sci. Water Res. Technol.* **2020**, *6* (10), 2902–2913. <https://doi.org/10.1039/D0EW00334D>.
- (202) Schoen, M. E.; Ashbolt, N. J. An In-Premise Model for Legionella Exposure during Showering Events. *Water Res.* **2011**, *45* (18), 5826–5836. <https://doi.org/10.1016/j.watres.2011.08.031>.
- (203) Allegra, S.; Leclerc, L.; Massard, P. A.; Girardot, F.; Riffard, S.; Pourchez, J. Characterization of Aerosols Containing Legionella Generated upon Nebulization. *Sci. Rep.* **2016**, *6* (1), 33998. <https://doi.org/10.1038/srep33998>.

- (204) Prussin, A. J.; Marr, L. C. Sources of Airborne Microorganisms in the Built Environment. *Microbiome* **2015**, *3* (1), 78. <https://doi.org/10.1186/s40168-015-0144-z>.
- (205) Ovrutsky, A. R.; Chan, E. D.; Kartalija, M.; Bai, X.; Jackson, M.; Gibbs, S.; Falkinham, J. O.; Iseman, M. D.; Reynolds, P. R.; McDonnell, G.; Thomas, V. Cooccurrence of Free-Living Amoebae and Nontuberculous Mycobacteria in Hospital Water Networks, and Preferential Growth of Mycobacterium Avium in Acanthamoeba Lenticulata. *Appl. Environ. Microbiol.* **2013**, *79* (10), 3185–3192. <https://doi.org/10.1128/AEM.03823-12>.
- (206) Proctor, C.; Garner, E.; Hamilton, K. A.; Ashbolt, N. J.; Caverly, L. J.; Falkinham, J. O.; Haas, C. N.; Prevost, M.; Prevots, D. R.; Pruden, A.; Raskin, L.; Stout, J.; Haig, S.-J. Tenets of a Holistic Approach to Drinking Water-Associated Pathogen Research, Management, and Communication. *Water Res.* **2022**, *211*, 117997. <https://doi.org/10.1016/j.watres.2021.117997>.
- (207) Ryan, M. P.; Adley, C. C. Ralstonia Spp.: Emerging Global Opportunistic Pathogens. *Eur. J. Clin. Microbiol. Infect. Dis.* **2014**, *33* (3), 291–304. <https://doi.org/10.1007/s10096-013-1975-9>.
- (208) Ryan, M. P.; Adley, C. C. Spingomonas Paucimobilis: A Persistent Gram-Negative Nosocomial Infectious Organism. *J. Hosp. Infect.* **2010**, *75* (3), 153–157. <https://doi.org/10.1016/j.jhin.2010.03.007>.
- (209) Sun, H.; Shi, B.; Bai, Y.; Wang, D. Bacterial Community of Biofilms Developed under Different Water Supply Conditions in a Distribution System. *Sci. Total Environ.* **2014**, *472*, 99–107. <https://doi.org/10.1016/j.scitotenv.2013.11.017>.
- (210) Huber, B.; Riedel, K.; Köthe, M.; Givskov, M.; Molin, S.; Eberl, L. Genetic Analysis of Functions Involved in the Late Stages of Biofilm Development in Burkholderia Cepacia H111. *Mol. Microbiol.* **2002**, *46* (2), 411–426. <https://doi.org/10.1046/j.1365-2958.2002.03182.x>.
- (211) Hansen, C. B.; Kerrouche, A.; Tatari, K.; Rasmussen, A.; Ryan, T.; Summersgill, P.; Desmulliez, M. P. Y.; Bridle, H.; Albrechtsen, H. J. Monitoring of Drinking Water Quality Using Automated ATP Quantification. *J. Microbiol. Methods* **2019**, *165*, 105713. <https://doi.org/10.1016/j.mimet.2019.105713>.
- (212) Bragonzi, A.; Farulla, I.; Paroni, M.; Twomey, K. B.; Pirone, L.; Lorè, N. I.; Bianconi, I.; Dalmastri, C.; Ryan, R. P.; Bevivino, A. Modelling Co-Infection of the Cystic Fibrosis Lung by Pseudomonas Aeruginosa and Burkholderia Cenocepacia Reveals Influences on Biofilm Formation and Host Response. *PLoS ONE* **2012**, *7* (12), e52330. <https://doi.org/10.1371/journal.pone.0052330>.
- (213) Stewart, C. R.; Muthye, V.; Cianciotto, N. P. Legionella Pneumophila Persists within Biofilms Formed by Klebsiella Pneumoniae, Flavobacterium Sp., and Pseudomonas Fluorescens under Dynamic Flow Conditions. *PLoS ONE* **2012**, *7* (11), e50560. <https://doi.org/10.1371/journal.pone.0050560>.

- (214) Cirillo, J. D.; Falkow, S.; Tompkins, L. S.; Bermudez, L. E. Interaction of Mycobacterium Avium with Environmental Amoebae Enhances Virulence. *INFECT IMMUN* **1997**, *65*, 9.
- (215) Cirillo, J. D.; Falkow, S.; Tompkins, L. S. Growth of Legionella Pneumophila in Acanthamoeba Castellanii Enhances Invasion. *Infect. Immun.* **1994**, *62* (8), 3254–3261.
- (216) Singh, R.; Hamilton, K. A.; Rasheduzzaman, M.; Yang, Z.; Kar, S.; Fasnacht, A.; Masters, S. V.; Gurian, P. L. Managing Water Quality in Premise Plumbing: Subject Matter Experts' Perspectives and a Systematic Review of Guidance Documents. *Water* **2020**, *12* (2), 347. <https://doi.org/10.3390/w12020347>.